

---

# Bioproduction of Natural Carotenoids by *Dietzia maris* and *Rhodococcus opacus*

---

A STUDY OF THE BIOPRODUCTION OF CANTHAXANTHIN BY *Dietzia maris* DSM 43672 AND  
ASTAXANTHIN BY *Rhodococcus opacus* DSM 43250

AUTHORS

ANDERS SØBYE  
MARIE-LOUISE KNOP LUND



**AALBORG UNIVERSITY**  
STUDENT REPORT  
SCHOOL OF ENGINEERING AND SCIENCE  
AALBORG UNIVERSITY 2018





**Title:**

Bioproduction of Natural Carotenoids  
by *Dietzia maris* and *Rhodococcus*  
*opacus*

**Project:**

Master Thesis

**Project Period:**

September 2017 - June 2018

**Participants:**

Anders Søbye  
Marie-Louise Knop Lund

**Supervisor:**

Peter Fojan

**Printed Copies:** 2

**Total Page Number:** 85

**Appendices:** 3

**Finished:** June 10<sup>th</sup>, 2018

**Abstract:**

The commercial interest for natural carotenoids have increased over the past decades due to their pro-vitamin, anti-oxidative, anti-cancer, anti-inflammatory, and fine pigmentation properties. The commercial production of carotenoids is, however, currently relying on chemical synthesis, which it is severely criticized due to inexpedient waste products and the adverse human reactions related to synthetic dyes. The natural sources of carotenoids are not limited, and microbial sources are of particular interest. However, only few organisms have reached commercial production levels and they mostly include  $\beta$ -carotene producers. The search for appropriate microbial sources has been extensive, but have mostly concerned single-organism batch reactions. Therefore this project proposes a two-organism biosynthesis reaction in the production of, firstly, the valuable keto-carotenoid canthaxanthin, and secondly, the valuable hydroxy-carotenoid astaxanthin. *D. maris* DSM 43672 is utilized for the production of canthaxanthin and *R. opacus* DSM 43250 for the production of astaxanthin, which will proceed through canthaxanthin as the precursor. The produced carotenoids were extracted using chloroform and non-toxic edible sunflower oil, where the oil-extraction was unsuccessful. However, it was discovered that during sonication of the *D. maris* cells in water, vesicles with a mean diameter of 255.79 nm were formed, encapsulating canthaxanthin, obtaining extractions yields of 152.72  $\mu\text{g/g}$ . The produced canthaxanthin vesicles were fed to *R. opacus*, which did not produce any astaxanthin during the 24 hours of incubation. Extraction of xanthophylls using water could be a new, high-yield extraction method in the production of natural xanthophylls without the use of organic solvents, providing they can be separated from the vesicles in which they reside.



---

# Preface

---

This project is written by Anders Søbye and Marie-Louise Knop Lund, Nanobiotechnology master students of Aalborg University, from September 2<sup>nd</sup> until June 10<sup>th</sup>. Lector Peter Fojan from the Department of Materials and Production is the primary supervisor, where Professor Reinhard Wimmer from the Department of Chemistry and Bioscience has been of extensive experimental assistance. The topic of this project is the biosynthesis of carotenoids by *Dietzia* and *Rhodococcus* species, where the production of canthaxanthin and astaxanthin by *D. maris* DSM 43672 and *R. opacus* DSM 43250, respectively, will be investigated. Furthermore, identification of carotenoids will rely on NMR spectroscopy, MS, NTA and TLC.

This project will introduce the current state of natural and synthetic carotenoid productions and the importance of efficient production methods of natural carotenoids. A description of the experiments will follow, leading to both the results and a discussion of the experiments according to relevant theory. All results not shown in the project are presented in the three appendices.

Throughout this project, each chapter and section will have numbered titles. Furthermore, all figures, significant equations, and tables will be numbered. The reference system applied is the numerical system and every reference is represented by a [number], which refers directly to a specific source in the bibliography. Figures with no citation are composed by the group itself.

---

Anders Søbye

---

Marie-Louise Knop Lund



---

## Significant Abbreviations

---

<b>ESI:</b>	Electrospray Ionization
<b>FT:</b>	Fourier Transform
<b>GS:</b>	Gym Streptomycin
<b>HSQC:</b>	Heteronuclear Single Quantum Coherence
<b>HPLC:</b>	High-Pressure Liquid Chromatography
<b>MS:</b>	Mass Spectrometry
<b>NMR:</b>	Nuclear Magnetic Resonance
<b>NTA:</b>	Nanoparticle Tracking Analysis
<b>PULCON:</b>	Pulse Length-based Concentration Determination
<b>TLC:</b>	Thin-Layer Chromatography
<b>TS:</b>	Tryptic Soy



---

# Table of Contents

---

<b>1</b>	<b>Introduction</b>	<b>9</b>
<b>2</b>	<b>Materials and Methods</b>	<b>15</b>
2.1	Chemicals . . . . .	15
2.2	Materials and Equipment . . . . .	16
2.3	Growth and Storage Conditions . . . . .	16
2.4	Preparation of Mineral Medium and Phosphate Buffer . . . . .	17
2.5	Mass Spectrometry Carotenoid Standard Curves . . . . .	17
2.6	Bioproduction of Canthaxanthin by <i>D. maris</i> . . . . .	18
2.6.1	Carotenoid Extraction using Chloroform . . . . .	19
2.6.2	Carotenoid Extraction using Water and Sonication . . . . .	19
2.6.3	Mass Spectrometry . . . . .	20
2.6.4	Nuclear Magnetic Resonance Spectroscopy . . . . .	21
2.6.5	Nanoparticle Tracking Analysis . . . . .	21
2.7	Bioproduction of Astaxanthin by <i>R. opacus</i> . . . . .	21
2.7.1	Thin-Layer Chromatography . . . . .	22
<b>3</b>	<b>Results and Discussion</b>	<b>23</b>
3.1	Mass Spectrometry Carotenoid Standard Curves . . . . .	24
3.1.1	Standard Curves and Characterization of Canthaxanthin . . . . .	24
3.1.2	Standard Curves and Characterization of Astaxanthin . . . . .	29
3.1.3	Standard Curves and Characterization of $\beta$ -carotene . . . . .	33
3.2	Bioproduction of Canthaxanthin by <i>D. maris</i> . . . . .	38
3.2.1	Carotenoid Extraction using Chloroform . . . . .	41
3.2.2	Carotenoid Extraction using Edible Sunflower Oil . . . . .	45
3.2.3	Carotenoid Extraction using Water and Sonication . . . . .	47
3.3	Bioproduction of Astaxanthin by <i>R. opacus</i> . . . . .	56
3.3.1	Thin-Layer Chromatography . . . . .	59
<b>4</b>	<b>Conclusion</b>	<b>61</b>
	<b>Bibliography</b>	<b>63</b>
	<b>Appendix A</b> <i>D. maris</i> and <i>R. ruber</i> NMR Measurements	<b>69</b>
	<b>Appendix B</b> Mass Chromatograms of Extracted Agar Plates	<b>75</b>
	<b>Appendix C</b> Nanoparticle Tracking Analysis Measurements	<b>83</b>



---

# 1. Introduction

---

Carotenoids are the most widely distributed natural yellow, orange, and red pigments found in nature, comprised of more than 600 characterized unique carotenoids found in plant species, algae, fungi, bacteria, and vertebrates where they exhibit important pro-vitamin, anti-oxidative, anti-inflammatory, and anti-cancer properties. Carotenoids constitute a class of apolar hydrocarbons (carotenes) and their oxygenated derivatives (xanthophylls), which can be further divided into epiphasic and hypophasic carotenoids depending on their solubility into petroleum ether or aqueous methanol, respectively [1–3]. Xanthophylls are generally substituted with hydroxyl-, keto-, methoxy-, epoxy-, or carboxyl groups [4]. The majority of carotenoids are long conjugated systems consisting of four central isoprene residues, and at least nine conjugated double bonds, exhibiting high molecular symmetry and giving rise to multiple geometrical and optical isomers through the extended double bonds. In addition, carotenoids are either acyclic or terminated by one or two cyclic end-groups, which mostly determine their binding capacity to proteins and their orientation on membranes [4, 5]. The extended conjugation of the central hydrocarbon chain naturally yields an all-trans configuration, with only few exceptions, due to a greater molecular stability and bioavailability, and lower steric hindrance, compared to the cis conformer [6]. The conjugated system is responsible for the characteristic yellow-to-red colours of carotenoids by allowing electrons of the double bonds to easily de-localize, causing the molecule to efficiently quench single oxygen and to retard lipid peroxidation and stabilize lipid-protein structures. [1–3, 5–11]

Several biosynthetic pathways have been confirmed to be responsible for the microbial production of carotenoids. The process generally starts with the precursor isopentenyl pyrophosphate, and proceeds through one of the most common steps in microbial carotenogenesis; the formation of all-trans lycopene and subsequently  $\beta$ -carotene ( $\beta,\beta$ -carotene), from which most other carotenoids are synthesized by hydroxylation, carbonylation, methoxylation, epoxidation, or carboxylation. Most of the involved enzymes are soluble proteins, but the later steps of carotenogenesis are dominated by membrane-bound proteins. [3]

Vertebrates cannot synthesize carotenoids *de novo* but rely on dietary sources of intake, and it is general consensus that a high amount of natural dietary carotenoids significantly reduces all-cause mortality in humans and that they are prominent chemo-protectives against cancer in general [6, 12]. Only approximately 40-50 different carotenoids constitute the entire human consumption of natural carotenoids, and only 6 (i.e.  $\beta$ -carotene, zeaxanthin, lutein, lycopene,  $\beta$ -cryptoxanthin,  $\alpha$ -carotene) comprise over 90 % of carotenoids detected in human serum and breast milk [2, 6, 13]. These serum carotenoids, and their respective metabolites, are concentrated in specific human organs, whether it is lycopene in the prostate,  $\beta$ -carotene in the corpus luteum, or zeaxanthin and lutein in the retina and brain neocortex, where they have been related to a natural retardation of disease development at those sites by an effective reduction of oxidative and inflammatory stress [2]. This natural disease retardation has not only increased the interest of natural carotenoids in daily products, but also in the treatment of various oxidative and inflammatory diseases, including cancer, by the scientific community. In addition, carotenoids tend to become more bioavailable when they are embedded in food products and display a higher anti-oxidant, and non-toxic, activity when derived from natural sources. [2, 6, 7]

Due to the high commercial prices of natural carotenoids and the highly effective synthetic chemical production methods for many of the compounds, the production and pursuit of rich natural sources of carotenoids were originally abandoned when they were first discovered [7]. Currently, the production of synthetic carotenoids is a heavy and dominating pigment industry, severely criticized due to chemical waste disposal, hazardous precursors and solvents, and non-biodegradable bi-products [7, 14]. In addition, serious health effects, including, but not limited to, toxic and neurologic adverse reactions, respiratory disorders, gastrointestinal problems, and dermatologic issues have given rise to a strong consumer concern about the application of synthetic dyes in everyday consumer products, ultimately increasing the market value and popularity of natural counterparts in food, cosmetic, paper, and agricultural industries over the past few decades [7, 10, 14, 15]. The market value of natural pigments surpassed 1.2 billion USD in 2010 (including fish and poultry fodder), and continues to increase with an annual growth of 2.3 % [3, 11]. Furthermore, from an industrial point of view, the chemical synthesis of carotenoids is not without problems, as the pathway of these compounds is often very complex, involves multiple organic solvents, and differs among all carotenoids. In addition, chemical synthesis produces a mixture of stereoisomers where some might not exhibit the desired health effects, and others may have undesired side effects [16]. Replacing the synthetic pigments is, however, challenging due to the lower stability, higher cost, and decreased colour intensity of the natural compounds. Nevertheless, this higher susceptibility of natural carotenoids to chemical attacks, may reflect some of the sought-after biological functions of these compounds. The natural molecules are easily degraded in the body, and their irreversible destruction over time is exactly their anti-oxidative and photo-protective function in action [5, 11]. [7–9]

Currently, the industry is gradually shifting away from the yellow carotenoids toward the considerably more valuable orange-to-red oxygenated carotenoids. The natural red carotenoids are not only more valuable in terms of high market value due to the current expensive commercial production methods, but also due to a high consumer demand for strong anti-oxidants and red food and cosmetic products in general [4, 10]. But what may be even more interesting in terms of disease treatments, is that orange-to-red carotenoids seem to exhibit an even more powerful anti-oxidant activity, compared to their yellow counterparts, potentially strengthening the immune system, decreasing the risk of degenerative diseases, and preventing cancer, cardiovascular diseases, macular degeneration, cataracts, and other terminal human diseases [2, 3, 10, 12]. Canthaxanthin ( $\beta$ ,  $\beta$ -carotene-4,4'-dione) is an orange-to-red keto-carotenoid, see Figure 1.1, that exhibit strong anti-oxidant activities and free radical scavenging properties, compared to carotenes such as  $\beta$ -carotene [3, 12], and which has proven the ability to reduce and protect against UV light-induced tumours/types of cancers [3, 17]. However, the hydroxylated keto-carotene astaxanthin (3,3'-dihydroxy- $\beta$ , $\beta$ '-carotene-4,4'-dione), see Figure 1.2, has proven to have the highest anti-oxidative activity amongst all carotenoids this far, and it might be ten (or even more) times higher than the activity of both  $\beta$ -carotene and even canthaxanthin and the hydroxylated carotene zeaxanthin [18]. These orange-to-red oxygenated carotenoids are primarily used in the poultry and aquacultural industries, where they are added to fish and poultry feed in order to obtain a more orange coloured egg-yolk, bright orange-to-red coloured feathers, and the pink colour of wild salmon, trout, and crustaceans in commercial fish species [3, 4, 11, 15, 17, 19].

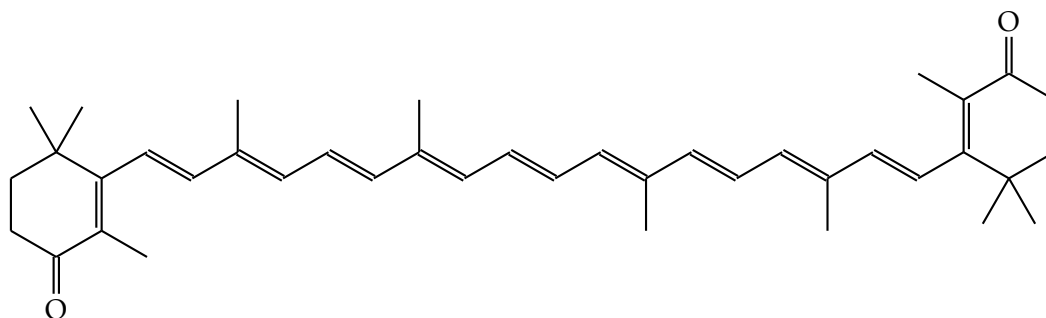


**Figure 1.1:** The chemical structure of all-*trans* canthaxanthin ( $\beta,\beta$ -Carotene-4,4'-dione).

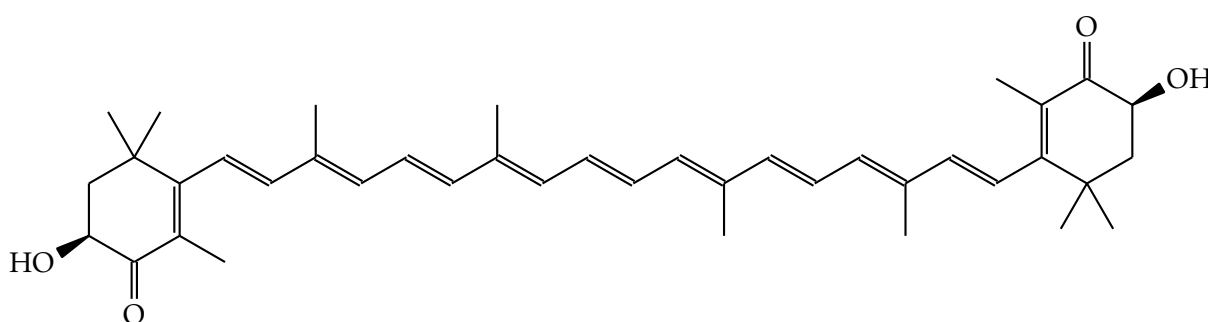


**Figure 1.2:** The chemical structure of all-*trans* astaxanthin (3,3'-dihydroxy- $\beta$ -carotene-4,4'-dione).

Several red pigments have been FDA and EU approved for human consumption, but only few of them are found naturally in the environment and the majority of these are still relying on multi-step chemical synthesis methods for commercial production [3]. The approved natural red pigments include betanin from beetroots, anthocyanins from, among others, elderberry, carmine from scale insects, and a range of oxygenated carotenoids (i.e. astaxanthin, canthaxanthin, capsanthin, and lycopene [14]). Even though a great variety of carotenoids exist in nature, only few have reached commercial production levels since few of these compounds yield significant quantities, both from chemical synthesis and solvent-based chemical extraction from their natural sources [3, 10]. [7, 20] Natural sources of carotenoids are not limited. The carotenoids are naturally most concentrated in green leafy vegetables and colourful fruits like tomatoes and paprika [2], but from the industrial point of view, these plant sources are generally influenced by seasonal variations, they are difficult to upscale, and they give rise to a significant loss of important human nutritional sources [6, 7, 20]. In addition, there exist no cheap exploitable commercial plant sources of the red keto-carotenoids [4]. Microbial fermentation is by far the most preferred production system of most compounds, including carotenoids, since it provides generally cheaper production, it is easy to upscale and control, it takes up far less physical space, there is no seasonal variations, and microbial processes can potentially recycle both agricultural and industrial wastewaters as growth substrates [6, 7, 10, 12, 20]. In addition, the majority of carotenoids are only found in microorganisms in appropriate exploitable quantities [21].

Several microorganisms are known to synthesize a variety of carotenoids, and some are even regarded as promising sources of these molecules. Few microorganisms have, however, reached commercial production levels, and mostly include  $\beta$ -carotene producers [6, 8, 9], due to a range of industrial

obstacles, leaving most microbial carotenoid productions at the R & D stage (and primarily on the R stage [15]). In particular, metabolically engineered *E. coli* have gained interest as a production host, including mutagenesis in natural producers, but the use of genetically modified organisms is still controversial, prohibited in food products, and it does not fit well with the consumer movement toward healthier and more natural products. [10, 11, 21]

The industrial production of natural astaxanthin is currently relying on the red *Haematococcus* algae (12-55 mg/g [11]) and to some extent the red *Phaffia* yeast (50-350 µg/g [10] up to 1.1 – 2.5 mg/g [19]). As astaxanthin is mainly used in fish feed, the main advantages of these organisms is that they are suitable delivery vesicles of astaxanthin, not requiring any further purification [16]. Nevertheless, the production cost is high due to the lack of leading fermentation and chemical synthesis methods, low production yields, and slow growth rates, resulting in an intense search for alternative cheaper production methods [3, 21]. Natural synthesis of canthaxanthin is still only on the research stage, and have stayed there for decades [3, 10, 19]. Several microorganisms that synthesize canthaxanthin have been discovered in the past several decades, but most suffer from low production yields, inaccessibility, or a very slow growth rate, leaving the commercial canthaxanthin production dominated by synthetic synthesis [10, 19]. Some strains, however, still provide commercial potentials, including *Haloferax alexandrines* (700 µg/g [3, 10, 22]) and *Dietzia maris* (191.5 µg/mL [23], 2.87 mg/L [24], and 121.6 mg/L [23, 24]).

Evidence of the biological function of carotenoids in microbes are generally conflicting, which is true for many secondary microbial metabolites, but they are believed to protect vital intracellular components from photo-degradation. The long  $\pi$ -system of the carotenoids is very electron mobile, providing the high reduction potential of the molecules [5]. By absorbing light in the gap of chlorophylls (420-500 nm), carotenoids harvest and mediate a trans-membrane proton transfer, which increases the active spectral range of photosynthesis and protect the cellular components like chlorophylls from excess light, explaining the widespread existence of carotenoids in green plants and algae [3, 25]. Furthermore, it has been demonstrated that carotenoids can reduce the penetration of singlet oxygen into the cell by decreasing the fluidity of the cell membrane [3, 4, 25]. Carotenoids are extremely rigid due to their linear backbone, which extends through and penetrates the hydrophobic zone of the cell membrane, decreasing the fluidity of the membrane in general and controlling the stability and the liability of the membrane to change with temperature [4, 5, 25].

Carotenoids are generally regarded as secondary metabolites in many species, but such metabolites are typically secreted during the stationary growth phase, and this is not the case of carotenoids which tend to be growth related instead [4]. Furthermore, carotenes are generally produced during both the growth and stationary phases [26]. Secretion is a typical key success factor of microbial fermentation systems, as the cells easily can be separated from the growth medium, the product is often water soluble, and purification is often cheap and straight forward. In addition, due to negative feedback systems, high intracellular concentrations are difficult to achieve for non-secreted products, and high concentrations might prove toxic for the cell, leading to an overall lower metabolism or viability of the cells in general [16]. In terms of production, one of the main problems with carotenoids is their extreme hydrophobicity and that they are membrane bound molecules, making natural secretion impossible, and extraction, processing, and purification cost intensive [7, 16]. In addition, the instability and tendency of the molecules to photo-degrade as a result of their anti-oxidative nature poses other industrial challenges, including storage and processing problems [7]. The underlying reaction of carotenoid loss during storage and processing is generally unknown, but includes geometric isomerization and oxidation as some of the major alternations [7].

---

The storage and extraction problems, arising from the extreme hydrophobicity of the carotenoids, have given rise to extensive research into alternative methods of processing. Encapsulation of carotenoids in water soluble forms have gained some industrial attention, as most food matrices are hydrosoluble [12, 27, 28], but most research concerns the replacement of extraction solvents and the application of industrial plant and fish waste as cheap carotenoid sources [11, 13, 29, 30].

The organic solvents are generally preferred in terms of high extraction yields, however, the most effective organic solvents, including chloroform, benzene and DMSO, are not GRAS approved and are thus prohibited for human consumption even at trace amounts [6]. As a result, much attention has been placed on green extraction methods involving cheap edible oil products as extraction solvents. Edible oils have the advantages of being non-toxic, eco-friendly, and can retard oxidation of the carotenoids. In addition, many carotenoids display a relatively well solubility into edible oils and the final enriched oil product may be directly incorporated into cosmetic and feed products. On the other hand, the high viscosity of oil can retard or slow diffusion, thus decreasing the extraction yield significantly. In order to extract the carotenoids from plant and microbial materials, heating of the oil is therefore often required, but at temperatures above 70 °C the carotenoids tend to be irreversibly destroyed. As a result, ultra-sonic assisted extraction has been widely applied instead of direct heating when extracting vulnerable anti-oxidants [10, 13]. Sonication enhances the extraction of anti-oxidants by propagating ultrasound pressure waves and causing micro cavitation bubbles to explosively collapse, locally disturbing and rupturing organic materials. [13, 30]

Due to the lack of leading fermentation methods in the commercial production of both canthaxanthin and astaxanthin, this project will seek to produce these carotenoids using the highly potent bacterial genera of *Rhodococcus* and *Dietzia*. Until now, the focus of carotenoid fermentation has been placed on single-organism systems, including metabolically engineered organisms. However, we propose a natural two-organism batch reaction system of, firstly, canthaxanthin and, secondly, astaxanthin by the hydroxylation of canthaxanthin.

Most known carotenoids naturally act as intermediates in the bioproduction of others. As mentioned,  $\beta$ -carotene is a highly common intermediate in the synthesis of most other carotenoids, and, in addition, both canthaxanthin and zeaxanthin act as intermediates in the biosynthesis of astaxanthin [3]. Therefore, we propose a system where the yellow-to-orange gram-positive aerobe bacterium *Rhodococcus ruber* is utilized for the production of natural  $\beta$ -carotene, which is the primary carotenoid of this species [31, 32], and the orange-to-red gram-positive aerobe bacterium *Dietzia maris* is utilized for the production of natural canthaxanthin, which is the most common carotenoid of this species [24]. The bacterial genera of *Rhodococcus* and *Dietzia* are closely related, where *Dietzia* was originally regarded as a species of *Rhodococcus* [25, 31]. For more detailed information about the *Rhodococcus* genera, we refer to our latest work with these bacteria [33, 34].

From earlier work with the genus of *Rhodococcus*, involving degradation of toxic compounds, it was discovered that the bacterium *Rhodococcus opacus* DSM 43250, when properly induced with phenol, possesses a highly active ring hydroxylation system, hydroxylizing aromatics as the first step toward complete mineralization. However, *R. opacus* showed difficulties with completely mineralizing bulky substrates and molecules substituted with highly electronegative and electron withdrawing substituents. This was observed when 4-fluorophenol was transformed into the dead-end lactone-enol intermediate and with 4-cyanophenol which was only hydroxylated, building up dead-end products over time. We propose that if *R. opacus* is able to hydroxylate the cyclic terminal groups of canthaxanthin as a step in dealing with carotenoids, it is possible that no further transformation can

take place due to the large bulky nature of the compound, and that the end-product thus is astaxanthin. The white gram-positive aerobic bacterium *R. opacus* is generally not associated with a high or effective natural production of carotenoids, and no degradation of these compounds have been reported for this bacterium. *R. opacus* is not associated with any natural production of canthaxanthin, and it is therefore possible that the bacterium will try to utilize canthaxanthin for energy production when it is the only carbon source presented. On the other hand, the genus is well adapted to degrade and transform hydrophobic toxic compounds, and generally survive in hydrophobic solvents [35], and it is therefore possible that the transformation of canthaxanthin is of little priority due to the low toxicity of the molecule. Nevertheless, the hydroxylation of carotenoids is regarded as a common phenomenon among all carotenoid producers, but the addition of a ketone group is a limited characteristic of few selected microbes [3]. Therefore, it was decided to utilize canthaxanthin as the precursor in the production of astaxanthin, and not zeaxanthin.

The produced canthaxanthin and  $\beta$ -carotene is fed to properly induced *R. opacus* cells, where the transformation into astaxanthin, but also the initial production of canthaxanthin and  $\beta$ -carotene, is monitored by extracting the carotenoids at different stages of the production. The carotenoids are extracted with both chloroform and edible organic sunflower oil, and the carotenoid content is quantitated via mass spectrometry (MS) and nuclear magnetic resonance (NMR) measurements.

---

## 2. Materials and Methods

---

This chapter will describe the method developed for the natural production, and quantitation, of canthaxanthin by *D. maris*, as well as the bioproduction of astaxanthin by *R. opacus*, proceeding through the canthaxanthin. The methods were empirically developed and adjusted throughout the experiment period. However, the methods presented in this chapter only accounts for the final working methods, and any variation from these will be presented in Chapter 3. This includes, in particular, experiments with *R. ruber*,  $\beta$ -carotene, and extraction with edible sunflower oil. For detailed theory on the NMR, TLC, and MS measurement techniques, see earlier work by the authors [33, 34]

### 2.1 Chemicals

#### Growth and Storage

- *Dietzia maris* strain DSM 43672 (DSMZ)
- *Rhodococcus opacus* strain DSM 43250 (DSMZ)
- *Rhodococcus ruber* strain DSM 43338 (DSMZ)
- 15 g/L Tryptic soy broth, for microbiology (Sigma Aldrich)
- 15 g/L Agar-agar with 2.0 - 4.5 % ash (Sigma Aldrich)
- 4 g/L D-(+)-Glucose, BioReagent (Sigma Aldrich)
- 4 g/L Yeast extract, for microbiology (Merck Ferm-Tech)
- 10 g/L Malt extract, for microbiology (Fluka Chemicals)

#### Mineral Medium and Phosphate Buffer

- 0.1 M Potassium phosphate dibasic, ACS reagent,  $\geq 98$  % (Sigma Aldrich)
- 0.1 M Potassium phosphate monobasic, for microbiology,  $\geq 99.0$  % (Sigma Aldrich)
- 1 g/L Ammonium nitrate, SigmaUltra,  $\geq 99.5$  % (Sigma Aldrich)
- 1 g/L Potassium phosphate dibasic, ACS reagent,  $\geq 98$  % (Sigma Aldrich)
- 1 g/L Potassium phosphate monobasic, for microbiology,  $\geq 99.0$  % (Sigma Aldrich)
- 0.2 g/L Magnesium sulfate heptahydrate, Ph.Eur (Fluka Chemicals)
- 0.026 g/L Calcium chloride dihydrate, ACS reagent, min. 99.5 % (MERCK)
- Saturated Iron(III) chloride hexahydrate solution, puriss p.a. Reag. Ph.Eur,  $\geq 99$  % (FLUKA)

**Production, Extraction and Identification of Carotenoids**

- All-trans analytical canthaxanthin,  $\geq 97.0$  % (DSM Nutritional Products Ltd.)
- All-trans analytical  $\beta$ -carotene,  $\geq 97.0$  % (DSM Nutritional Products Ltd.)
- Astaxanthin, for HPLC from *Haematococcus pluvialis*,  $\geq 97$  % (Sigma Aldrich)
- Chloroform, ACS reagent,  $\geq 99.8$  % (Sigma Aldrich)
- Chloroform-D + 0.03 % TMS, 99.80 % D (Euriso-Top)
- Deuterium oxide with 99.9 atom % D (Sigma Aldrich) + 0.0038 wt% TMP-D<sub>4</sub>
- Methanol, HPLC grade,  $\geq 99.9$  % (Sigma Aldrich)
- Canthaxanthin, ChemCruz LOT A2317 (Santa Cruz Biotechnology Inc.)
- $\beta$ -carotene, 16837 (Cayman Europe OÜ)
- Petroleum Ether, 40-60 °C, BAKER ANALYZED<sup>®</sup> Reagent (J.T. Baker)
- Acetone, for HPLC,  $\geq 99.8$  % (Sigma Aldrich)

**2.2 Materials and Equipment****Growth and Storage**

- Biowizard Flow Cabinet from KOJAIR<sup>®</sup> TECH
- InnOva<sup>™</sup> 4230 Refrigerated incubator shaker from New Brunswick Scientific
- JP Selecta Autoclave

**Production, Extraction and Identification of Carotenoids**

- Elite LaChrom VWR Hitachi Mass Spectrometer setup; including organizer, pump, autosampler, column oven for HPLC, diode array detector, and UV detector, along with one Bruker NMR-MS-BRIDGE Compact. Includes software Bruker Compass Hystar 3.2 and Bruker Compass Data Analysis
- Acentis<sup>®</sup> Xpress C18, 3 Micron, 15x4.6 cm column for HPLC
- Acentis<sup>®</sup> Xpress RP-amide, 2.7 Micron, 15x4.6 column for HPLC
- Bruker AVIII-600 MHz NMR Spectrophotometer with a Cryogenic Triple Resonance Probehead. Including software Bruker Topspin 3.5
- Minisart<sup>®</sup> SRP hydrophobic PTFE, 0.2  $\mu$ m (non-sterile), single-use syringe filter units
- Minisart<sup>®</sup> sartorius stedim (biotech), 0.2  $\mu$ m non-pyrogenic hydrophilic, single-use syringe filter units
- Sonics<sup>®</sup> Vibra Cell(TM) CV 33 ultra-sonicator
- Thermo Scientific Sorvall Lynx 4000 Centrifuge with F12 096-062375 LEX rotor
- Eppendorf 5804 R centrifuge with F-34-6-38 rotor
- Christ Alpha 1-4 LD freeze-dryer with an RC 6 chemistry hybrid vacuum pump from VacuumBrand
- VWR glass wool 1-04086 E 1.11, 1913-08
- NanoSight Ltd<sup>™</sup> LM12 Nanoparticle Analysis System with a Tension microscope and MARIIN F-0333 ASG camera, including the software NanoSight NTA 3.2
- Silica gel 60 F254 aluminium sheets for TLC (MERCK)

**2.3 Growth and Storage Conditions**

*D. maris*, *R. ruber*, and *R. opacus* cells were received, handled, and maintained in accordance with supplier protocols. Recovered cells were suspended in either Tryptic Soy (TS) broth or Gym Streptomycin (GS) broth, or onto corresponding agar plates.

## 2.4. Preparation of Mineral Medium and Phosphate Buffer

---

The TS broth was prepared by dissolving 15 g/L tryptic soy broth in milli-Q water, where the pH was adjusted toward 7.3. Additionally, for preparation of TS agar plates, 15 g/L agar was added to the broth. The GS broth was prepared by dissolving 4 g/L glucose, 4 g/L yeast extract, and 10 g/L malt extract in milli-Q water, where the pH was adjusted towards 7.2. Both TS and GS media were autoclaved at 121 °C, 1 bar above the atmospheric pressure, for 30 minutes. Finally, both broth and solidified agar plates were stored at 4 °C for up to four months.

Meanwhile, *D. maris* cells were maintained in 5 mL TS broths and on TS agar plates, and *R. ruber* and *R. opacus* cells were maintained in 5 mL GS broths, throughout the period of experiments, where cells were re-inoculated into new suspensions or onto new plates every 4 days of growth.

Broth suspensions were utilized as pre-cultures for some carotenoid production experiments, while agar plates were used directly in other production experiments.

The cells were, throughout the experiment period, unless mentioned otherwise, incubated at 28 °C, at 250 RPM (liquid cultures) and in full light under a household white light bulb, for 4 days before application. In addition, to some extent, variations in the bacterial density and colour of the cultures can occur, in particular for agar plates with *D. maris* cells. However, only agar plates with bright red cultures and significant biomasses were utilized in the experiments.

Lastly, all bacterial work were carried out under high laminar flow in a sterile cabinet, using sterilized and disinfected surfaces and equipment. Additionally, all milli-Q water used throughout the experiments were autoclaved at 121 °C, 1 bar above atmospheric pressure for 30 minutes before application.

## 2.4 Preparation of Mineral Medium and Phosphate Buffer

The 0.01 M phosphate buffer was prepared by diluting 38.5 mL autoclaved 0.1 M potassium phosphate monobasic solution and 61.5 mL autoclaved 0.1 M potassium phosphate dibasic solution into milli-Q water, yielding a total volume of 1 L and achieving pH 7.2.

The mineral medium was prepared by dissolving 1 g/L potassium phosphate monobasic, 1 g/L potassium phosphate dibasic, 0.2 g/L magnesium sulphate, 0.026 g/L calcium chloride, 2 drops of saturated iron chloride, and 1 g/L ammonium nitrate into milli-Q water, in that order. In order to minimize insoluble precipitation of the minerals, the chemicals were autoclaved individually (not including ammonium nitrate) and mixed afterwards achieving appropriate concentrations and volumes. Furthermore, magnesium sulphate and calcium chloride were added slowly during stirring into a cold solution. Ammonium nitrate was, at last, dissolved into the medium. The final pH of the mineral medium was 7.2, and the medium was stored at 4 °C for up to four months.

## 2.5 Mass Spectrometry Carotenoid Standard Curves

In order to quantitate any production of both canthaxanthin and astaxanthin by *D. maris* and *R. opacus*, respectively, MS standard curves with known concentrations of the pure compounds (analytical standards) were prepared as the concentration reference standards. The reference standards were prepared by dissolving canthaxanthin or astaxanthin into a 5 mM stock solution in chloroform. This stock solution was diluted into a logarithmic series of 7 concentrations, ranging from 0.001 mM to 1 mM. Each stock solution was prepared, and diluted, in triplicates, and each triplicate was measured upon within 12 hours of preparation.

In order to form the standard curves, three MS chromatograms were measured for each concentration triplicate, in random order on different days. The triplicates were evaporated and separated by the

reverse phase C18 HPLC column, whereafter the masses were recorded in time by the calibrated HPLC/ESI-MS setup for 10 minutes at 40 °C, in positive ionization mode. In addition, an isocratic mobile phase with 99 % acetonitrile, a flowrate of 1 mL/min, an injection volume of 5  $\mu$ L, and 10 minutes of pre-run with pure acetonitrile between all measurements were utilized.

From the full MS chromatograms, the appropriate adduct signals were extracted for canthaxanthin or astaxanthin, see Table 2.1, resulting in the extracted ion chromatograms. Subsequently, the main mass peak was identified, and integrated manually using the existing software. The integrals of the triplicates of the triplicates were averaged, and plotted in relation to the concentration, resulting in the MS standard curves. The linear section of the plot was identified (with  $R^2$  values above 0.98 when forced through (0,0)), and utilized for quantitation of carotenoid content in all further experiments. Since the carotenoids were weighed directly into HPLC vials, and due to their sticky nature, a PULCON  $^1\text{H}$  NMR spectrum was measured directly on the stock solution triplicates in order to confirm the concentration of the 5 mM. In addition, a carbon and HSQC spectrum were measured for later comparison between produced carotenoids and the analytical standards. For all NMR measurements, 150  $\mu$ L of the 5 mM stock solution was diluted into a total volume of 600  $\mu$ L deuterium-locked chloroform. But in the case of astaxanthin, this step was repeated for the 0.5 mM triplicates, which was completely evaporated after MS measurements and diluted into 600  $\mu$ L deuterium-locked chloroform, due to the lower solubility of this compound in chloroform compared to both  $\beta$ -carotene and canthaxanthin.

For the PULCON  $^1\text{H}$  NMR measurements, a spectral width of 20 ppm and a pulse angle of 90° (four times) were utilized, and 32 scans were recorded where 65,536 data points were used for data acquisition. For the  $^{13}\text{C}$  measurements, a spectral width of 230 ppm and a pulse angle of 30° were utilized, and 1024 scans were recorded, where 131,072 data points were used for data acquisition. The  $^1\text{H}$  NMR spectra were calibrated internally according to tetramethylsilane, where the  $^{13}\text{C}$  spectra were referenced indirectly according to the  $^1\text{H}$  spectra ( $\Xi = 0.25145020$ ). Additionally, the spectra were phase corrected both horizontally and according to the individual peaks.

For the HSQC 2D NMR experiments,  $^1\text{H}$  and  $^{13}\text{C}$  nuclei were correlated in order to identify directly bonded carbon and hydrogen atoms. The HSQC NMR experiment was carried out with an ecco/antiecco-TPPI gradient selection with decoupling during acquisition, while using trim pulses inept transfer with multiplicity editing during selection steps, with matched sweep adiabatic pulses (program HSCQEDTGPSISP 2.3). Eight scans were recorded with a spectral width of 160 and 11 ppm. The HSQC NMR spectra were referenced indirectly according to the  $^1\text{H}$  NMR spectra ( $\Xi = 0.25145020$  for  $^{13}\text{C}$ ). All NMR experiments were conducted at 25 °C.

## 2.6 Bioproduction of Canthaxanthin by *D. maris*

In order to determine the appropriate light conditions during the bacterial growth of *D. maris* and *R. ruber*, for carotenoid production, four 100 mL broths were, initially, prepared in 250 mL Erlenmeyer flasks. The cultures were prepared by suspending either 100 mL TS broth or 100 mL GS broth, depending on the organism, and 2 mL pre-culture, which had been grown for 4 days, into the Erlenmeyer flasks. Of the two cultures containing *D. maris* cells, one was incubated in full light, while the other one was wrapped in aluminium foil before incubation ( $\text{OD}_{540} = 0.062$ ). The same was the case with the two *R. ruber* cultures ( $\text{OD}_{540} = 0.02$ ). On the fourth day of incubation, the cultures were centrifuged twice at 10,000  $\cdot$  g for 10 minutes, where the GS and TS broths were, subsequently, completely discarded. The fresh cells were extracted directly with 30 mL chloroform twice, vigorously shaken, and centrifuged at 10,000  $\cdot$  g for 10 minutes in between. Afterwards, a total volumes of 40 mL

enriched chloroform was recovered from each culture and completely evaporated under a laminar flow of nitrogen. The evaporated extracts were stored in amber glass containers at  $-80\text{ }^{\circ}\text{C}$  in an argon atmosphere.

### 2.6.1 Carotenoid Extraction using Chloroform

In order to determine the highest carotenoid content available for general extraction, the most efficient solvent was initially utilized, and later compared with other extraction methods.

Twelve TS agar plates were inoculated and incubated with  $50\text{ }\mu\text{L}$  *D. maris* pre-culture. On the fourth day of incubation, the cellular content of the plates were either directly extracted with chloroform or transferred onto the second series of TS agar plates, see Figure 2.1.

It has been proposed that the canthaxanthin production by *Dietzia* species is most efficient at pH 5.5 and in media containing yeast extracts [23]. Therefore, some of the secondary TS agar plates were prepared with the addition of  $7\text{ g/L}$  yeast extract and with a pH of 5.5. The secondary TS plates were incubated for another 4 days before carotenoid extraction.

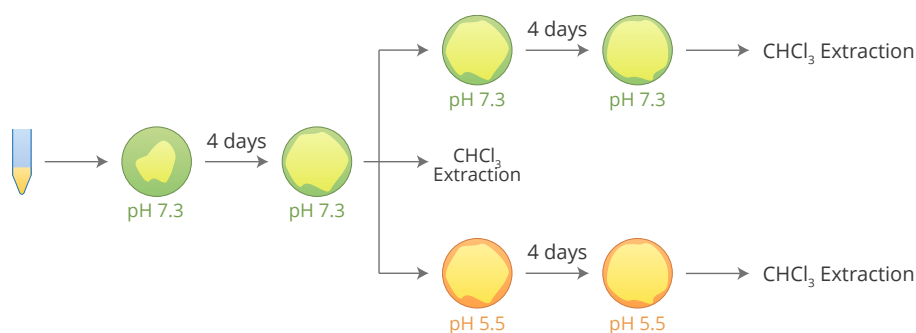


**Figure 2.1:** The work flow of the different agar plates used for carotenoid extraction using chloroform.

For the extraction of the carotenoids, the cellular content of the TS agar plates were transferred, weighed, and extracted directly with  $5\text{ mL}$  chloroform twice, vigorously shaken, and centrifuged at  $10,000\cdot\text{g}$  for 10 minutes in between. In the end, a total volume of  $10\text{ mL}$  chloroform was recovered from each plate, filtrated through a  $0.2\text{ }\mu\text{m}$  hydrophobic filter, and completely evaporated under a laminar flow of nitrogen. The evaporated extracts were stored in amber glass vials at  $4\text{ }^{\circ}\text{C}$  in an argon atmosphere until the next day.

### 2.6.2 Carotenoid Extraction using Water and Sonication

As a green non-toxic alternative to the carotenoid extraction using chloroform, ultra-sonication of the *D. maris* cells in milli-Q water was attempted for extraction of the carotenoids. Eight TS agar plates were inoculated and incubated with  $50\text{ }\mu\text{L}$  *D. maris* pre-culture. On the fourth day of incubation, the cellular content of the plates were either directly extracted with water or transferred onto the second series of TS agar plates with a pH value of 5.5, see Figure 2.2. The secondary TS plates were incubated for another 4 days before carotenoid extraction.

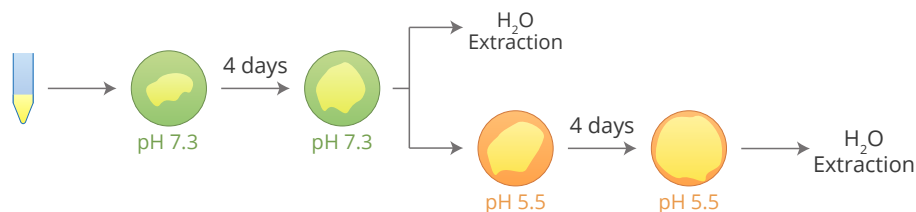


**Figure 2.2:** The work flow of the different agar plates used for carotenoid extraction using water and sonication.

For the extraction of the carotenoids, the cellular content of these TS agar plates were weighed and transferred into 5 mL of milli-Q water. Following, the water fractions were directly ultra-sonicated at 148 W (37 % of 400 W) for a total of 5 minutes with an alternating sequence of 15 seconds of sonication and 30 second breaks. Subsequently, the water fractions were centrifuged at  $10,000 \cdot g$  for 10 minutes, and the 5 mL water fraction was recovered without cell debris. This extraction was repeated twice. In the end, the water fractions were filtrated through a  $0.2 \mu\text{m}$  hydrophilic filter, and 1 mL was stored in amber glass vials for MS measurements at  $4 \text{ }^\circ\text{C}$  until the next day. The rest of the water fractions were freeze-dried for 24 hours and stored at  $-80 \text{ }^\circ\text{C}$  for later measurements.

### 2.6.3 Mass Spectrometry

Before the MS measurements of the light condition experiments, the evaporated extracts were diluted into 5 mL chloroform, where 2 mL was filtrated twice through compressed glass wool in order to remove any left-over cell debris.

Furthermore, the evaporated carotenoid extracts of the agar plates extracted with chloroform were diluted into 1.5 mL chloroform, where  $300 \mu\text{L}$  of the water fraction, from the agar plates extracted with water and ultra-sonication, were diluted into  $300 \mu\text{L}$  methanol.

All samples were then evaporated and separated by the reverse phase C18 HPLC column, whereafter the masses were recorded by the calibrated HPLC/ESI-MS setup for 10 minutes at  $40 \text{ }^\circ$ , in positive ionization mode in triplicates. In addition, an isocratic mobile phase with 99 % acetonitrile, a flow rate of  $1 \text{ mL/min}$ , an injection volume of  $5\text{-}15 \mu\text{L}$ , and 10 minutes of pre-run with pure acetonitrile between the measurements were utilized.

All MS measurements in this project were conducted the following day after the extraction.

From the resulting full mass chromatograms, the appropriate adduct  $m/z$  signals were extracted for several carotenoids, see Table 2.1, resulting in the extracted ion chromatograms. Subsequently, the main mass peaks were identified for canthaxanthin and astaxanthin, and integrated manually using the existing software. The peak areas of the triplicates of the quadruplicates were compared to the respective MS standard curves, averaged, and plotted in relation to the carotenoid content per litre culture broth or per gram bacterial cells.

Carotenoid	m/z	
	Monoisotopic mass	Extracted Adducts
$\beta$ -cryptoxanthin	552.4331	552.4300
$\beta/\alpha$ -carotene/Lycopene	536.4382	536.4382
Canthaxanthin	564.3967	565.3900
Zeaxanthin/Lutein	568.4280	568.4280
Astaxanthin	596.3865	597.3758

**Table 2.1:** Utilized and extracted  $m/z$  values of the monoisotopic masses ( $[M]^+$ ) and the ( $[M^+H]^+$ ) adducts, at positive ionization mode for all detected carotenoids.

### 2.6.4 Nuclear Magnetic Resonance Spectroscopy

In order to verify the presence of canthaxanthin and  $\beta$ -carotene in *D. maris* and *R. ruber*, respectively, and the structures of the carotenoids in the water-extracted samples, 1D and 2D FT-NMR spectroscopy measurements were performed.

For the light-condition experiments, the sample used for MS measurements from both experiments were completely evaporated and re-diluted into 600  $\mu$ L deuterium-locked chloroform.

For the water-extracted samples, the left-over water fractions after all measurements and feeding experiments, were mixed and freeze-dried for 48 hours. Before the NMR measurements, the freeze-dried sample was re-hydrated into 2 mL deuterium oxide containing 0.0038 wt% 3-(trimethylsilyl)propanoic-2,2,3,3- $d_4$  acid (TMP). For NMR measurements, 600  $\mu$ L was recovered with the least amount of cell debris, centrifuged and utilized.

For the  $^1\text{H}$  NMR measurements, a spectral width of 14 ppm and a pulse angle of  $30^\circ$  were utilized, and 16 scans were recorded, where 65,536 data points were used for data acquisition. In addition, for the light-condition experiments, a  $^{13}\text{C}$  NMR spectrum was measured with a spectral width of 230 ppm and a pulse angle of  $30^\circ$  and 1024 scans were recorded, where 131,072 data points were used for data acquisition. The  $^1\text{H}$  NMR spectra were calibrated internally according to tetramethylsilane or TMP, where the  $^{13}\text{C}$  spectra were referenced indirectly according to the  $^1\text{H}$  spectra ( $\Xi = 0.25145020$ ). Additionally, the spectra were phase corrected both horizontally and according to the individual peaks. The HSQC NMR measurement of the water-extracted sample was performed as described in Section 2.5. Furthermore, all the NMR experiments were conducted at  $37^\circ\text{C}$ .

### 2.6.5 Nanoparticle Tracking Analysis

In order to determine how the insoluble carotenoids became water-soluble during the water extraction and ultra-sonication, nanoparticle tracking analysis (NTA) was utilized as it was hypothesized that vesicles were formed during the extraction. For the tracking measurements, 100  $\mu$ L water-extracted sample was diluted into a total volume of 1000  $\mu$ L milli-Q water. The sample was injected into the setup, and the movement of the vesicles were tracked for 60 seconds at three different sample spots in triplicates, with a 1 second delay and 30 frames per second. The detection threshold was set to 18 with a minimum track length of 6 in order to cancel background noise and non-moving particles from the measurements. From the tracked movements of the vesicles, their sizes were estimated by the existing software.

## 2.7 Bioproduction of Astaxanthin by *R. opacus*

Firstly, one main culture was prepared by suspending 2 mL *R. opacus* GS pre-culture, which had been grown for four days, into one 250 mL Erlenmeyer flask containing 100 mL GS broth.

On the fourth day of incubation, the main culture was centrifuged twice at  $10,000 \cdot g$  for 10 minutes, where the GS broth was exchanged with 0.01 M phosphate buffer, and where supernatants were, subsequently, completely discarded.

The fresh, washed cells were rehydrated and re-inoculated into a total volume of 300 mL mineral medium, containing 200 mg/L phenol as the inducer, which was equally distributed into three 250 mL Erlenmeyer flasks ( $\text{OD}_{540} = 0.975\text{-}1.05$ ). The cultures were incubated at  $28^\circ\text{C}$  and 250 RPM, and after 10 hours of incubation, another 200 mg/L phenol, along with 5 mg/L  $\beta$ -carotene in 1 mL chloroform, were suspended into the cultures. After an additional 24 hours of incubation, the cells were again harvested by centrifugation.

The fresh, washed cells were rehydrated and re-inoculated into eight 100 mL Erlenmeyer flasks each containing a total volume of 20 mL mineral medium ( $OD_{540} = 0.648-0.824$ ).

The two initial freeze-dried water-extracted samples, containing the highest concentration of canthaxanthin, were rehydrated into 5 mL milli-Q water each. Following, 3 mL of each water sample was equally distributed into six of the cultures. The last two 20 mL cultures, without canthaxanthin, served as reference cultures.

In order to determine the conversion of canthaxanthin by *R. opacus*, the metabolic profile was determined after 0 and 24 hours of incubation, in triplicates. The two reference cultures were incubated for 0 and 24 hours, respectively.

The eight cultures were extracted two times with 5 mL chloroform, recovered and filtrated through a 0.2  $\mu\text{m}$  hydrophobic filter, and completely evaporated under a laminar flow of nitrogen.

For the MS measurements, the evaporated extracts were diluted into 1.5 mL chloroform, and evaporated and separated by the reverse phase C18 HPLC column, whereafter the masses were recorded in time by the calibrated HPLC/ESI-MS setup for 10 minutes at 40 °, in positive ionization mode. In addition, an isocratic mobile phase with 99 % acetonitrile, a flow rate of 1 mL/min, an injection volume of 15  $\mu\text{L}$ , and 10 minutes of pre-run with pure acetonitrile between the measurements were utilized.

From the resulting full mass chromatograms, the appropriate adduct  $m/z$  signals were extracted for several carotenoids, see Table 2.1, resulting in the extracted ion chromatograms. Subsequently, the main mass peaks were identified for canthaxanthin and astaxanthin, and integrated manually using the existing software. The integrals of the triplicates were compared to the respective MS standard curves, averaged, and compared to the initial concentrations.

### 2.7.1 Thin-Layer Chromatography

After the verification of the presence of vesicles in the water-extracted samples, a thin-layer chromatogram was prepared in order to draw-out carotenoids and compare them with known carotenoid standards and the carotenoids present in *R. opacus* after incubation with the water-extracted samples.

Approximately 1.5  $\mu\text{L}$  of the water-extracted samples, and the chloroform extracts from the *R. opacus* experiments, were suspended onto a thin-layer chromatography (TLC) plate, along with known carotenoid standards. The normal phase TLC was developed with a petroleum ether-acetone (75:25) mobile phase, and after evaporation of the solvent, metabolites were visualized in visible and UV light at 350 nm.

---

## 3. Results and Discussion

---

This chapter will present the results and the relevant discussion simultaneously, in order to elucidate how the results of each experiment have been utilized to identify carotenoids, and have contributed to the development and improvement of the final methods utilized. In addition, this project will only show the MS chromatograms of one of the prepared triplicates or quadruplicates, and for one of the experiments. Furthermore, NMR and MS spectra will only show the relevant ppm and time ranges, respectively, and MS spectra will only show the relevant high-intensity adducts used for concentration calculations, even though multiple adducts and fragments were extracted and evaluated from the full chromatograms.

The initial intention of this project was to focus on the biosynthesis of astaxanthin by *R. opacus*, adjusting and developing a production method, and in the end, designing a two-organism batch reactor for the complete reaction proceeding from a carotenoid precursor into astaxanthin. Based on the metabolic capabilities of *R. opacus*, two different carotenoids were chosen as starting compounds, where *D. maris* was used for the bioproduction of canthaxanthin, and *R. ruber* for the production of  $\beta$ -carotene. In order to carry out a series of astaxanthin production optimization experiments, high quantities of the two precursor carotenoids were required, but they are both expensive, and sufficient amounts were thus difficult to come by. Finally after months of searching, analytical standards were acquired, and 5 g of  $\beta$ -carotene and 10 g of canthaxanthin were bought from Cayman Europe OU and Santa Cruz Biotechnology Inc., respectively, and delivered by AH Diagnostics. The compounds were delivered after a few weeks, and subsequently, one week was spent culturing *R. opacus* cells, and inducing the bacterium with phenol. When the time came for the first series of feeding experiments, efforts were made to dissolve canthaxanthin in chloroform, which is one of the few solvents in which the compound is soluble. However, the assumed canthaxanthin proved to be completely insoluble in chloroform, but was, surprisingly, highly soluble in water. As all other carotenoids, canthaxanthin is completely insoluble in water, and MS measurements revealed, that the red compound did not contain any canthaxanthin, and that it contained high amounts of sucrose and polymers instead. See Figure 3.1 for the  $^1\text{H}$  NMR spectrum of the compound.

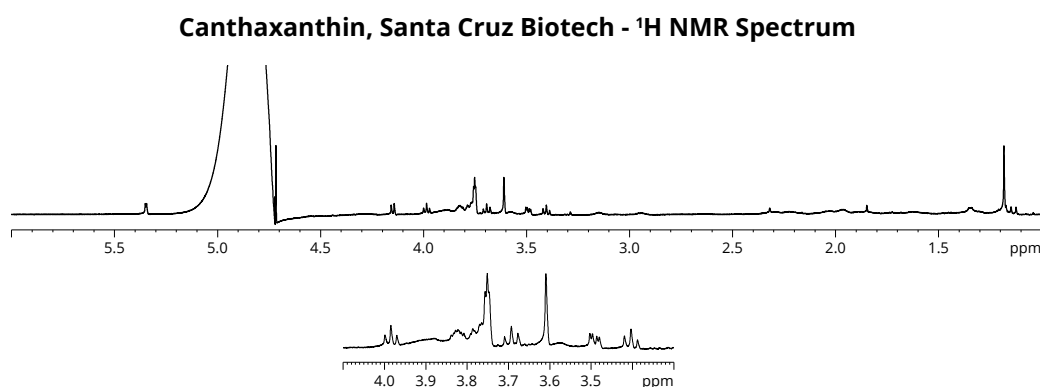


**Figure 3.1:**  $^1\text{H}$  NMR spectrum of canthaxanthin bought from Santa Cruz Biotechnology Inc., diluted into deuterium oxide. The insert shows sucrose. No peaks related to canthaxanthin, or any other carotenoid, were identified.

Due to the lack of canthaxanthin in the compound provided by Santa Cruz Biotechnology Inc., it was decided to utilize *D. maris* for the production of this carotenoid, and focus on its extraction methods. It is well established that canthaxanthin is a primary carotenoid produced by *Dietzia* bacteria [11, 23, 25, 26, 36]. Due to problems with  $\beta$ -carotene, see Section 3.1.3, it was decided only to use canthaxanthin as a precursor in the natural synthesis of astaxanthin.

### 3.1 Mass Spectrometry Carotenoid Standard Curves

In order to quantitate any production of both canthaxanthin and astaxanthin by *D. maris* and *R. opacus*, respectively, MS standard curves were prepared as concentration references using analytical standards of the compounds. It was also attempted to prepare a standard curve for the quantitation of  $\beta$ -carotene produced by *R. ruber*.

After weeks of tracking down industrial suppliers, DSM Nutritional Products in Switzerland was kind enough to donate two analytical standards of canthaxanthin and  $\beta$ -carotene, making quantitation of these compounds possible using MS [37, 38]. These analytical standards did not contain enough compound for the original feeding experiments, but the amounts were sufficient for the preparation of the MS standard curves.

The extraction, handling, and mass separation of carotenoids can be challenging due to their extreme hydrophobicity and the pronounced sensitivity of the molecules to the working environment [12]. Additionally, the high similarity between several carotenoids can make their identification and separation by NMR in complex solutions challenging, and thus much effort was made to map the behaviour of these compounds during, and address the challenges when using, both MS and NMR methods.

#### 3.1.1 Standard Curves and Characterization of Canthaxanthin

The canthaxanthin MS standard curve was developed from extracted ion chromatograms ( $m/z$   $565.3900 \pm 0.05$  ( $[M + H]^+$ )) for the different concentration triplicates. See Figure 3.2 for the extracted ion chromatogram of the analytical standard of canthaxanthin.

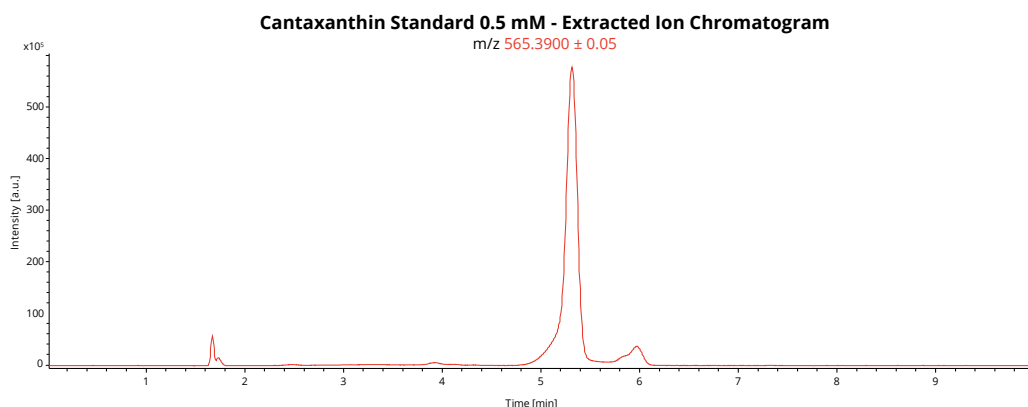


**Figure 3.2:** HPLC/ESI-MS  $m/z$   $565.3900 \pm 0.05$  ( $[M + H]^+$ ) extracted ion chromatogram of one of the 0.5 mM analytical canthaxanthin standard triplicates, at positive ionization. The mass chromatogram is measured in chloroform with an isocratic mobile phase of 99 % acetonitrile on the C18 HPLC column. In addition, a 10 minute pre-run with pure acetonitrile, followed by a running time of 10 minutes, was utilized with a 5  $\mu$ L injection volume. The main mass peak of canthaxanthin is identified between 5 and 6 minutes, with one minor isomeric shoulder at 6 minutes.

### 3.1. Mass Spectrometry Carotenoid Standard Curves

From Figure 3.2, it is visible that during the current measurement conditions, canthaxanthin has a retention time between 5 and 6 minutes. This conforms with a study made by LaFountain *et al.*, who, using a gradient of primarily methanol, observed a retention time of 5.1 minutes [39]. Furthermore, there is a shoulder visible after the high intensity mass peak with the same mass profile, suggesting that they both belong to canthaxanthin, but that there is a difference in the stereochemistry of the molecule. This was also observed by Goswami *et al.* [40]. Thus both peaks were identified as the main mass peak of canthaxanthin, and were both integrated. These two peaks could arise from the fact that the all-trans canthaxanthin standards contains 1.3 *cis*-canthaxanthin, according to the supplier. According to Lesellier *et al.*, the retention of xanthophylls increases as the *cis* double bond moves towards the middle of the molecule, and thus, the largest and first peak corresponds to the *trans* configuration, while the minor shoulder is most likely due to the *cis* configuration. This phenomenon is argued to arise from the difference, between *cis* and *trans* conformers, in interactions between the stationary phase and the carotenoid, and is highly dependent on the polarity and structure of both the stationary and mobile phases. [41–45]

From the extracted ion chromatograms, the isotopic distribution of the compound can be visualized, see Figure 3.3. This isotopic abundance elucidates what adducts should be searched for in later experiments, and can be utilized to compare synthetic and natural canthaxanthin.

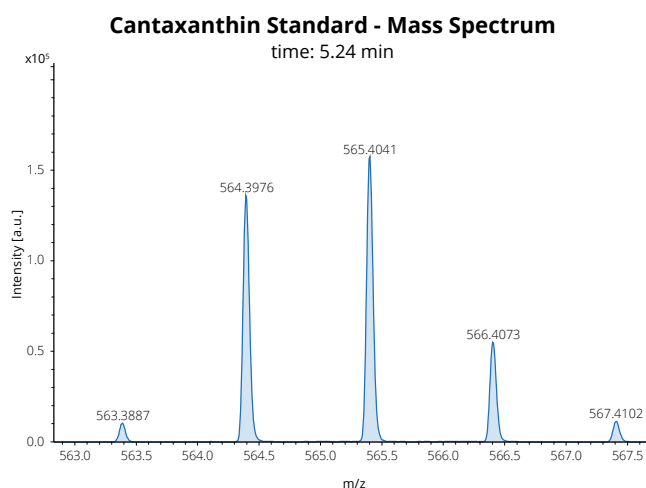


**Figure 3.3:** HPLC/ESI-MS mass spectrum, from the extracted ion chromatogram of the analytical canthaxanthin standard in Figure 3.2, at positive ionization,  $565.3900 \pm 0.05$  ( $[M + H]^+$ ), at 5.24 minutes. The isotopic distribution is visible, where the base peak is also the  $[M + H]^+$  adduct, closely followed by the molecular ion at 564.3976 ( $[M]^+$ ).

In Figure 3.3, the isotopic distribution of the canthaxanthin is visible with five isotopomers with relatively high mass intensities. In this case, the  $[M + H]^+$  adduct at  $m/z$  565.4041 is the base peak, closely followed by the molecular ion at  $m/z$  564.3975 ( $[M]^+$ ). From the isotopic distribution, it is possible to estimate the number of carbon atoms in a molecule, provided that the number of carbons do not exceed 40. The intensity of the signal of the  $M+1$  isotopomer at  $m/z$  566.4073 is approximately 37 % of the base peak, where the  $M+2$  isotopomer is approximately 8 %. From the abundance of  $^{13}\text{C}$  (1.1 %), this will give an estimation of  $34 \pm 2$  carbons in the molecule, which, for canthaxanthin with 40 carbon atoms, is a fair estimation. The estimation would be far more precise for smaller molecules, in particular those with less than 5 carbon atoms, due to the  $^{13}\text{C}$  abundance [46]. In addition, the isotopomers indicate a charge state of 1, which points to the fact that  $m/z$  565.4041 is the  $[M + H]^+$  adduct. From this spectrum, it will be assumed that the  $[M + H]^+$  adduct will be the base peak in any

further experiments. Lastly, these observations of how canthaxanthin as a molecule behaves in the current MS setup, including the isomeric shoulder, base peak, and retention time, should make it easier to identify the molecule in later experiments.

From integrating the extracted ion chromatograms, the canthaxanthin MS standard curves were finally composed. See Figure 3.4 for the full MS standard curve of canthaxanthin, and Figure 3.5 for the linear section of the standard curve, which can be used for quantitation of the compound.

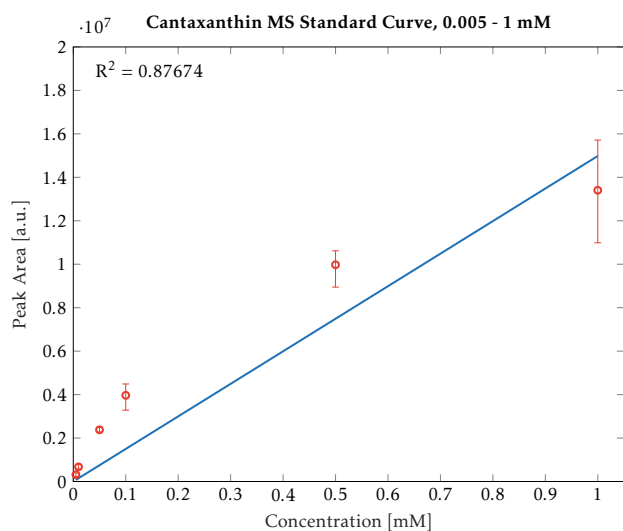


**Figure 3.4:** Full MS standard curve of canthaxanthin, with concentrations ranging from 0.005 mM to 1 mM. The extracted ion chromatograms at  $m/z$   $565.3900 \pm 0.05$  ( $[M + H]^+$ ) have been integrated manually for each concentration triplicate in triplicates. The area is plotted as a function of the concentration, and linearly fitted, forcing the fit through (0,0), ultimately obtaining the  $R^2$  value of 0.87674. The concentrations have been corrected using the exact concentration calculated from the corresponding PULCON  $^1\text{H}$  NMR spectra.

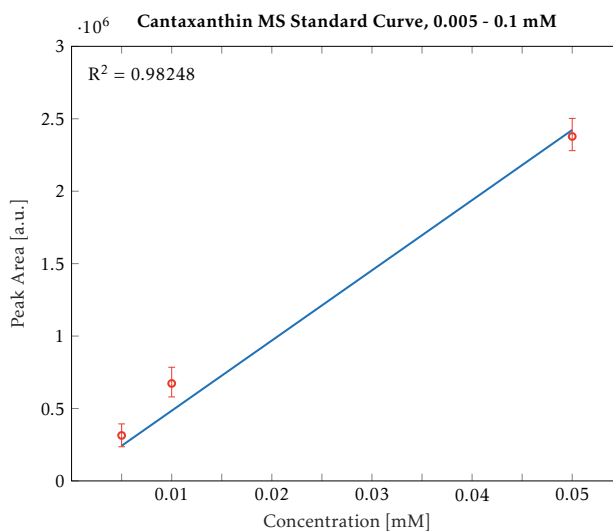


**Figure 3.5:** Linear section of the full MS standard curve of canthaxanthin, with concentrations ranging from 0.005 mM to 0.1 mM. The extracted ion chromatograms at  $m/z$   $565.3900 \pm 0.05$  ( $[M + H]^+$ ) have been integrated manually for each concentration triplicate in triplicates. The area is plotted as a function of the concentration, and linearly fitted, forcing the fit through (0,0), ultimately obtaining the  $R^2$  value of 0.98248. The concentrations have been corrected using the exact concentration calculated from the corresponding PULCON  $^1\text{H}$  NMR spectra.

The complete data set from Figure 3.4 resembles a power function, and can only be poorly linearly fitted ( $R^2 = 0.87674$ ). Thus, the three lowest concentrations (0.005 - 0.1 mM) were chosen for a more suitable and precise concentration range for quantitation, which greatly improved the linear fit ( $R^2 = 0.98248$ ). This means that samples in later experiments were diluted in order to obtain concentrations within this range.

Due to the sticky nature of the compound, the concentrations of the 5 mM stock solutions used for standard curves were verified using a  $^1\text{H}$  NMR PULCON program, with glucose as the concentration reference. See Figure 3.6 for one of the PULCON  $^1\text{H}$  NMR spectra of one of the 5 mM canthaxanthin stock solutions, and Table 3.1 for the calculated concentrations.

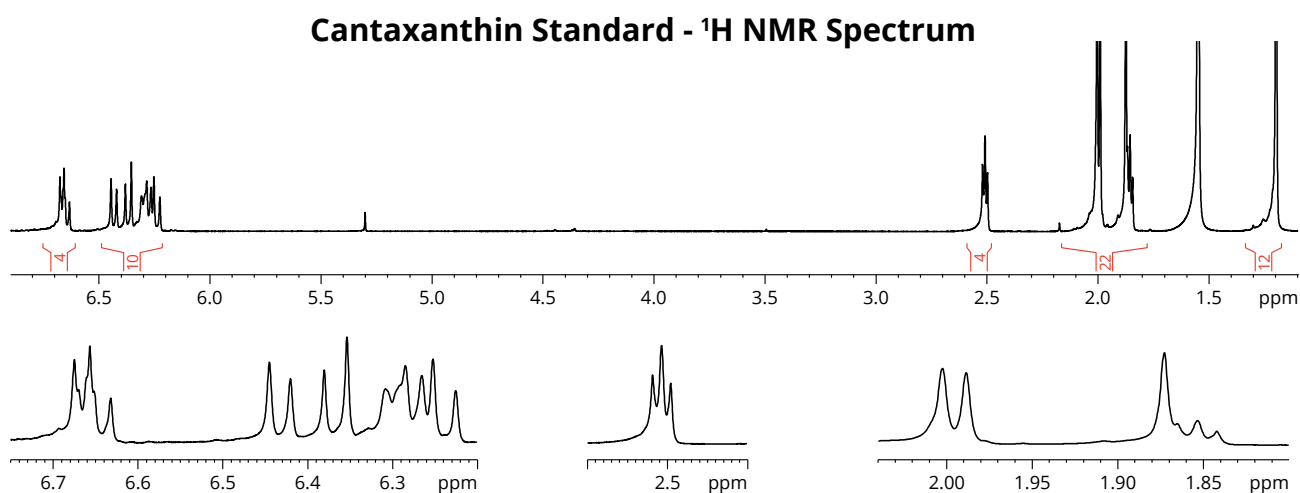


**Figure 3.6:** PULCON  $^1\text{H}$  NMR spectrum of one of the 5 mM analytical canthaxanthin stock solutions, diluted into deuterium-locked chloroform. The inserts show the 52 hydrogens of canthaxanthin, whose abundance was utilized to estimate the exact concentration of the compound in solution. In addition, the peaks fit well with expected shifts.

In Figure 3.6, the chemical shifts of the 52 hydrogens of canthaxanthin can be seen, with the inserts showing their splitting patterns. The chemical shifts correspond well with expected value from the Human Metabolome Database (HMDB ID: HMDB0003154). With shifts of the single hydrogens of the backbone being between 6.24 and 6.65 ppm, shifts of the hydrogens of the methyl groups being below 2.5 ppm, the NMR spectrum of the molecular backbone is consistent with most carotenoids when residing in a complex solution. This fact makes distinction between these similar compounds difficult. However, the chemical shifts of the hydrogen atoms bonded to, or next to, those ring carbons on which substitutions occur, can be distinguished between different carotenoids. In the case of canthaxanthin, the double-bonded oxygen atom in both ring systems gives rise to a significantly higher shift of the hydrogen atom next to the keto group, compared to the same hydrogen in  $\beta$ -carotene. The shifts of these hydrogen atoms are similar to those of the olefinic hydrogens and not to those of the hydrogens in the methyl groups, which would otherwise be the case.

In addition to the PULCON  $^1\text{H}$  NMR spectrum, a  $^{13}\text{C}$  NMR spectrum, identifying carbon atoms, and an HSQC 2D NMR spectrum, identifying directly coupled hydrogen and carbon atoms, were measured for each analytical compound. The  $^1\text{H}$ ,  $^{13}\text{C}$ , and HSQC NMR spectra together with MS measurements, make it possible to detect, and verify, the presence of canthaxanthin in complex biological media. See Figure 3.7 for the  $^{13}\text{C}$  NMR spectrum of the analytical canthaxanthin standard, and Figure 3.8 for the  $^1\text{H}$  coupled  $^{13}\text{C}$  HSQC spectrum of canthaxanthin.

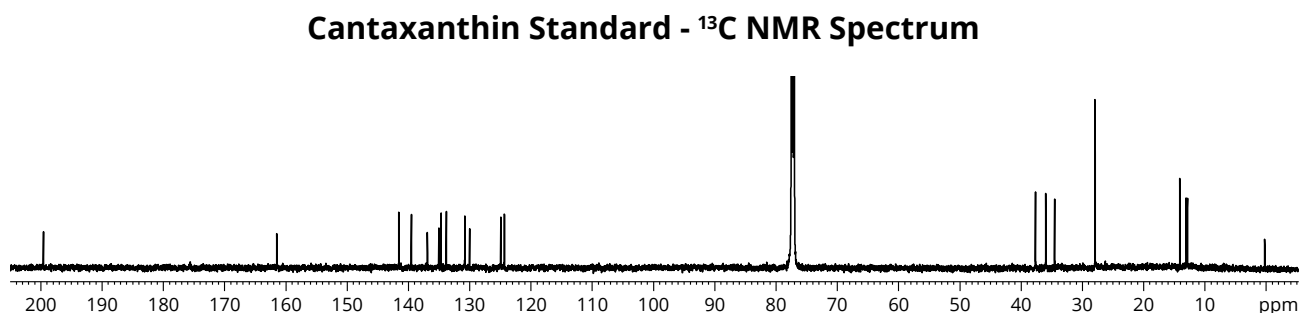


**Figure 3.7:**  $^{13}\text{C}$  NMR spectrum of one of the 5 mM analytical canthaxanthin stock solutions, diluted into deuterium-locked chloroform. The carbon shifts correspond well with expected chemical shifts of canthaxanthin.

In Figure 3.7, the chemical shifts of the 40 carbons of canthaxanthin can be seen. The chemical shifts correspond well with expected values from the LipidBank (ID: VCA0040), but as with the chemical shifts of the hydrogens, it is mainly the substituted carbon atoms, or their neighbouring atoms, that can be used for distinction between the different carotenoids in complex media. The chemical shifts below 40 ppm corresponds to the methyl groups [47], and all shifts between 120 and 140 ppm correspond to the olefinic methine carbon atoms which tend to have chemical shifts above 100-110 ppm due to the electron deficient environment of the double bonds [47]. The peak at 198.7 ppm corresponds to the two carbon atoms of the keto groups [48], in agreement with general shifts of carbonyls above 160 ppm [47].

### Cantaxanthin Standard - HSQC Spectrum

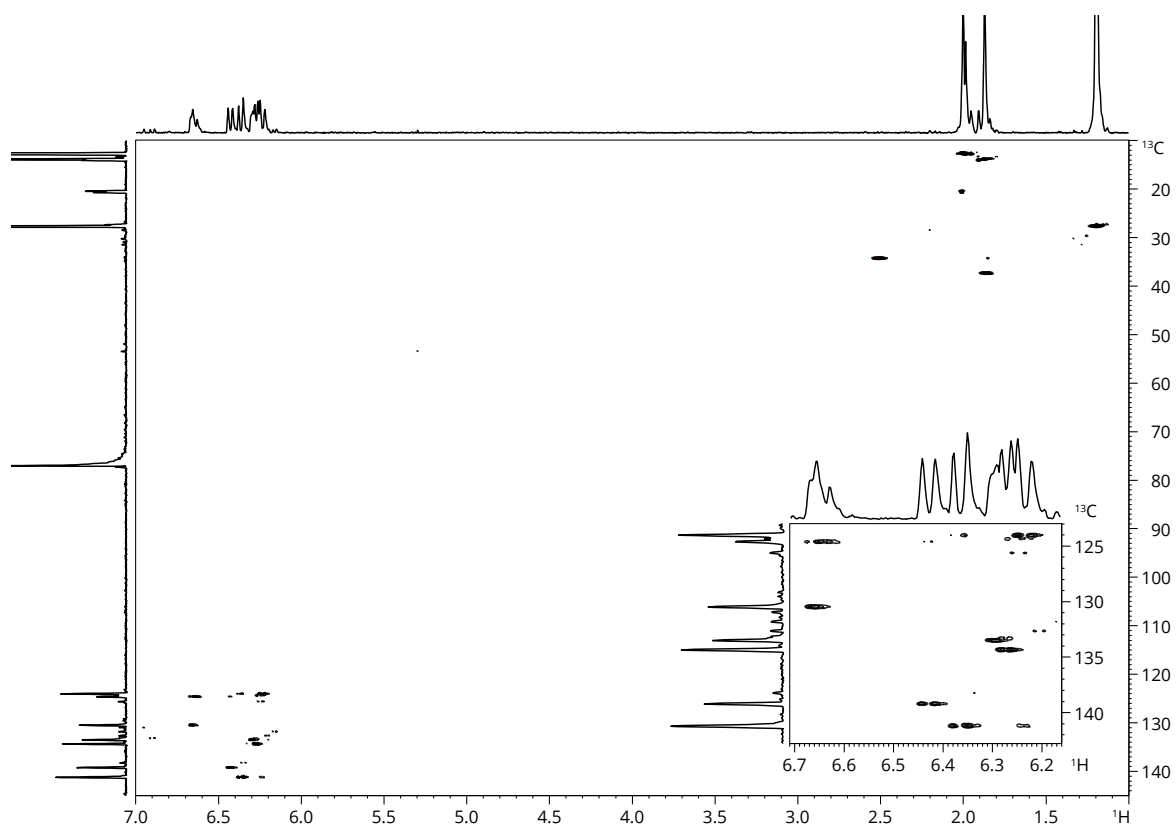


**Figure 3.8:**  $^1\text{H}$  coupled  $^{13}\text{C}$  HSQC 2D NMR spectrum of one of the 5 mM analytical canthaxanthin stock solutions, diluted into deuterium-locked chloroform.

In Figure 3.8, the direct couplings between the hydrogen and carbon atoms of canthaxanthin are visible. The HSQC was mainly measured in order to quickly identify canthaxanthin in a complex carotenoid solution. The NMR experiments, however, in particular the carbon and HSQC measurements, require significantly higher concentrations of the compound, when compared to MS [49].

Lastly, due to the pronounced instability, and tendency toward photodegradation, of carotenoids, one of the analytical standard triplicates were stored at room temperature, in full light, for 48 hours before an additional MS measurement of the solution. See Figure 3.9 for the extracted ion chromatogram of canthaxanthin after 48 hours of storage.

### 3.1. Mass Spectrometry Carotenoid Standard Curves

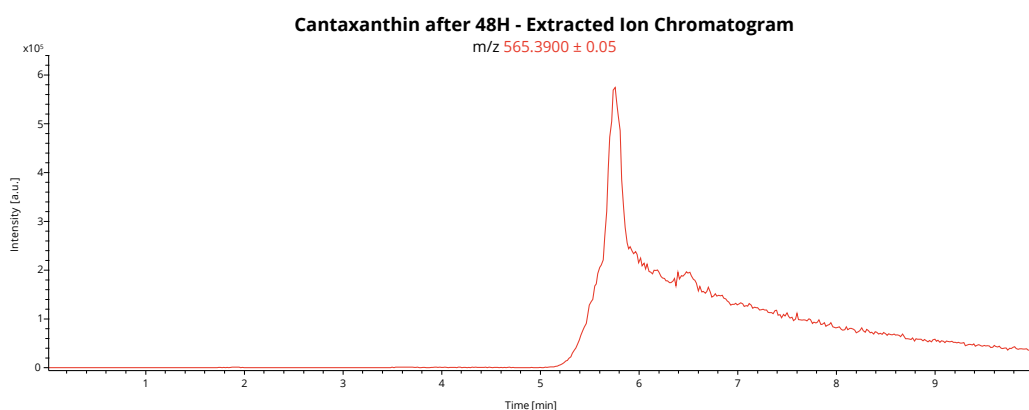


**Figure 3.9:** HPLC/ESI-MS  $m/z$   $565.3900 \pm 0.05$  ( $[M + H]^+$ ) extracted ion chromatogram of one of the 0.5 mM analytical canthaxanthin standard triplicates, which had been stored at room temperature, in full light, and for 48 hours, at positive ionization. The mass chromatogram is measured in chloroform with an isocratic mobile phase of 99 % acetonitrile on the C18 HPLC column. In addition, a 10 minute pre-run with pure acetonitrile, followed by a running time of 10 minutes, was utilized with a 5  $\mu$ L injection volume. The main mass peak of canthaxanthin is identified between 5 and 6 minutes, with one minor isomeric shoulder at 6 minutes.

Some concentration of carotenoids is normally lost during storage, but it appears that high concentrations of canthaxanthin is still present in the sample, even after 48 hours of storage. However, it appears that the amount of isomeric conformers have increased in the solution, see Figure 3.9, and it was therefore decided to complete all MS measurements of all later experiments within 24 hours of extraction, and to store the extracts in cool dark places in between.

#### 3.1.2 Standard Curves and Characterization of Astaxanthin

In addition to the canthaxanthin MS standard curves, an astaxanthin MS standard curve was developed for the quantitation of astaxanthin. It was developed using the extracted ion chromatograms at  $m/z$   $597.3758 \pm 0.05$  ( $[M + H]^+$ ). See Figure 3.10 for the extracted ion chromatogram of the analytical astaxanthin standard.

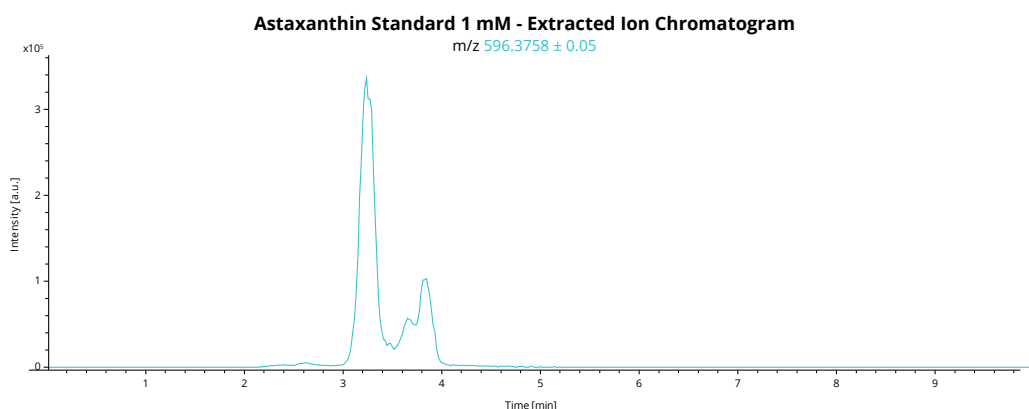


**Figure 3.10:** HPLC/ESI-MS  $m/z$   $597.3758 \pm 0.05$  ( $[M + H]^+$ ) extracted ion chromatogram of one of the 0.5 mM analytical astaxanthin standard triplicates, at positive ionization. The mass chromatogram is measured in chloroform with an isocratic mobile phase of 99 % acetonitrile on the C18 HPLC column. In addition, a 10 minute pre-run with pure acetonitrile, followed by a running time of 10 minutes, was utilized with a 5  $\mu$ L injection volume. The main mass peak of astaxanthin is identified between 3 and 4 minutes, with one minor isomeric shoulder at 4 minutes.

From Figure 3.10, it is visible that astaxanthin has a retention time between 3 and 4 minutes under the current measuring conditions. Furthermore, there is again a shoulder visible after the high intensity mass peak with the same mass profile, suggesting that they both belong to astaxanthin, but with a

differing stereochemistry. Thus both peaks were identified as the main mass peak of astaxanthin, and both were integrated for quantitation. As with canthaxanthin, the analytical standard of astaxanthin should mostly contain molecules in the *trans* configuration, but it appears that some molecules with a *cis* configuration are present, accounting for the shoulder. However, the fact, that there appears to be two shoulders, instead of one, points to the fact, that there might be two *cis* conformations in the standard, with two different positions of the *cis* double bond. It is difficult to elucidate how much of the non-*trans* conformers present in the analytical standards originate from the production methods and how much originates from storage/transportation, as isomerization of carotenoids is known to occur during long-term storage.

From the extracted ion chromatograms, the isotopic distribution of astaxanthin can be visualized, see Figure 3.11. This isotopic abundance can help predict the primary mass detected in further experiments, and can be utilized for a comparison between synthetic and natural astaxanthin.

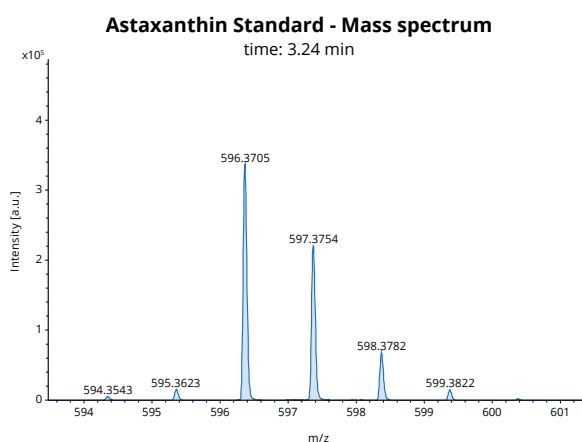


**Figure 3.11:** HPLC/ESI-MS mass spectrum, from the extracted ion chromatogram of the analytical astaxanthin standard in Figure 3.10, at positive ionization,  $m/z$  597.3758  $\pm$  0.05 ( $[M + H]^+$ ), at 3.24 minutes. The isotopic distribution is visible, where the base peak is also the molecular ion.

In Figure 3.11, the isotopic distribution of the astaxanthin is visible with six isotopomers with relatively high mass intensities. In this case, the molecular ion at  $m/z$  596.3706 is the base peak, followed by the  $[M + H]^+$  adduct at  $m/z$  597.3754. The intensity of the signal of the M+1 isotopomer at  $m/z$  566.4073 is approximately 65 % of the base peak, and the M+2 isotopomer is approximately 21 %. From the abundance of  $^{13}\text{C}$  (1.1 %), this will give an estimation of  $59 \pm 2$  carbons in the molecule, which for a larger molecule like canthaxanthin with 40 carbon atoms, is a poor estimation. In addition, the isotopomers indicate charge state of 1, which fits when assuming that  $m/z$  597.3754 is the  $[M + H]^+$  adduct. From this spectrum, it will be assumed that the molecular ion will be the base peak in any further experiments. Lastly, these observations should make it easier to identify the molecule in later experiments.

From integration of the extracted ion chromatograms, the astaxanthin MS standard curves were finally composed. See Figure 3.12 for the full MS standard curve of astaxanthin, which can be used for quantitation of the compound.



In Figure 3.13, the chemical shifts of the 52 hydrogens of astaxanthin can be seen, with the inserts showing their splitting patterns. The chemical shifts correspond well with expected values determined by Yokoyami *et al.* [50]. Again most of the olefinic backbone hydrogens are found to have chemical shifts between 6.20 and 6.70 ppm and the hydrogens of the methyl groups show shifts below 2.5 ppm. However, in the case of astaxanthin, the terminal ring systems are both hydroxylated and contain a keto group each, where canthaxanthin is not hydroxylated, and is only substituted with two keto groups in total. Therefore, the hydrogen atoms located at the same carbon atoms as the hydroxyl groups are of particular interest when distinguishing the two carotenoids from one another. The chemical shift observed at 4.32 ppm belongs to the two equivalent hydrogens located at the carbon atoms harbouring the aforementioned hydroxyl groups of astaxanthin, and the chemical shift at 3.67 ppm belongs to the equivalent hydrogen atoms of the hydroxyl groups themselves.

Sample	Initial [mM]	Exact [mM]
Canthaxanthin	5.00	$6.56 \pm 0.64$
Astaxanthin	0.56	$0.61 \pm 0.05$

**Table 3.1:** The estimated concentration of the canthaxanthin stock solutions and the 0.5 mM astaxanthin solutions used for MS, calculated from the amount directly weighted into the vials, compared to the exact concentration calculated from the PULCON  $^1\text{H}$  NMR measurements. The 0.5 mM astaxanthin solutions were utilized instead of the 5 mM stock solutions in order to obtain the most precise calculation, due to the lower solubility of the compound into chloroform compared to other carotenoids. It is visible that the exact concentrations calculated from the PULCON measurements are slightly higher than the concentrations initially calculated, while still having the same order of magnitude.

In addition to the PULCON  $^1\text{H}$  NMR spectrum, a  $^{13}\text{C}$  NMR spectrum, identifying carbon atoms, and an HSQC 2D NMR spectrum, identifying directly coupled hydrogen and carbon atoms, were measured for each analytical compound. The  $^1\text{H}$ ,  $^{13}\text{C}$ , and HSQC NMR spectra together with MS measurements, would make it possible to detect, and verify the presence of astaxanthin in complex biological media. See Figure 3.14 for the  $^{13}\text{C}$  NMR spectrum of the analytical standard of astaxanthin, and Figure 3.15 for the  $^1\text{H}$  coupled  $^{13}\text{C}$  HSQC spectrum of astaxanthin.

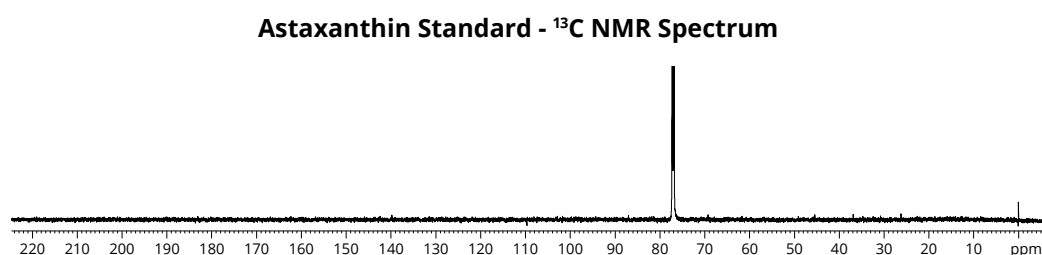


**Figure 3.14:**  $^{13}\text{C}$  NMR spectrum of one of the 5 mM analytical astaxanthin stock solutions, diluted into deuterium-locked chloroform. No carbon shifts of astaxanthin is observed.

The  $^{13}\text{C}$  spectrum in Figure 3.14 does surprisingly not show any carbons at all. The reason behind this is unknown, but it is most likely due to some human error during the setup of either the samples or the measurements, since the  $^{13}\text{C}$  NMR spectrum of astaxanthin has been successfully recorded in the literature [51]. In section 3.1.3, it will furthermore become apparent that there also were some problems with the  $^{13}\text{C}$  spectrum of  $\beta$ -carotene. Nevertheless, the carbon atoms of astaxanthin were related to their directly coupled hydrogens in the HSQC spectrum, which was recorded right after the aforementioned  $^{13}\text{C}$  spectrum of astaxanthin, see Figure 3.15.

## Astaxanthin Standard - HSQC Spectrum

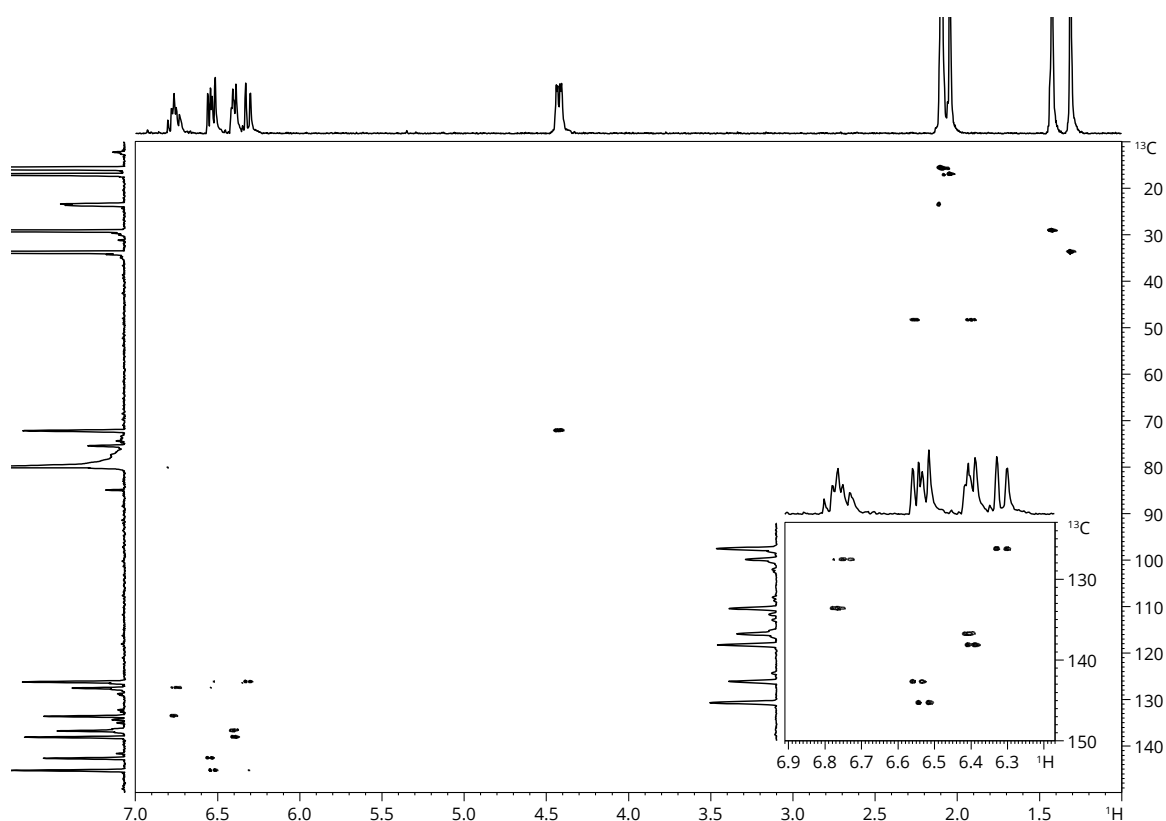


**Figure 3.15:**  $^1\text{H}$  coupled  $^{13}\text{C}$  HSQC 2D NMR spectrum of one of the 5 mM analytical astaxanthin stock solutions, diluted into deuterium-locked chloroform. The direct coupling between the substituted carbon at 72.1 ppm, and the hydrogen at 4.32 ppm would be one of the main couplings used for the distinction between carotenoids.

In Figure 3.15, the direct couplings between the hydrogen and carbon atoms of astaxanthin are visible. The HSQC was mainly measured in order to quickly identify astaxanthin in complex carotenoid solutions, where the direct coupling between the substituted carbon at 72.1 ppm, and the hydrogen at 4.32 ppm would be one of the main identifiers of the molecule.

### 3.1.3 Standard Curves and Characterization of $\beta$ -carotene

It was initially intended to utilize *R. ruber* for the bioproduction of  $\beta$ -carotene, which could be transformed by *R. opacus* into astaxanthin, canthaxanthin, or zeaxanthin. Therefore, as with astaxanthin and canthaxanthin, a  $\beta$ -carotene MS standard curve was prepared in order to quantitate any produced  $\beta$ -carotene. See Figure 3.16 for the extracted ion chromatograms of the analytical  $\beta$ -carotene standard at  $m/z$   $536.4382 \pm 0.05$  ( $[\text{M}]^+$ ) and  $m/z$   $537.4382 \pm 0.05$  ( $[\text{M} + \text{H}]^+$ ).

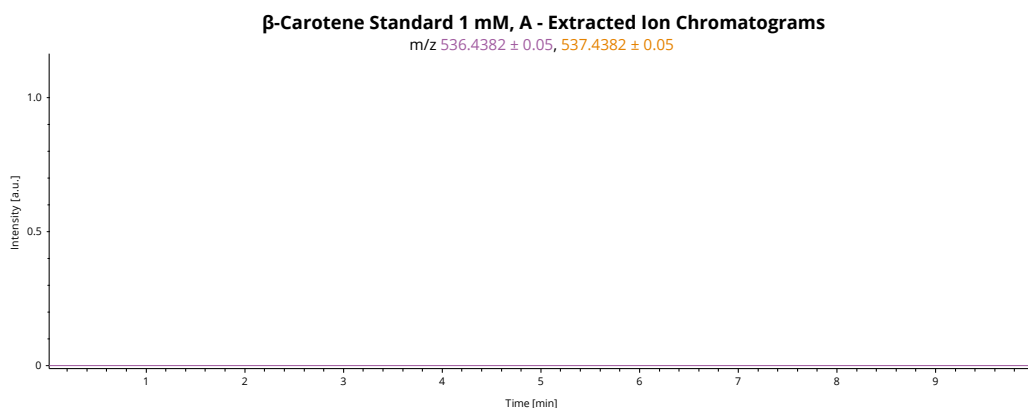


**Figure 3.16:** HPLC/ESI-MS m/z 536.4382  $\pm$  0.05 ( $[M]^+$ ) and m/z 537.4382  $\pm$  0.05 ( $[M+H]^+$ ) extracted ion chromatograms of one of the 1 mM analytical  $\beta$ -carotene standard triplicates, at positive ionization. The mass chromatogram is measured in chloroform with an isocratic mobile phase of 99 % acetonitrile on the C18 HPLC column. In addition, a 5 minute pre-run with pure acetonitrile, followed by a running time of 10 minutes, was utilized with a 5  $\mu$ L injection volume. No  $\beta$ -carotene was found in this solution.

From the full mass chromatogram, both the molecular ion  $[M]^+$  and the hydrogenated adduct  $[M+H]^+$  were extracted. However, none of these masses appear to be present in the solution. This could be the result of a very poor solubility of  $\beta$ -carotene in acetonitrile, a high degree of adsorption onto the C18 HPLC column, or a lacking ability of the compound to vaporize and ionize in the current MS setup. The extracted ion chromatogram in Figure 3.16 was extracted from the first  $\beta$ -carotene measurement that day. The extracted ion chromatogram of the measurement on the second triplicate that followed, shows quite a different story, see Figure 3.17.

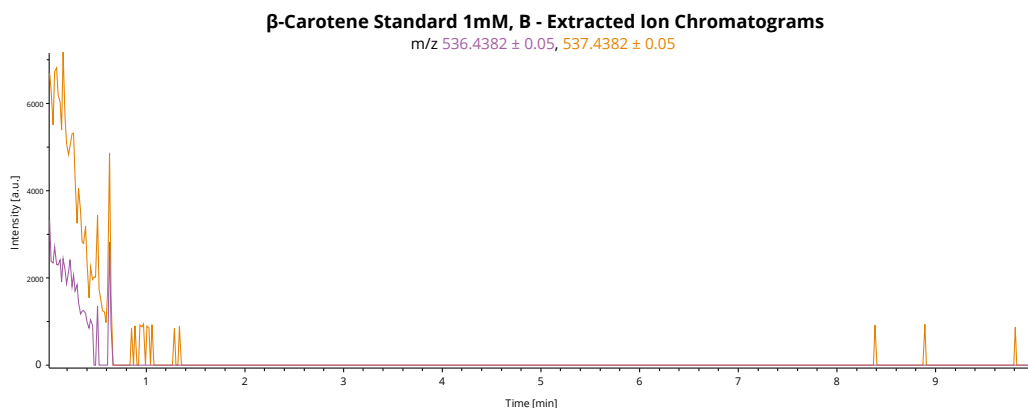


**Figure 3.17:** HPLC/ESI-MS m/z 536.4382  $\pm$  0.05 ( $[M]^+$ ) and m/z 537.4382  $\pm$  0.05 ( $[M+H]^+$ ) extracted ion chromatograms of one of the 1 mM analytical  $\beta$ -carotene standard triplicates, at positive ionization. The mass chromatogram is measured on the second  $\beta$ -carotene solution in chloroform, with an isocratic mobile phase of 99 % acetonitrile on the C18 HPLC column. In addition, a 5 minute pre-run with pure acetonitrile, followed by a running time of 10 minutes, was utilized with a 5  $\mu$ L injection volume.  $\beta$ -carotene appears to be present in this solution.

From Figure 3.17, it can be seen, that both  $\beta$ -carotene adducts are present in the spectrum, but they are suspected to be a part of the "dead volume" of the machine, which is sample volume left over from previous measurements, primarily consisting of sticky molecules residing on the column. The dead volume is normally washed out during the pre-run or very early during the running time, often right before the calibration solution. It was therefore natural to assume that the running time of 10 minutes simply was too short for the observation of  $\beta$ -carotene, and that this compound would appear later than canthaxanthin and astaxanthin if both the running time and pre-run was increased. This tendency was observed randomly throughout the 18 measurements done on different stock solutions

### 3.1. Mass Spectrometry Carotenoid Standard Curves

and dilutions of  $\beta$ -carotene. Furthermore, it was also observed that the Cayman Europe OÜ  $\beta$ -carotene was absent during the first measurement with a running time of 10 minutes. It was then decided to increase the running time to 30 minutes, with a pre-run of 10 minutes, in order to observe  $\beta$ -carotene. See Figure 3.18 for the extracted ion chromatogram of this measurement.

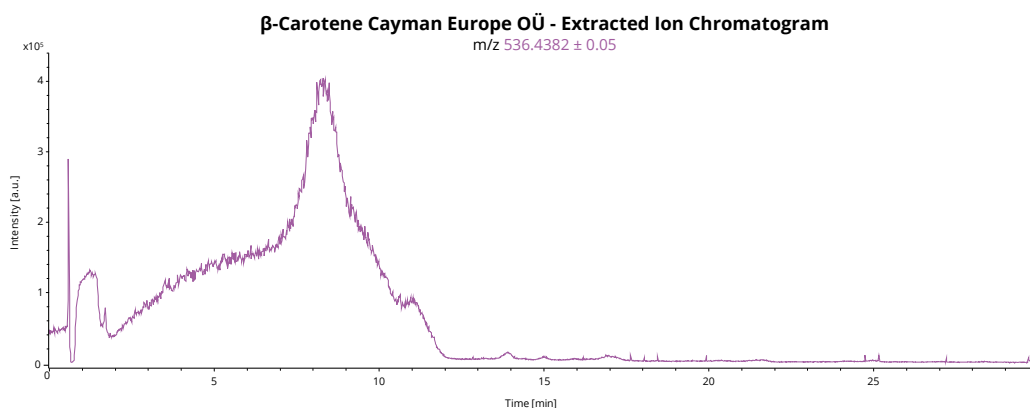


**Figure 3.18:** HPLC/ESI-MS  $m/z$   $536.4382 \pm 0.05$  ( $[M]^+$ ) extracted ion chromatogram of the  $\beta$ -carotene from Cayman Europe OÜ, at positive ionization. The mass chromatogram is measured in chloroform, with an isocratic mobile phase of 99 % acetonitrile on the C18 HPLC column. In addition, a 10 minute pre-run with pure acetonitrile, followed by a running time of 30 minutes, was utilized with a 5  $\mu$ L injection volume. This time  $\beta$ -carotene appear all over the spectrum.

In Figure 3.18,  $\beta$ -carotene appear all over the chromatogram during the first 10 minutes of running time. It is possible that the peculiar and unpredictable behaviour of  $\beta$ -carotene during these MS measurements, is a result of its higher hydrophobicity compared to both canthaxanthin and astaxanthin, causing the compound to be less soluble in acetonitrile and to have an increased tendency to adsorb onto the highly hydrophobic C18 HPLC column. In order to verify this hypothesis, and to combat the problem, a less hydrophobic RP-amide HPLC column, was utilized. A mass chromatogram was recorded on a mixture of all three carotenoids to elucidate whether they could be measured simultaneously using the RP-amide column, see Figure 3.19.

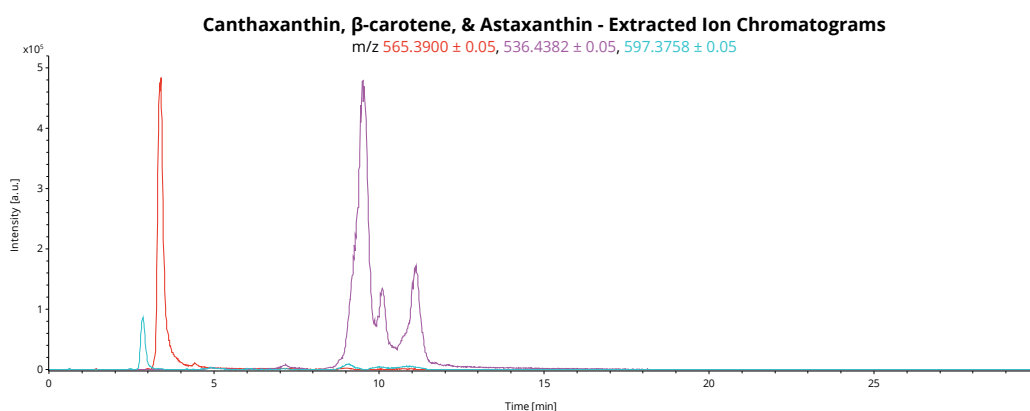


**Figure 3.19:** HPLC/ESI-MS extracted ion chromatogram of a mixture of analytical canthaxanthin ( $565.3900 \pm 0.05$  ( $[M + H]^+$ )), astaxanthin ( $597.3758 \pm 0.05$  ( $[M + H]^+$ )), and  $\beta$ -carotene ( $m/z$   $536.4382 \pm 0.05$  ( $[M]^+$ )), at positive ionization using the RP-amide HPLC column. In addition, a 10 minute pre-run with pure acetonitrile, followed by a running time of 30 minutes, was utilized with a 5  $\mu$ L injection volume. It is visible that astaxanthin has a retention time of 2.9 minutes (green), canthaxanthin at 3.5 minutes (blue), and  $\beta$ -carotene between 9 and 12 minutes (red).

In Figure 3.19, it is clear, that with the RP-amide HPLC column, it is possible to get a mass chromatogram of all three analytical standards simultaneously. Along with canthaxanthin and astaxanthin, the analytical  $\beta$ -carotene standard also appear to contain one or more stereoisomers. When using

reverse-phase HPLC separation, the *trans* configuration of  $\beta$ -carotene will have the shortest retention time, while the *cis* isomers will have different retention times based on the position of the *cis* double bond. The closer to the middle of the molecule the double bond is, the longer retention time is displayed, and thus, the first mass peak corresponds to *trans*  $\beta$ -carotene, while the second and third peaks most likely correspond to the 9-*cis* and 15-*cis* isomers, respectively. These two isomers are most common in the literature. However, it cannot be verified whether isomeric shoulders are results of *cis* isomers or some other conformers. [41, 52–55]

Unfortunately, through multiple tests, it became evident that the MS standard curves made from measurements on the C18 column were not applicable for quantitation on the RP-amide column, and it was therefore decided to continue using the C18 column for further experiments, and to discontinue the  $\beta$ -carotene production by *R. ruber*, focusing solely on the canthaxanthin production by *D. maris* and its extraction. It became evident, however, that if high concentrations of  $\beta$ -carotene were present in one of the samples in later experiments, there is a risk of a continuous flow of  $\beta$ -carotene during MS measurements using the C18 HPLC column, ultimately risking shielding of the canthaxanthin and astaxanthin mass signals, decreasing their actual integrals. The area under the curve of canthaxanthin decreased by 30 % for samples containing high concentrations of  $\beta$ -carotene, compared to equivalent concentrations in samples free of  $\beta$ -carotene. Nevertheless, the problem can now be addressed by checking for the presence of high concentrations of  $\beta$ -carotene on the RP-amide HPLC column, evaluating the extent of the shielding problem on the C18 column.

Fortunately,  $\beta$ -carotene behaves completely normal during NMR measurements when dissolved in chloroform. As with canthaxanthin and astaxanthin, a PULCON  $^1\text{H}$ ,  $^{13}\text{C}$ , and HSQC NMR spectra were measured. See Figure 3.20 for the PULCON  $^1\text{H}$  NMR spectrum of the analytical  $\beta$ -carotene standard.

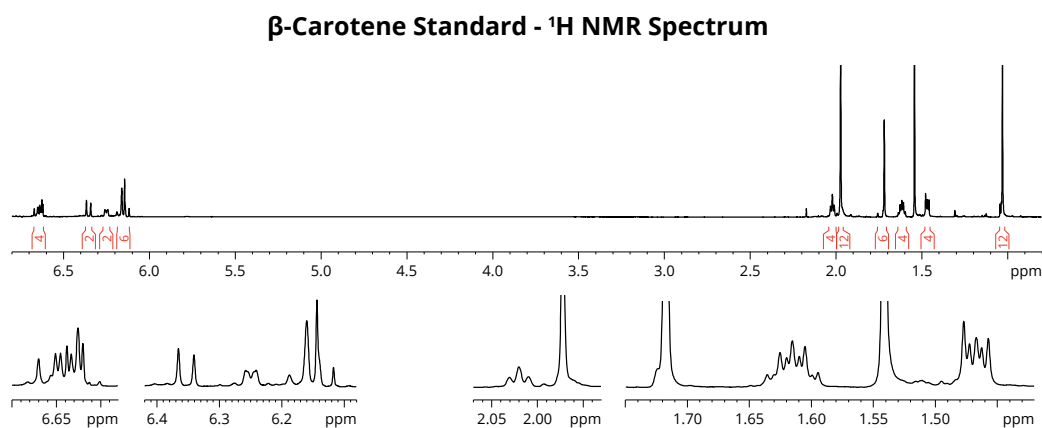


**Figure 3.20:** PULCON  $^1\text{H}$  NMR spectrum of one of the 5 mM analytical  $\beta$ -carotene stock solutions, diluted into deuterium-locked chloroform. The insert shows the 56 hydrogens of  $\beta$ -carotene, whose abundance was utilized to calculate the exact concentration of the compound in the solution. In addition, the peaks fit well with expected shifts.

In Figure 3.20, the chemical shifts of the 56 hydrogens of  $\beta$ -carotene can be seen, with the inserts showing their splitting patterns. The chemical shifts correspond well with expected values determined by G. P. Moss [48]. Again most of the olefinic backbone hydrogens are found to have shifts between 6.20 and 6.70 ppm and the hydrogens of the methyl groups have shifts below 2.5 ppm.

In addition to the PULCON  $^1\text{H}$  NMR spectrum, a  $^{13}\text{C}$  NMR spectrum, identifying carbon atoms, and an HSQC 2D NMR spectrum, identifying directly coupled hydrogen and carbon atoms, were measured. The  $^1\text{H}$ ,  $^{13}\text{C}$ , and HSQC NMR spectra together with MS measurements, make it possible to

detect, and verify the presence of  $\beta$ -carotene in complex biological media in later experiments. See Figure 3.21 for the  $^{13}\text{C}$  NMR spectrum of the analytical  $\beta$ -carotene standard, and Figure 3.22 for the  $^1\text{H}$  coupled  $^{13}\text{C}$  HSQC spectrum of  $\beta$ -carotene.

#### $\beta$ -Carotene Standard - $^{13}\text{C}$ NMR Spectrum

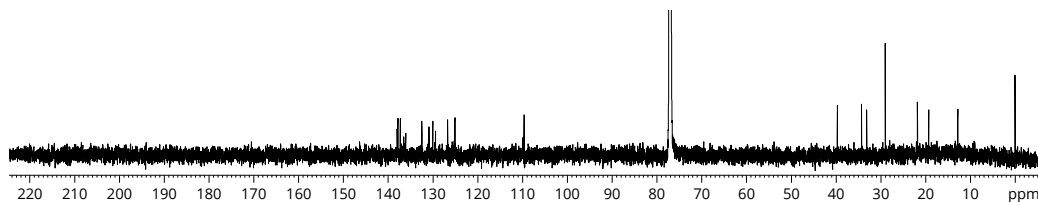


**Figure 3.21:**  $^{13}\text{C}$  NMR spectrum of one of the 5 mM analytical  $\beta$ -carotene stock solutions, diluted into deuterium-locked chloroform. The carbon shifts correspond well with expected chemical shifts of  $\beta$ -carotene.

In Figure 3.21, the chemical shifts of the 40 carbons of  $\beta$ -carotene can be seen. The chemical shifts correspond well with expected values from the LipidBank (ID: VCA0001). The chemical shifts below 40 ppm correspond to the methyl groups [47], where the shifts between 120 and 140 ppm correspond to the olefinic methine carbon atoms. However, for some reason one of the methine carbon atoms is visible at 110 ppm in Figure 3.21 but not in the HSQC spectrum in Figure 3.22.

#### $\beta$ -Carotene Standard - HSQC Spectrum

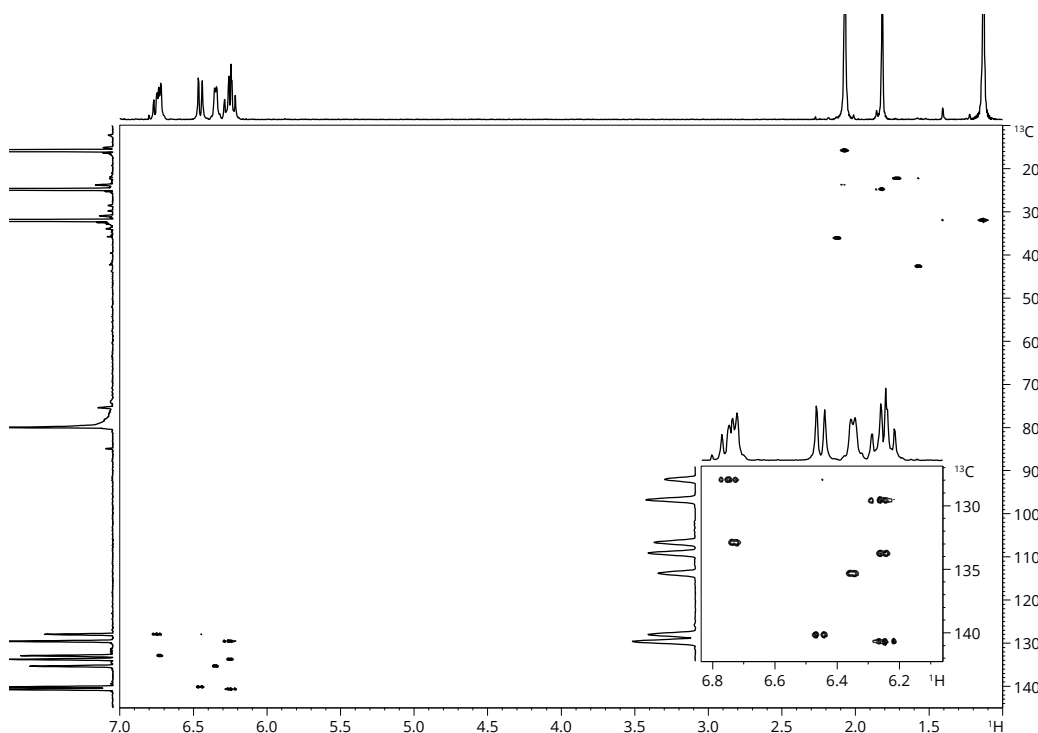


**Figure 3.22:**  $^1\text{H}$  coupled  $^{13}\text{C}$  HSQC 2D NMR spectrum of one of the 5 mM analytical  $\beta$ -carotene stock solutions, diluted into deuterium-locked chloroform.

In Figure 3.22, the direct couplings between the hydrogen and carbon atoms of  $\beta$ -carotene are visible. The HSQC spectrum was mainly measured in order to quickly identify  $\beta$ -carotene in a complex carotenoid solution. The NMR experiments, however, in particular the carbon and HSQC measurements, require significantly higher concentrations of the compound, compared to MS.

As has been established, the NMR spectra of the three carotenoids presented in this chapter are highly similar, with only minor differences in the chemical shifts. Using HSQC NMR for distinguishing the carotenoids from one another while in a complex solution might prove difficult, since only astaxanthin has a distinct direct coupling between a hydrogen and carbon atom which is not shared by either canthaxanthin or  $\beta$ -carotene.  $^{13}\text{C}$  NMR might be more suitable for the task, but, as with HSQC, it requires high concentrations and purity to be effective.

### 3.2 Bioproduction of Canthaxanthin by *D. maris*

For some micro-organisms, visible light is essential for an effective production of carotenoids due to their anti-oxidant and photosynthetic nature, while for others, complete darkness may enhance the production [56]. In order to achieve the most efficient carotenoid production by *D. maris* DSM 43672, and *R. ruber* DSM 43338, it was investigated whether the cells should be grown in full light or in complete darkness. In addition, this experiment served as a baseline for what carotenoids *D. maris* DSM 43672 produced under normal growth conditions. For the full mass chromatogram and extracted ion chromatograms of several carotenoids produced by *D. maris*, in complete darkness and in full light, see Figure 3.23.

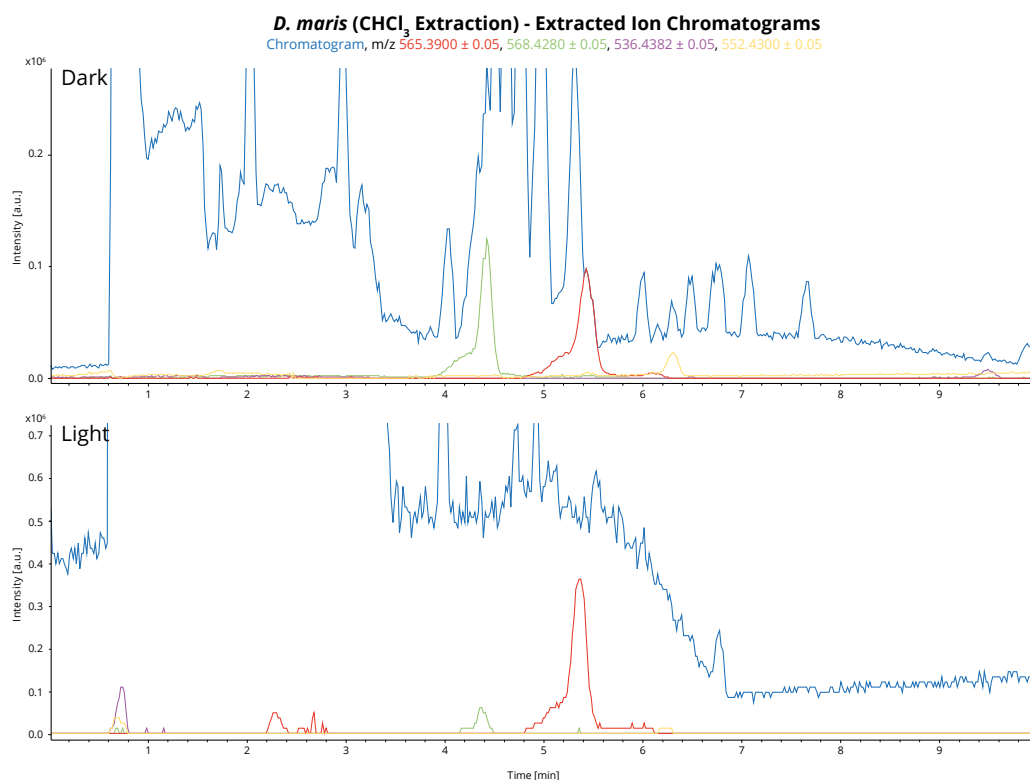


**Figure 3.23:** HPLC/ESI-MS full mass chromatogram and extracted ion chromatograms of the *D. maris* cultures grown in complete darkness and in full light, at positive ionization. The mass chromatogram is measured in chloroform with an isocratic mobile phase of 99 % acetonitrile on the C18 HPLC column. In addition, a 5 minute pre-run with pure acetonitrile, followed by a running time of 10 minutes, was utilized with a 5  $\mu\text{L}$  injection volume. Canthaxanthin at  $m/z$   $565.3900 \pm 0.05$  ( $[\text{M} + \text{H}]^+$ ), zeaxanthin/lutein at  $m/z$   $568.4280 \pm 0.05$  ( $[\text{M}]^+$ ),  $\beta$ -carotene/lycopene at  $m/z$   $536.4382 \pm 0.05$  ( $[\text{M}]^+$ ), and  $\beta$ -cryptoxanthin at  $m/z$   $552.4331 \pm 0.05$  ( $[\text{M}]^+$ ) have been extracted from the full chromatogram (dark blue). The highest concentration of canthaxanthin was produced during growth in full light.

From Figure 3.23, it is evident that *D. maris* DSM 43672 synthesizes different carotenoids under the current growth conditions. Besides canthaxanthin, there is also a carotenoid, which is assumed to be

### 3.2. Bioproduction of Canthaxanthin by *D. maris*

either zeaxanthin or lutein, with an  $m/z$  value of 568.4280. According to Sander *et al.*, when using reverse phase HPLC, zeaxanthin and lutein will have a shorter retention time than canthaxanthin, which fits with the retention time in Figure 3.23 [57]. Furthermore, the compound with an  $m/z$  value of 552.4331 is assumed to be  $\beta$ -cryptoxanthin, which should have a longer retention time than canthaxanthin [57]. These carotenoids were expected to be present in the solution, since they have been shown to be natural secondary metabolites of the *D. maris* species [58–60].

The bioproduction of canthaxanthin was most efficient during incubation in full light, compared to incubation in full darkness. This is in agreement with findings from other *Dietzia* species, whose canthaxanthin production can be notably increased, by white-light irradiation due to enhanced growth and enzymatic stimulation [24]. See Figures 3.24 and 3.25 for the mass spectra extracted from Figures 3.23 at 5.33 minutes for the dark experiment and 5.36 minutes for the light experiment, respectively.

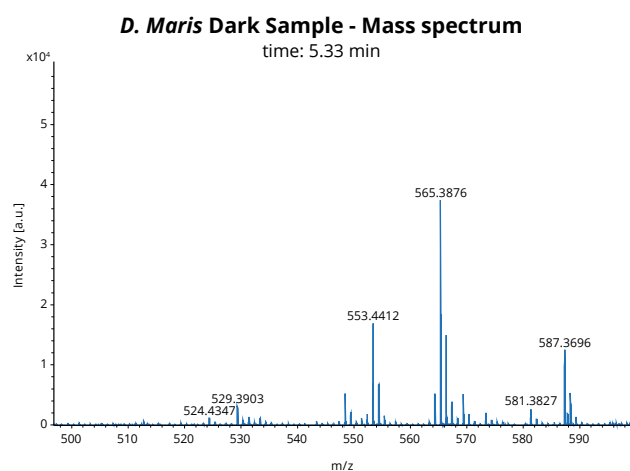


**Figure 3.24:** HPLC/ESI-MS mass spectrum, from the extracted ion chromatogram of the *D. maris* culture grown in complete darkness in Figure 3.23, at positive ionization, at 5.33 minutes. The isotopic distribution is visible for canthaxanthin, where the base peak is the  $[M + H]^+$  adduct at  $m/z$  565.3876. In addition, several other compounds, which appear to be carotenoids, or fractions hereof, are visible.

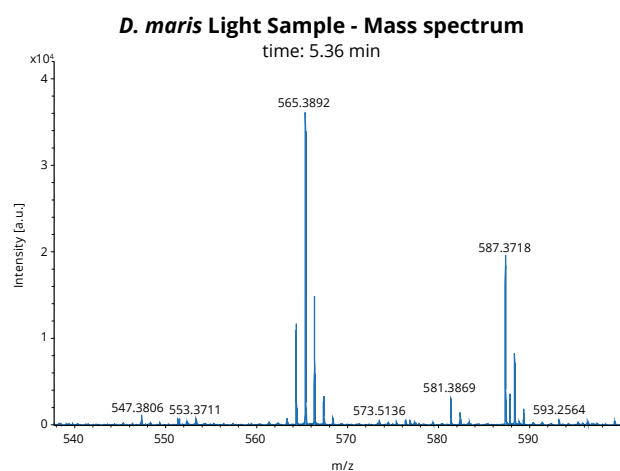


**Figure 3.25:** HPLC/ESI-MS mass spectrum, from the extracted ion chromatogram of the *D. maris* culture grown in full light in Figure 3.23, at positive ionization, at 5.36 minutes. The isotopic distribution is visible for canthaxanthin, where the base peak is the  $[M + H]^+$  adduct at  $m/z$  565.3892. In addition, several other compounds, which appear to be carotenoids, or fractions hereof, are visible.

From Figures 3.24 and 3.25, it can be seen that the  $[M + H]^+$  adduct is clearly the base peak for canthaxanthin in both experiments, which is in agreement with the base peak observed from the analytical standard of the compound. There is however, a significant reduction in the intensity of the molecular ion in both experiments, where the  $[M]^+$  and  $[M + H]^+$  adducts were generally close to one another in intensity in the analytical standards.

It is clear from Figure 3.23, that both samples contain significant quantities of contaminants, which may be left-over cell debris or cellular constituents. As was seen with  $\beta$ -carotene, the contaminants will shield the mass signal of canthaxanthin, decreasing the mass intensity and the actual integrals. Nevertheless, the integrals were measured, see Figure 3.26.

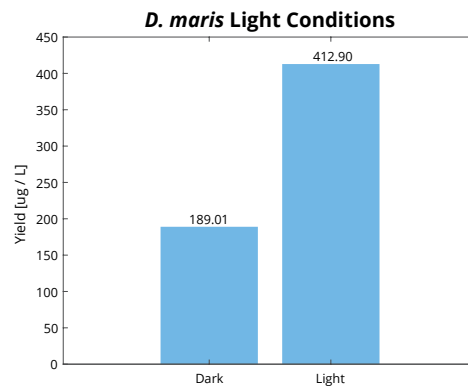


**Figure 3.26:** Bar plot showing the canthaxanthin yield per litre growth medium harvested for extraction using chloroform. The light sample contained 118.4 % more canthaxanthin than the sample grown in complete darkness.

From Figure 3.26, it is evident that the production of canthaxanthin was 118.4 % higher in the culture exposed to light, compared to the culture grown in complete darkness. However, the concentrations calculated from the extracted ion chromatograms should only be regarded as an indicator rather than an exact concentration, due to the high degree of shielding by the sample contaminants in these experiments. Lastly, since canthaxanthin acts as part of the oxidation defence of *D. maris*, it could be argued that exposure to high intensity UV light in short periods of time might enhance the production further [61].

As with *D. maris* DSM 43672, the carotenoid production of *R. ruber* DSM 43338 was determined using an identical experiment. See Figure 3.27 for the full mass chromatogram and extracted ion chromatograms of the concentrated *R. ruber* samples that were shielded from, and exposed to, light.

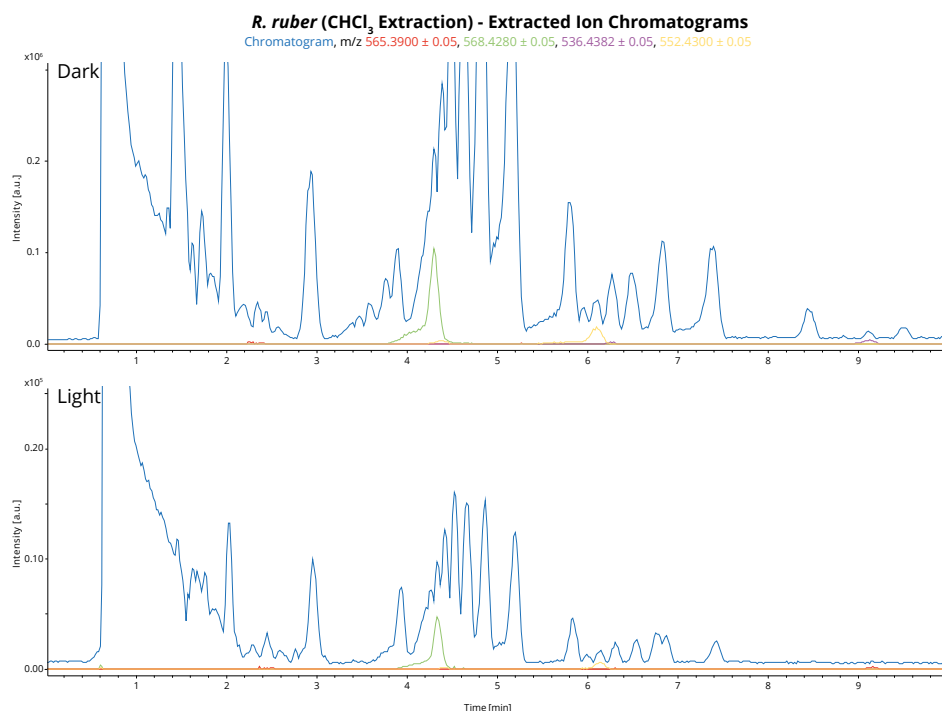


**Figure 3.27:** HPLC/ESI-MS full mass chromatogram and extracted ion chromatograms of the *R. ruber* cultures grown in complete darkness and in full light, at positive ionization. The mass chromatogram is measured in chloroform with an isocratic mobile phase of 99 % acetonitrile on the C18 HPLC column. In addition, a 5 minute pre-run with pure acetonitrile, followed by a running time of 10 minutes, was utilized with a 5 µL injection volume. Canthaxanthin at m/z 565.3900 ± 0.05 ([M + H]<sup>+</sup>), zeaxanthin/lutein at m/z 568.4280 ± 0.05 ([M]<sup>+</sup>), β-carotene/lycopene at m/z 536.4382 ± 0.05 ([M]<sup>+</sup>), and β-cryptoxanthin at m/z 552.4331 ± 0.05 ([M]<sup>+</sup>) have been extracted from the full chromatogram (dark blue).

As is visible in Figure 3.27, the mass chromatogram is similar to that of the *D. maris* bacteria, except for the fact, that there is no traceable amount of canthaxanthin present in any of the two samples. Furthermore, it was not possible to measure any  $\beta$ -carotene/lycopene in this sample either, even though it is the main carotenoid of the *R. ruber* species.

Subsequent to the MS measurements of both organisms, PULCON  $^1\text{H}$ ,  $^{13}\text{C}$ , and HSQC 2D NMR spectra were measured, but due to the high degree of contamination, and the relatively low concentration of canthaxanthin in both *D. maris* experiments, none of the characteristic peaks associated with the hydrogen or carbon atoms of either canthaxanthin or  $\beta$ -carotene were detected. For all NMR spectra, see Appendix A.

### 3.2.1 Carotenoid Extraction using Chloroform

Chloroform is one of the most effective solvents for carotenoid extraction. Therefore, in order to determine the highest carotenoid content available for general extraction, chloroform was initially utilized for later comparison with other extraction methods. As seen in Figure 3.26, canthaxanthin was indeed the primary carotenoid produced by *D. maris* DSM 43672, and the production was most efficient when the cells were incubated in full light. In addition to the optimization of the production parameters, agar plates were utilized for the production of canthaxanthin due to the larger surface area, increasing the exposure of the cells to both light and oxygen. Lastly, it was investigated whether a modified TS medium containing yeast extract with a pH of 5.5 would optimize the production of canthaxanthin any further, as has been reported by Goswami *et al.* and Gharibzahedi *et al.* [23, 24, 26, 40].

The plates were prepared in quadruplicates and extracted with chloroform, whereafter three mass chromatograms were measured for each quadruplicate. See Figure 3.28 for the full mass chromatogram and the extracted ion chromatograms of one of the quadruplicates which were incubated at pH 7.3 for a total of four days.

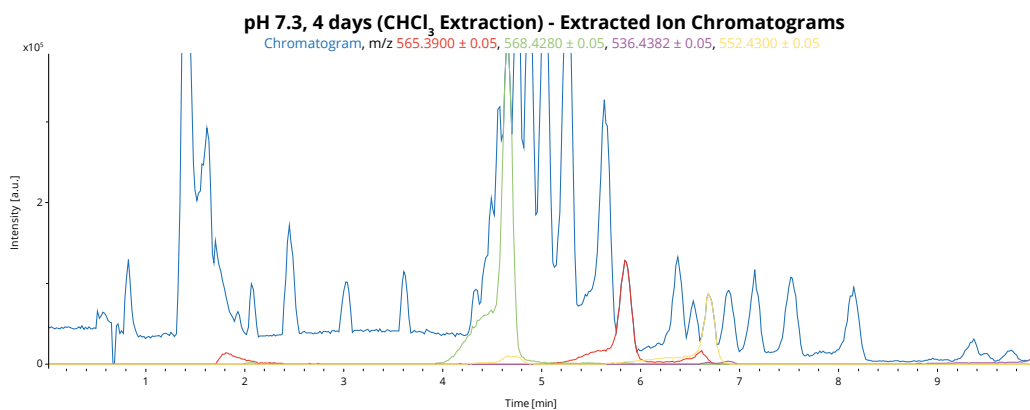


**Figure 3.28:** HPLC/ESI-MS full mass chromatogram and extracted ion chromatograms of one of the *D. maris* agar plates which had been incubated at pH 7.3 for 4 days, at positive ionization. The mass chromatogram is measured in chloroform with an isocratic mobile phase of 99 % acetonitrile on the C18 HPLC column. In addition, a 10 minute pre-run with pure acetonitrile, followed by a running time of 10 minutes, was utilized with a 5  $\mu\text{L}$  injection volume. Canthaxanthin at  $m/z$  565.3900  $\pm$  0.05 ( $[\text{M} + \text{H}]^+$ ), zeaxanthin/lutein at  $m/z$  568.4280  $\pm$  0.05 ( $[\text{M}]^+$ ),  $\beta$ -carotene/lycopene at  $m/z$  536.4382  $\pm$  0.05 ( $[\text{M}]^+$ ), and  $\beta$ -cryptoxanthin at  $m/z$  552.4331  $\pm$  0.05 ( $[\text{M}]^+$ ) have been extracted from the full chromatogram (dark blue).

In Figure 3.28, it is evident that both canthaxanthin at  $m/z$  565.3900  $\pm$  0.05, zeaxanthin/lutein at  $m/z$  568.4280  $\pm$  0.05, and  $\beta$ -cryptoxanthin at  $m/z$  552.4331  $\pm$  0.05 are produced by the bacterium during these incubation conditions. This was observed within all of the quadruplicates, whose mass chromatograms can be found in Appendix B. In addition, it is observed that no contaminations seem

to shield the mass signal of all carotenoids extracted from the full chromatogram.

It was hypothesized that a higher incubation time, along with a transfer to fresh agar plates, might increase the canthaxanthin yield even further. It has been shown that carbon and nitrogen starvation can impede carotenoid biosynthesis [24], and since it is suggested that the accumulation of canthaxanthin has no inhibitory effect on the cellular growth of the organism [23], it was decided to transfer the bacterial cells after 4 days of incubation onto new agar plates in order to maximize the canthaxanthin yield. See Figure 3.29 for the full mass chromatogram and the extracted ion chromatograms of one of the quadruplicates which were incubated at pH 7.3 for a total of eight days.

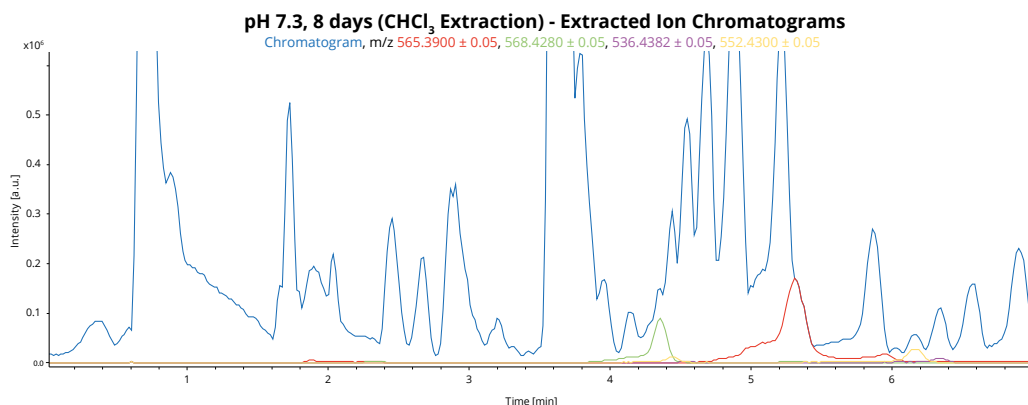


**Figure 3.29:** HPLC/ESI-MS full mass chromatogram and extracted ion chromatograms of one of the *D. maris* agar plates which had been incubated at pH 7.3 for 8 days, at positive ionization. The mass chromatogram is measured in chloroform with an isocratic mobile phase of 99 % acetonitrile on the C18 HPLC column. In addition, a 10 minute pre-run with pure acetonitrile, followed by a running time of 10 minutes, was utilized with a 5 µL injection volume. Canthaxanthin at  $m/z\ 565.3900 \pm 0.05$  ( $[M + H]^+$ ), zeaxanthin/lutein at  $m/z\ 568.4280 \pm 0.05$  ( $[M]^+$ ),  $\beta$ -carotene/lycopene at  $m/z\ 536.4382 \pm 0.05$  ( $[M]^+$ ), and  $\beta$ -cryptoxanthin at  $m/z\ 552.4300 \pm 0.05$  ( $[M]^+$ ) have been extracted from the full chromatogram (dark blue).

From Figure 3.29, it is again evident that both canthaxanthin at  $m/z\ 565.3900 \pm 0.05$ , zeaxanthin/lutein at  $m/z\ 568.4280 \pm 0.05$ , and  $\beta$ -cryptoxanthin at  $m/z\ 552.4331 \pm 0.05$  are produced by the bacterium during these incubation conditions. This was observed within all of the quadruplicates, whose mass chromatograms can be found in Appendix B. Furthermore, it became evident that the canthaxanthin yield increased after eight days of incubation, which can be attributed to the increase in biomass. Lastly, some shielding of the canthaxanthin signal may have had occurred, but not to the same extent as in the light condition experiments in Figure 3.23. In order to further increase the canthaxanthin yield, new pH 7.3 agar plates were incubated for four days, whereafter the biomass was transferred to fresh pH 5.5 plates which contained yeast extract. It was also attempted to use pH 5.5 plates for the first four days of incubation, but the cells did not grow well, if at all, under these conditions. Nevertheless, when incubated on pH 5.5 agar plates, subsequent to growth on pH 7.3 plates, the canthaxanthin yield increased even further compared to when only pH 7.3 plates were used. See Figure 3.30 for the full mass chromatogram and the extracted ion chromatograms of one of the quadruplicates which were incubated at pH 5.5 for a total of eight days.

### 3.2. Bioproduction of Canthaxanthin by *D. maris*

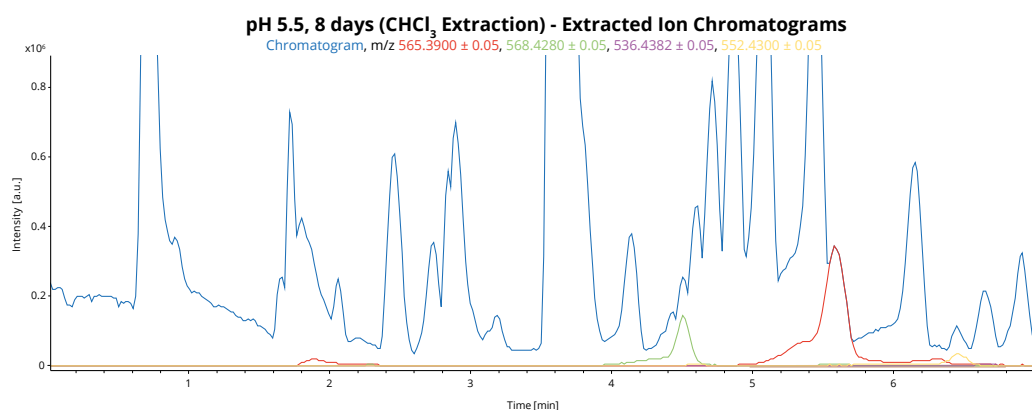


**Figure 3.30:** HPLC/ESI-MS full mass chromatogram and extracted ion chromatograms of one of the *D. maris* agar plates which had been incubated at pH 5.5 for 8 days, at positive ionization. The mass chromatogram is measured in chloroform with an isocratic mobile phase of 99 % acetonitrile on the C18 HPLC column. In addition, a 10 minute pre-run with pure acetonitrile, followed by a running time of 10 minutes, was utilized with a 5  $\mu$ L injection volume. Canthaxanthin at  $m/z$   $565.3900 \pm 0.05$  ( $[M+H]^+$ ), zeaxanthin/lutein at  $m/z$   $568.4280 \pm 0.05$  ( $[M]^+$ ),  $\beta$ -carotene/lycopene at  $m/z$   $536.4382 \pm 0.05$  ( $[M]^+$ ), and  $\beta$ -cryptoxanthin at  $m/z$   $552.4300 \pm 0.05$  ( $[M]^+$ ) have been extracted from the full chromatogram (dark blue).

From Figure 3.30, it is again evident that both canthaxanthin at  $m/z$   $565.3900 \pm 0.05$ , zeaxanthin/lutein at  $m/z$   $568.4280 \pm 0.05$ , and  $\beta$ -cryptoxanthin at  $m/z$   $552.4331 \pm 0.05$  are produced by the bacterium during these incubation conditions. This was observed within all of the quadruplicates, whose mass chromatograms can be found in Appendix B. In addition, it can be seen that the canthaxanthin yield increased even further, but that the zeaxanthin/lutein yield remained relatively low. This was the case for both experimenters with longer incubation times, compared to the four day incubation, which could suggest that zeaxanthin/lutein might act as a precursor in the biosynthesis of canthaxanthin by *D. maris*. Furthermore, it has been shown in earlier work with the *R. opacus* bacterium, that the accumulation of hydroxylated species over time can result in their spontaneous oxidization into quinone derivatives [62, 63], meaning that the increase in canthaxanthin might be a result of a spontaneous process rather than an enzymatic one.

For all three experiments, the extracted ion chromatograms were integrated and averaged for all the triplicate measurements of the quadruplicates. Subsequently, the concentration was related to the biomass, which was harvested for extraction, in order to make the experiments comparable, see Figure 3.31.

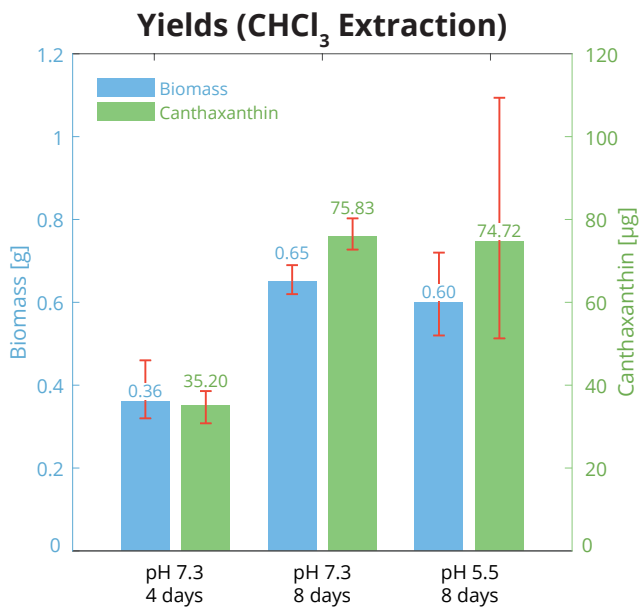


**Figure 3.31:** Bar plot showing the average biomass and canthaxanthin yields for all three experiments extracted with chloroform. It is evident that both yields increase with the incubation time. In addition, the margin of error of the 8 day experiment at pH 5.5 is significantly larger than the ones of the other experiments.

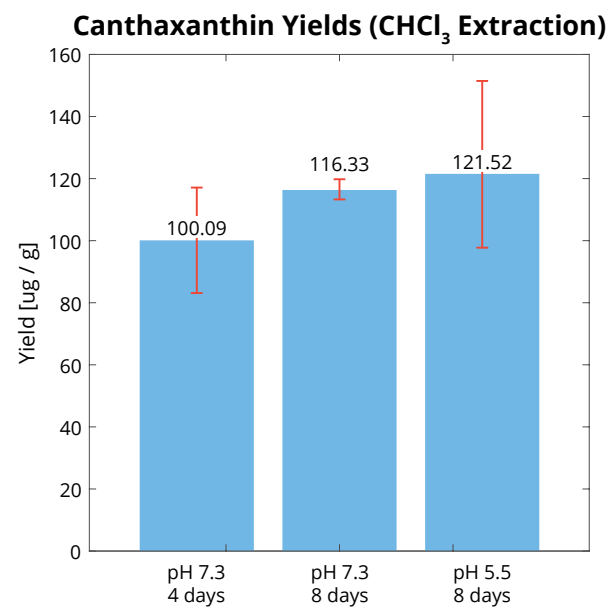


**Figure 3.32:** Bar plot showing the average canthaxanthin yield per gram biomass harvested for extraction for all three experiments extracted with chloroform.

From Figures 3.31 and 3.32, it is evident that, as the biomass increases, the canthaxanthin concentration increases as well. As the biomass and canthaxanthin yield nearly doubles when the incubation time increases until 8 days in total, there is only a marginal difference between the pH 7.3 agar plates and the pH 5.5 plates containing yeast extract. But the margin of error of the pH 5.5 experiment is significantly higher than the two other experiments, describing a large fluctuation in the canthaxanthin yield for identical extractions. This is contrary to the findings of Goswami *et al.* who found a significantly higher canthaxanthin concentration in *D. maris* cultures grown at pH 5.5, compared to all other pH values [23, 24, 40]. When visualized as canthaxanthin per gram bacteria, the canthaxanthin yield of the 4 day experiment is 100.09 µg/g, where it was 116.33 µg/g for the 8 day experiment at pH 7.3, and 121.52 µg/g for the 8 day experiment at pH 5.5. Thus, since there is only a small increase in the yield per gram of biomass with a total incubation time of eight days, it would appear that it would be more efficient to extract every fourth day of growth. However, this is a consequence of the simultaneous doubling of both the biomass, incubation time and canthaxanthin yield, and it can be argued that it would be more cost-effective to extract once every eight days. This process could be optimized if growing the cells on the same agar plates for eight days of incubation would lead to an equally high yield, or if the *D. maris* cells would experience carbon and nitrogen starvation which is related to an impeded canthaxanthin production.

Furthermore, the yields per gram biomass are in the same order of magnitude, compared to what is achieved in the literature by different organisms. Asker *et al.* obtained yields of 691 µg/g using *Haloflex alexandrinus* [22]. Khodaiyan *et al.* were able to get maximum yields of 683 µg/g from *Dietzia natronolimnaea* [36], and Miguel *et al.* extracted a total carotenoid yield of 227 µg/g from *Gordonia jacobaea* [64]. However, one study by Goswami *et al.* reported yields as high as 16,509 µg/g, by optimizing the growth parameters [23].

### 3.2.2 Carotenoid Extraction using Edible Sunflower Oil

Many carotenoids are relatively soluble in edible oil products, increasing the scientific interest of these liquids as extraction solvents, serving as an eco-friendly, cheap, and non-toxic alternative to organic solvents. In addition, long-term storage of natural carotenoids are generally challenging due to the low stability of the molecules, but edible oil might prove to retard carotenoid oxidation by excluding oxygen, and to some extent light, from the solution. [13, 30]

Before any experiments involving the carotenoid extraction using edible organic sunflower oil from Urtekram, a combination of canthaxanthin, astaxanthin, and  $\beta$ -carotene dissolved into sunflower oil, was tested on the MS setup in order to determine dilution factors and any mass shielding effects. The enriched oil was diluted into chloroform (1:10), whereafter the sample was evaporated and separated by the C18 HPLC column. See Figure 3.33 for the extracted ion chromatograms of the sunflower oil enriched with canthaxanthin, astaxanthin and  $\beta$ -carotene.

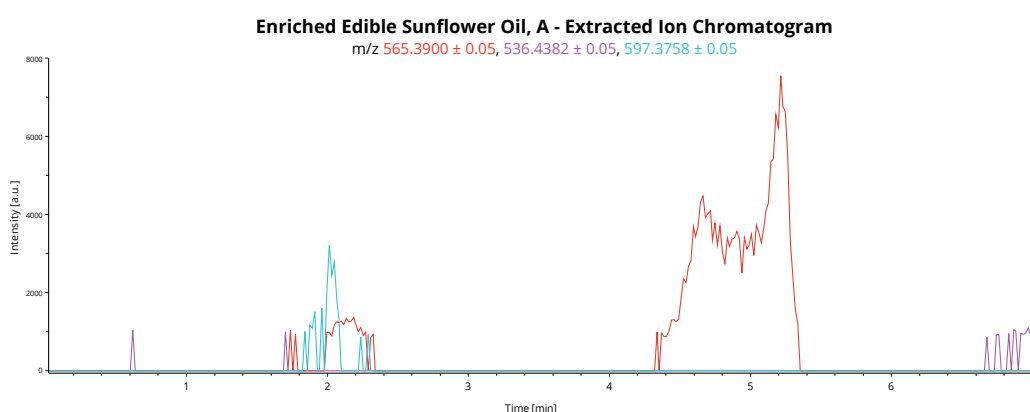


**Figure 3.33:** HPLC/ESI-MS extracted ion chromatograms of sunflower oil enriched with canthaxanthin, astaxanthin and  $\beta$ -carotene, at positive ionization. The mass chromatogram is measured in chloroform (1:10) with an isocratic mobile phase of 99 % acetonitrile on the C18 HPLC column. In addition, a 10 minute pre-run with pure acetonitrile, followed by a running time of 10 minutes, was utilized with a 15  $\mu$ L injection volume and a post-run sequence with pure isopropanol of 10 minutes. Canthaxanthin at  $m/z$  565.3900  $\pm$  0.05 ( $[M + H]^+$ ),  $\beta$ -carotene/lycopene at  $m/z$  536.4382  $\pm$  0.05 ( $[M]^+$ ), and astaxanthin at  $m/z$  597.3776  $\pm$  0.05 ( $[M + H]^+$ ) have been extracted from the full chromatogram.

It is evident from Figure 3.33, that both canthaxanthin and astaxanthin dissolved into oil, have expected retention times, where  $\beta$ -carotene, as usual, is unpredictable. It is, however, evident that the concentrations of both canthaxanthin and astaxanthin are very low in this diluted solution. The oil suspension was prepared with carotenoid concentrations comparable with the chloroform-extracted samples. However, when diluted further into chloroform, the carotenoids in the oil suspension became less detectable, making quantitation difficult, further complicated by the fact that the concentration of oil in the MS sample cannot be increased. In addition, the mass signals of the sunflower oil are highly dominant throughout the entire chromatogram, decreasing the mass signal of the carotenoids even further.

Due to the successful separation using the RP-amide HPLC column in Figure 3.19, efforts were made to elucidate whether this column was more fit for the separation of samples containing oil. See Figure 3.34 for the extracted ion chromatograms of the sunflower oil enriched with canthaxanthin, astaxanthin and  $\beta$ -carotene, separated using the RP-amide HPLC column.

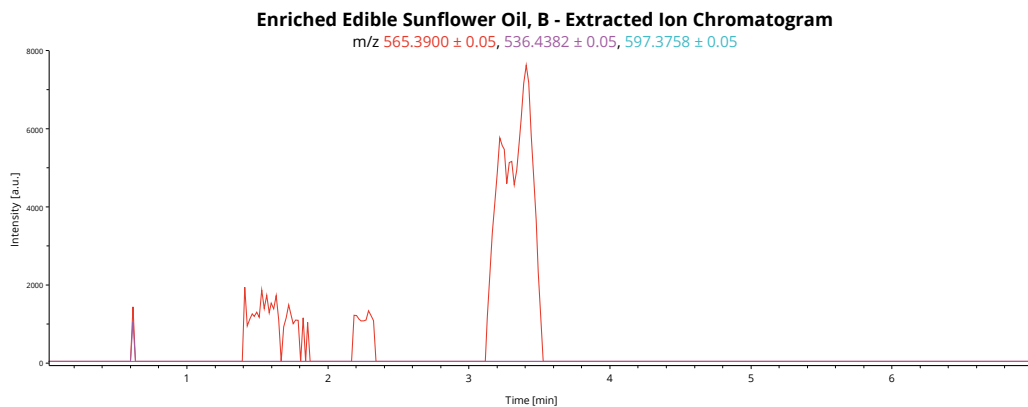


**Figure 3.34:** HPLC/ESI-MS extracted ion chromatogram of sunflower oil enriched with canthaxanthin, astaxanthin and  $\beta$ -carotene, at positive ionization. The mass chromatogram is measured in chloroform (1:10) with an isocratic mobile phase of 99 % acetonitrile on the RP-amide HPLC column. In addition, a 10 minute pre-run with pure acetonitrile, followed by a running time of 10 minutes, was utilized with a 15  $\mu$ L injection volume and a post-run sequence with pure isopropanol at 10 minutes. Canthaxanthin at  $m/z$  565.3900  $\pm$  0.05 ( $[M + H]^+$ ),  $\beta$ -carotene/lycopene at  $m/z$  536.4382  $\pm$  0.05 ( $[M]^+$ ), and astaxanthin at  $m/z$  597.3758  $\pm$  0.05 ( $[M + H]^+$ ) have been extracted from the full chromatogram.

From Figure 3.34, it can be seen that the carotenoids are even less detectable when using the RP-amide HPLC column compared to the C18 HPLC column in Figure 3.33. It became evident in earlier experiments with the RP-amide HPLC column, that the integral decreased for canthaxanthin when using this column, compared to the C18 HPLC column, explaining why the carotenoids are even less detectable on the RP-amide HPLC column in these low concentrations.

In order to increase the carotenoid concentration in the edible oil after extraction, another extraction setup was attempted. It was hypothesized that a water-oil phase separation could increase the carotenoid content of the oil over time, by the bacteria continuously releasing carotenoids into the oil. Like *Rhodococcus*, the bacterial envelope of *D. maris* is surrounded by an outer lipid layer composed primarily of mycolic acids, which act as an outer hydrophobic barrier. As a result, the bacteria are well adapted to survival in hydrophobic, and some times toxic, solvents and to degrade and metabolize hydrophobic substrates. Therefore, it was hypothesized that in a mineral medium-sunflower oil solution, the bacteria might form micro-emulsions at the interface, and utilize the lipids of the oil as the primary carbon source, subsequently secreting carotenoids into the oil phase over time. This phenomenon was reported by Haas *et al.*, who used a mineral oil medium with a higher density than water [65]. However, due to the lower density of the sunflower oil, compared to water, the result was that the edible oil layer impeded the oxygen flow of the culture, ultimately choking the aerobic bacterium although the cultures were regularly shaken. Therefore, it was decided to focus on direct extraction with oil, where the bacterium has been grown under normal aerobic conditions in full light. One agar plate was grown with *D. maris* cells for four days at pH 7.3, and the extraction of the carotenoids were attempted with the edible sunflower oil. Plant and microbial material is often grounded and freeze-dried before being extracted directly with edible oil and exposed to a series of short high-intensity ultrasonic waves [13]. Therefore, it was decided to transfer the bacterial cells directly into 5 mL sunflower oil, and ultra-sonicate the sample once at 148 W (37 % of 400 W) for a total of 2 minutes with an alternating sequence of 15 seconds of sonication and 30 second breaks. The enriched oil was then centrifuged and filtrated through a 0.2  $\mu$ m hydrophobic filter. The enriched oil was diluted into chloroform, and the carotenoids were detected using the calibrated MS setup and the C18 HPLC column. See Figure 3.35 for the extracted ion chromatograms of the oil-extracted sample.

## 3.2. Bioproduction of Canthaxanthin by *D. maris*

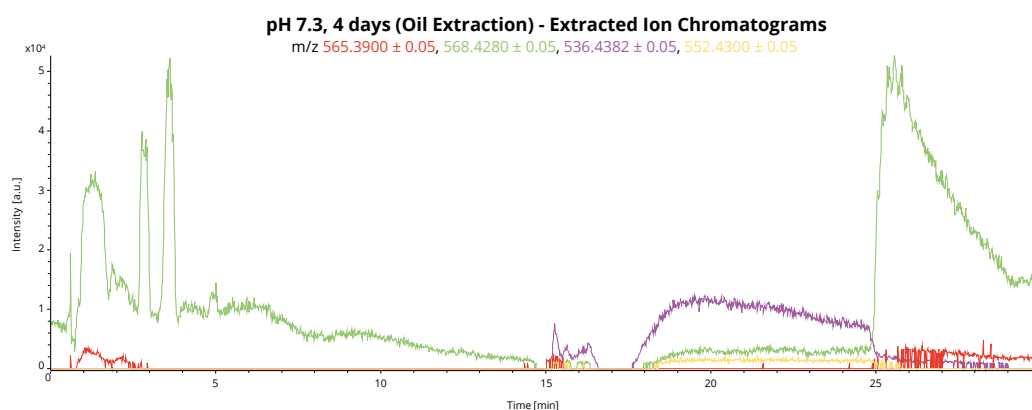


**Figure 3.35:** HPLC/ESI-MS extracted ion chromatograms of the oil-extracted sample, at positive ionization. The mass chromatogram is measured in chloroform (1:10) with an isocratic mobile phase of 99 % acetonitrile on the C18 HPLC column. In addition, a 10 minute pre-run with pure acetonitrile, followed by a running time of 30 minutes, was utilized with a 15  $\mu$ L injection volume and a post-run sequence with pure isopropanol of 10 minutes. Canthaxanthin at  $m/z$  565.3900  $\pm$  0.05 ( $[M + H]^+$ ), zeaxanthin/lutein at  $m/z$  568.4280  $\pm$  0.05,  $\beta$ -carotene/lycopene at  $m/z$  536.4382  $\pm$  0.05 ( $[M]^+$ ), and  $\beta$ -cryptoxanthin at  $m/z$  552.4300  $\pm$  0.05 ( $[M + H]^+$ ) have been extracted from the full chromatogram.

From Figure 3.35 it can be seen that all detected carotenoids tend to continuously separate from the HPLC column, resulting in a continuous flow of mass. It was seen in Figure 3.33 that canthaxanthin and astaxanthin, despite being in low concentrations and suspended in oil, had the expected retention times. This is not the case in Figure 3.35, which contained the same concentration of oil and was extracted from agar plates with original concentrations of carotenoids comparable with the ones in Figure 3.33. Therefore, it can be argued that the extracted masses in Figure 3.35 do not belong to the particular carotenoids. Furthermore, if there are no carotenoids related to the *D. maris* bacterium present in the extract, it can be hypothesized that the result might be a consequence of the high viscosity of the oil which can retard, or slow down, diffusion of carotenoids into the oil, decreasing the extraction yield significantly [13, 66]. In order to verify, that extraction and measurements of oil-extracted samples might be even more challenging than first anticipated, the experiment was repeated. This time however, it was hypothesized, that a phase separation would improve the extraction result during sonication, and thus, water was added to the bacteria-in-oil solution. This led to the surprising observation, that the water began to change into a bright red colour, while the oil remained unchanged. This was unexpected due to the fact that canthaxanthin is completely insoluble in water, where it is soluble in sunflower oil [67, 68]. Thus, it was speculated, that oil might not be the ideal extraction solvent for this project. This is in spite of the fact that using vegetable oils for the extraction of carotenes from especially plants and fish waste is a growing trend in the literature [13, 69, 70].

### 3.2.3 Carotenoid Extraction using Water and Sonication

Subsequent to the red water discovery, the extraction using edible oil was abandoned and new experiments were devised to explore this water phenomenon further, and to see if it was possible to reproduce the effect in quadruplicates. Thus, *D. maris* cells were incubated on eight TS agar plates at pH 7.3, for four days, where the biomasses of four of the plates were transferred onto new agar plates at pH 5.5 and incubated for another four days. For the extraction, the complete biomasses of the plates were transferred to 5 mL milli-Q water which was ultra-sonicated for 5 minutes twice, as well as centrifuged and filtrated in order to remove cell debris. See Figure 3.36 for the full mass chromatogram and the extracted ion chromatograms of one of the water-extracted quadruplicates which was incubated at pH 5.5 for eight days in total. All other mass chromatograms

of the water-extracted samples can be seen in Appendix B.

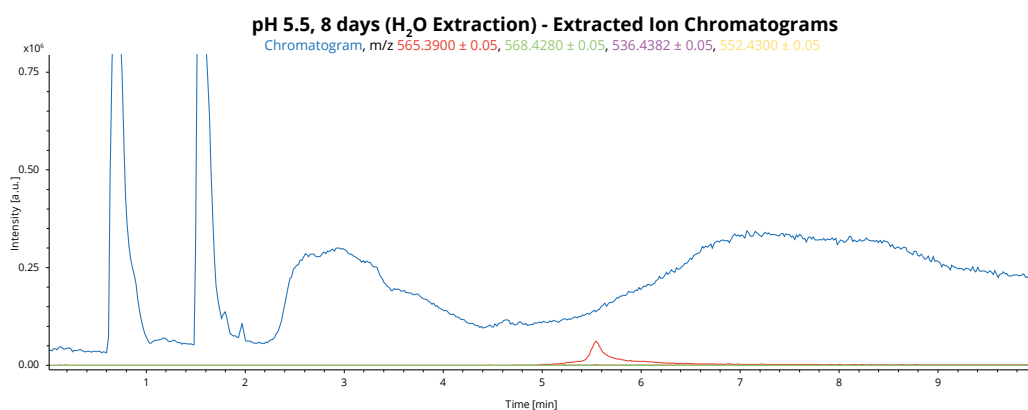


**Figure 3.36:** HPLC/ESI-MS full mass chromatogram and extracted ion chromatograms of one of the water-extracted quadruplicates which had been incubated for 8 days at pH 5.5, at positive ionization. The mass chromatogram is measured in methanol (1:1) with an isocratic mobile phase of 99 % acetonitrile on the C18 HPLC column. In addition, a 10 minute pre-run with pure acetonitrile, followed by a running time of 10 minutes, was utilized with a 5  $\mu$ L injection volume. Canthaxanthin at  $m/z$  565.3900  $\pm$  0.05 ( $[M + H]^+$ ), zeaxanthin/lutein at  $m/z$  568.4280  $\pm$  0.05,  $\beta$ -carotene/lycopene at  $m/z$  536.4382  $\pm$  0.05 ( $[M]^+$ ), and  $\beta$ -cryptoxanthin at  $m/z$  552.4300  $\pm$  0.05 ( $[M + H]^+$ ) have been extracted from the full chromatogram (dark blue).

From Figure 3.36, it is evident that canthaxanthin is present in the water-extracted samples in significant amounts, at the expected retention time. There is however, a high degree of contamination, shielding the mass signal of canthaxanthin. This was the case in all of the mass chromatograms of all water-extracted samples, including those incubated for only four days, see Appendix B. This contamination can be explained by the extraction method as most cellular components are water soluble, and thus may not be filtrated from the sample through the 0.2  $\mu$ m hydrophilic filter, which was the only purification step utilized.

As with the chloroform-extracted samples, the canthaxanthin content in both water-extracted experiments, involving the two different agar plates and incubation times, were calculated from the extracted ion chromatograms, compared to the MS standard curve, and averaged for each quadruplicate, see Figures 3.37 and 3.38.

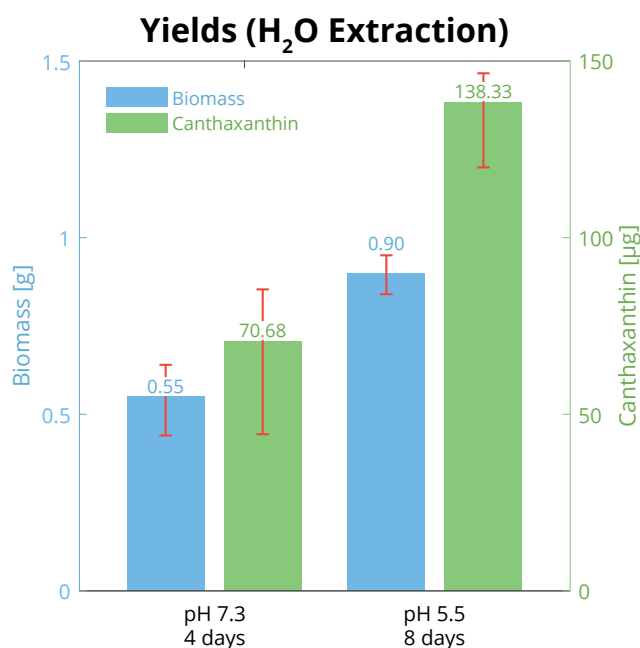


**Figure 3.37:** Bar plot showing the average biomass and canthaxanthin yields for both experiments extracted with water and sonication. It is evident that both yields increase with the incubation time. In addition, the margin of error of the 4 day experiment is significantly larger than the one of the other experiment.

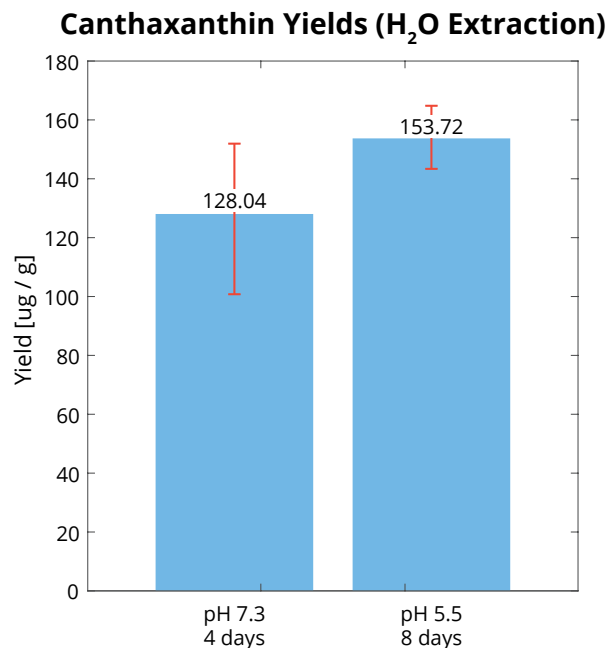


**Figure 3.38:** Bar plot showing the average canthaxanthin yield per gram biomass harvested for extraction for both experiments extracted with water and sonication.

From Figures 3.37 and 3.38, it is evident that, as the biomass increases, the canthaxanthin concentration increases as well. The canthaxanthin yields obtained from the water-extraction after eight days of growth is 102 % higher compared to the yield obtained after just four days of incubation. The canthaxanthin yield increases proportionally to the biomass, and thus the yield per gram biomass from both experiments is only marginally different. This was also the case with the chloroform-extracted samples, and therefore it can again be argued whether it is worth doubling the incubation time, when both experiments require the same number of agar plates to obtain similar canthaxanthin yields. It is, however, possible to use both half the volume of chloroform, and the time spent on extraction, if the cells were only extracted every eight days of growth.

Interestingly, the maximum yield of the water-extracted samples is approximately 25 % higher than the maximum yields of the chloroform-extracted samples, and therefore, it appears that larger yields can be achieved using water, instead of chloroform, as extraction solvent.

One could argue that during the ultra-sonication of the *D. maris* cells, the membrane structure was disrupted, inducing an emulsification process forming self-assembly structures, encapsulating the hydrophobic carotenoids and making them water-soluble. It is generally accepted that sonication leads to inactivation of bacterial strains and other microorganisms, where it is well established that cavitation events are largely responsible for this bactericidal effect. The exact mechanism of cavitation, through which sonication is lethal to microorganisms, is yet to be fully uncovered [71]. Nevertheless, it has been shown, that low-frequency sonication have deteriorating effects on the integrity of gram-negative bacteria [72], where the same is only true for some gram-positive bacteria, as they appear to be more resistant to sonication due to their thicker cell wall [73]. Thus, when exposed to sonication, larger chunks of the membrane may dissociate from the bacterial envelope, forming self-

assembling structures and leaving the cell wall more or less intact. In addition, individual polar lipids may themselves dissociate from the entire cell envelope [74]. Therefore, one could argue, that since the carotenoids are membrane bound in general, and the bacterial membrane is dissociated during ultra-sonication, it is possible that a high percentage of the canthaxanthin available for extraction, will follow the membrane lipids into vesicle structures in the solution, leaving the remaining envelope structures to be discarded during filtration and centrifugation.

### Nanoparticle Tracking Analysis

In order to verify the presence of vesicles, formed from the membrane constituents of the bacterial cells during sonication, NTA was utilized for each of the water-extracted quadruplicates. Dynamic light scattering is the most widespread technique used for determination of the size of vesicles in a sample, but the method suffers from some inherent drawbacks. One of these drawbacks comes from the fact that the method relies on light scattering fluctuations from the brownian motion of the particles. Since the scattering intensity is proportional to the sixth power of the particle diameter, accurate size measurement is easily interrupted by any presence of large contaminants such as dust particles [75, 76]. NTA is a viable alternative to dynamic light scattering techniques, relying on light scattering microscopy and a charge-coupled device camera to track individual vesicles and their motion in a solution. Subsequently, the brownian motion is related to the size of the vesicles using the Stokes-Einstein equation [75]. Filipe *et al.* evaluated NTA along with dynamic light scattering, and found that NTA was a highly suitable measurement method for nano-carrier systems consisting of vesicles [75]. The same favourable conclusion of NTA has been drawn in other papers [77, 78].

For each quadruplicate of the water extracted samples, the size of the vesicles were estimated from the movement of the particles in the water-based solution on three different spots three times. The measurements for one spot were averaged, showing a relatively narrow size distribution. See Figure 3.39 for the size distribution of one of the spots on one of the water-extracted samples.

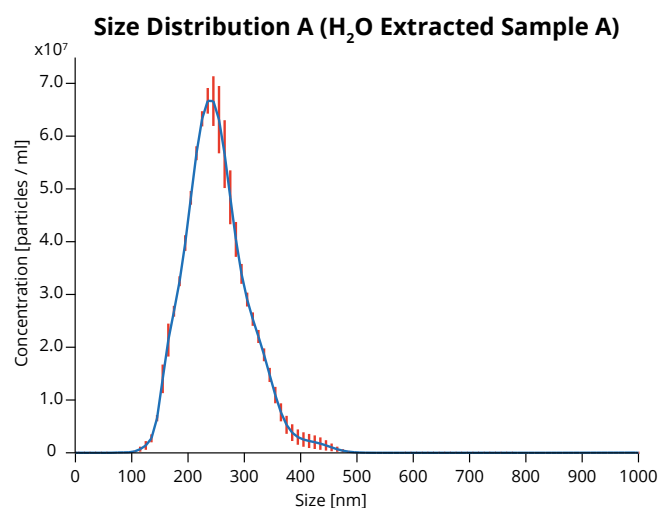


**Figure 3.39:** A plot showing the average size distribution of the vesicles in one spot of one water-extracted sample, formed during ultra-sonication of the *D. maris* cells from the membrane constituents, encapsulating the bacterial canthaxanthin.

From Figure 3.39, as well as the remaining size distributions shown in Appendix C, a relatively narrow size distribution of the vesicles can be seen, ranging from 100 - 400 nm. For all of the median diameters from all measurements on each quadruplicate, see Table 3.2.

Sample	Median Diameters [nm]		
	Measurement A	Measurement B	Measurement C
A	251.6 ± 3.0	254.3 ± 2.2	254.4 ± 3.1
B	260.5 ± 9.4	245.9 ± 0.8	259.3 ± 1.9
C	220.9 ± 9.9	237.0 ± 3.3	245.7 ± 3.2
D	290.0 ± 1.2	276.1 ± 5.7	273.8 ± 2.6

**Table 3.2:** Median diameters from measurements on all spots of the vesicles formed in all samples during ultra-sonication of the *D. maris* cells from the membrane constituents, encapsulating the bacterial canthaxanthin. The overall average diameter of the vesicles in all four water-extracted samples is 255.79 nm.

As can be seen in Figure 3.39, there are clearly some type of vesicles in the sample, with a size distributions as seen in Table 3.2. The overall average of the median diameters of the vesicles is 255.79 nm. This could conform with either micelles or liposomes being present in the sample, although the size would be quite large for micelles, since they are typically around 10 - 80 nm in diameter due to the stabilization of the involved surfactants [79]. It was, however, not possible to find any studies to date, who have characterized vesicles formed from the sonication of bacterial cells. In addition, it should be noted, that the samples were all filtrated using a 200 nm filter, which may have had an impact on the vesicles present in the final samples. Furthermore, it should also be noted that the parameters used by the software to calculate the diameters of the vesicles, were chosen manually to some extent, excluding non-moving particles, particles with small movements, and what appeared to be background noise.

From the median diameters, it is indicated that the sonication of the cells have resulted in the formation of bilayer vesicles like liposomes, which generally are larger in size compared to micelles. In addition, it was not possible to dissolve the freeze-dried vesicles with canthaxanthin into chloroform, or extracting the canthaxanthin from inside the vesicles using chloroform as the extraction solvent. This could indicate that the vesicles are highly stabilized in the solution by other molecules. In addition, under normal circumstances, the rigidity of canthaxanthin reduces the fluidity of the bacterial membrane, and this effect might be pronounced in the smaller membrane of the newly formed vesicles [4, 5, 25]. Without stabilizers, the vesicles would leak out canthaxanthin into the solution [80], as simple micelles and liposomes tend to become disrupted during chloroform extraction as they would completely or partially dissolve into the organic solvent [81]. As was seen from the MS measurements of the water extracted samples, a high degree of contamination was present in the samples, beside the carotenoids. These contaminations could be the constituents comprising the vesicle structures. In addition, the cells were extracted in water and no efforts were made to purify the samples further, making it possible that the vesicles are stabilized by many different biological molecules, as the bacterial cell envelope is a complex structure composed of multiple lipid species, proteins and other constituents. Furthermore, the lipid molecules composing the lipid bilayer of the bacterial membrane are most likely to form other bilayer structures like liposomes, due to their size and shape, determining their packing parameter.

Furthermore, both the membrane-bound proteins, as well as canthaxanthin, normally reside in the bacterial membrane, extending through the hydrophobic zone of the lipid barrier. Thus by assuming a lipid bilayer structure like liposomes, the membrane constituents are allowed to stay in their natural cellular environment where they might contribute to the stabilization of the smaller vesicles. There are however, to the knowledge of the authors, no studies, which have meticulously sonicated bacteria similar to *D. maris* and analysed any resulting vesicles.

### Nuclear Magnetic Resonance Spectroscopy

In addition to the NTA measurements, 1D and 2D NMR measurements were conducted in order to confirm the presence of canthaxanthin in the water-extracted samples. However, in order to increase the concentration of the samples, left-over vesicle samples were mixed, freeze-dried, and diluted directly into 2 mL deuterium oxide. See Figure 3.40 for the  $^1\text{H}$  NMR spectrum of the mixed water-extracted sample.

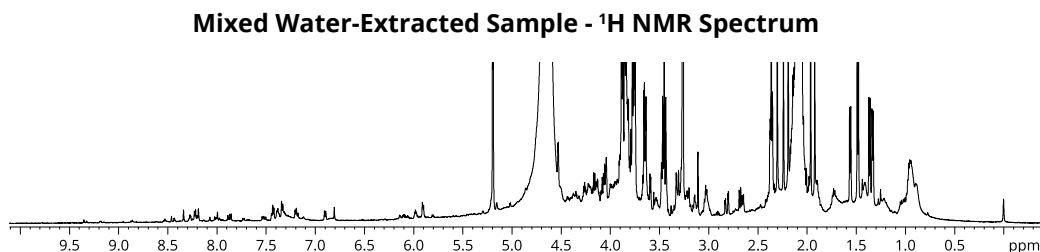


**Figure 3.40:**  $^1\text{H}$  NMR spectrum of the mixed water-extracted sample, diluted into deuterium oxide. No peaks were related to canthaxanthin.

Contrary to the MS measurements on the water-extracted samples, no canthaxanthin is visible in the  $^1\text{H}$  spectra of this mixed solution. This may be attributed to the fact that the maximum concentration of canthaxanthin achieved in the solution was 0.3 mM, where 1 mM usually gives a fine NMR result [49]. Nevertheless, there are many peaks in the spectrum, which may correspond to the many different biological molecules which may be present in the sample. There are many peaks which have a very broad appearance, which would conform with the presence of micelles or liposomes larger than 100 nm in the sample [82–84]. The large size of the vesicles leads to a large molecular tumbling time, making it hard or impossible to average any anisotropic interactions, leading to a broad peak. This limitation could be overcome using more advanced NMR techniques, such as the High-Resolution Magic Angle Spinning technique [83]. Lastly, the presence of the broad peaks might result in the weak signals from the carotenoids being effectively invisible in the NMR spectrum.

Unfortunately, the low concentration of canthaxanthin means that it is even more difficult to achieve a good quality HSQC spectrum. This is evident in Figure 3.41, which shows the  $^1\text{H}$  coupled  $^{13}\text{C}$  HSQC 2D NMR spectrum of the mixed water-extracted sample. There are no traces of canthaxanthin in the NMR spectrum.

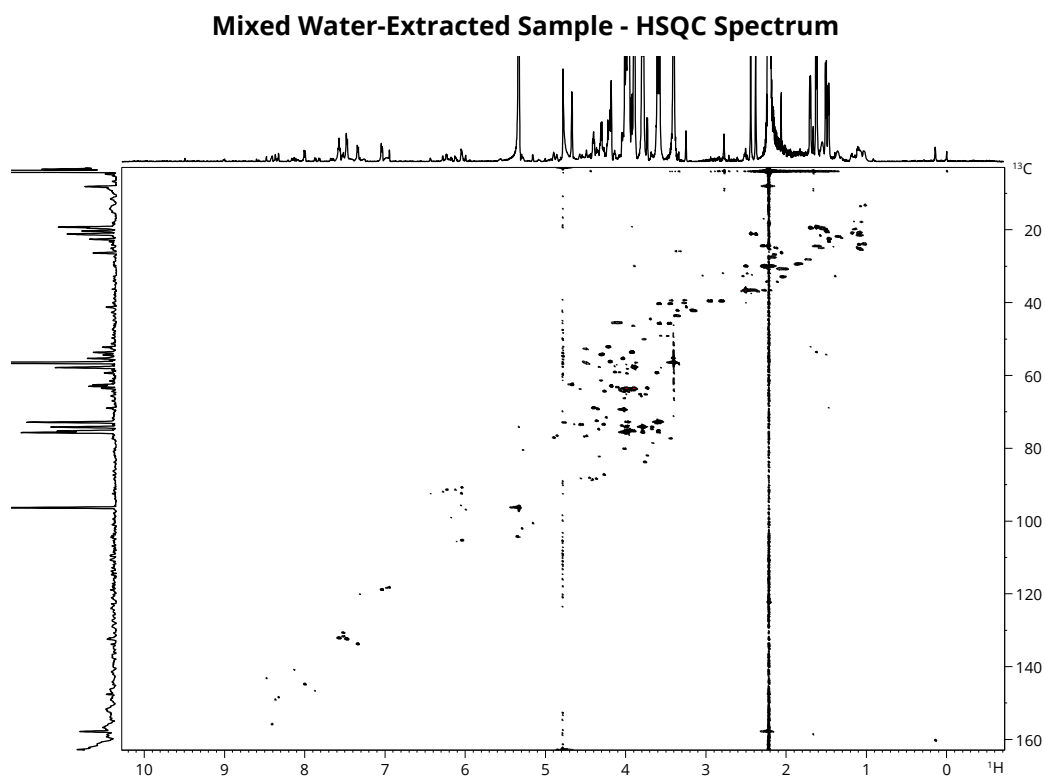


**Figure 3.41:**  $^1\text{H}$  coupled  $^{13}\text{C}$  HSQC 2D NMR spectrum of the mixed water-extracted sample, diluted into deuterium oxide. No peaks were related to canthaxanthin.

Surprisingly, it appears that a high canthaxanthin yield can be achieved by using a water-based extraction instead of using organic solvents. There is however, the problem arising from the purity of the extract. It clearly became evident from the MS and NMR measurements from both extraction methods that, even though they were both filtrated through a  $0.2\ \mu\text{m}$  filter, the chloroform extracted samples were less contaminated with other cellular constituents. However, since chloroform is a toxic solvent and prohibited in the production of human consumption products, efforts should be made to purify the canthaxanthin from the water-extracted samples. When cellular constituents are present in human consumption products, there is an increased risk of allergic reactions and an increased risk of food borne pathogenic DNA. It has even been found that complete strands of genomic DNA can enter the bloodstream when ingested from foods [85]. The cavitation process of the sonication however, might have fragmented much of the DNA present, but there is at the moment no guarantee of this being the case, as sonication is not effective at destroying all types of DNA of all sizes. Small fragments seem to be especially resistant to degradation from sonication [86, 87].

The canthaxanthin in the water extracts may be purified using existing commercial methods like preparative and semi-preparative HPLC, which cannot be utilized directly on live cells, but may be used on smaller liposomes where most cell debris is removed. In this project, the motivation was to purify the water extracts, obtaining a more concentrated sample for NMR measurements. However, the separation autosampler of the MS setup, collecting exact masses at exact retention times, was out of order. Therefore, semi-preparative HPLC was discussed. But before any semi-preparative HPLC separation could take place, it was investigated how well the canthaxanthin would dissolve into acetonitrile from the liposomes, which would give an estimate of how much time and solvent would be necessary for purification using the present HPLC setup. The mixed water-extracted sample was freeze-dried and dissolved into 5 mL acetonitrile. The solution was ultra-sonicated twice at 148 W (37 % of 400 W) for 30 minutes with an alternating sequence of 15 seconds of sonication and 30

second breaks. The solution was centrifuged, and 1 mL of the enriched acetonitrile was used for MS measurements. See Figure 3.42 for the resulting extracted ion chromatograms of the enriched acetonitrile.

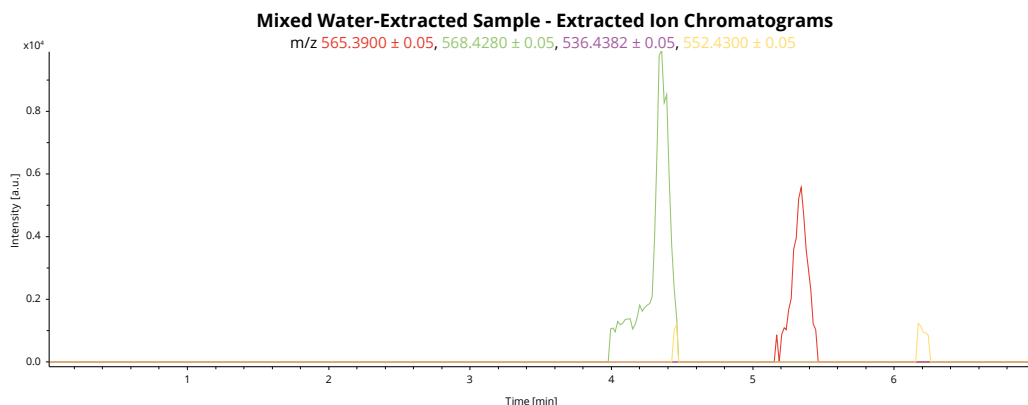


**Figure 3.42:** HPLC/ESI-MS extracted ion chromatograms of the mixed water-extracted sample dissolved into acetonitrile, at positive ionization. The mass chromatogram was measured with an isocratic mobile phase of 99 % acetonitrile on the C18 HPLC column. In addition, a 10 minute pre-run with pure acetonitrile, followed by a running time of 10 minutes, was utilized with a 5  $\mu$ L injection volume. Canthaxanthin at  $m/z$   $565.3900 \pm 0.05$  ( $[M + H]^+$ ), zeaxanthin/lutein at  $m/z$   $568.4280 \pm 0.05$ ,  $\beta$ -carotene/lycopene at  $m/z$   $536.4382 \pm 0.05$  ( $[M]^+$ ), and  $\beta$ -cryptoxanthin at  $m/z$   $552.4300 \pm 0.05$  ( $[M + H]^+$ ) have been extracted from the full chromatogram.

From Figure 3.42, canthaxanthin is visible with a low mass intensity. Interestingly, the mass signal of zeaxanthin/lutein at  $m/z$   $568.4280 \pm 0.05$  is more intensive compared to canthaxanthin, even though it was virtually undetectable during the first MS measurements on the water-extracted samples. One explanation is that the compound is finally present in the solution at significant quantities, due to the mixing of the four water-extracted samples, and that the compound is more soluble in acetonitrile, compared to canthaxanthin. The presence of the hydroxyl groups in the molecule might facilitate the diffusion into the solvent.

The canthaxanthin extracted ion chromatogram was integrated in triplicates, averaged, and compared to the MS standard curve. The resulting concentration of canthaxanthin in the enriched acetonitrile was  $0.076 \mu\text{M}$  which is only 0.07% of the canthaxanthin present in the entire water-extracted sample. Due to the poor solubility of the compound in acetonitrile under the current conditions, it was decided not to use semi-preparative HPLC for purification of canthaxanthin from the liposomes. This process would require massive volumes of acetonitrile and risk an irreversible absorption of the compound onto the HPLC column. It was however, evident from this experiment, that the MS setup was able to separate the compound using acetonitrile as a solvent. It was hypothesized that, the minuscule amount of dissolved canthaxanthin, found in Figure 3.42, was due to a very poor solubility of the compound in acetonitrile. If this was the case, it would invalidate any quantitation made in this project, and would mean that the actual concentrations of produced canthaxanthin would be order of magnitudes higher than what was measured. There are currently no reports on the solubility of canthaxanthin in acetonitrile, and efforts made to dissolve the carotenoid in acetonitrile in this project were ultimately unsuccessful. Nevertheless, acetonitrile is a very common solvent for MS measurements of carotenoids [18, 23, 88, 89].

In this project, the maximum yields of canthaxanthin when using chloroform as an extraction solvent were  $121.52 \mu\text{g/g}$ , and  $153.72 \mu\text{g/g}$  when using water as an extraction solvent. Although these yields are in the same order of magnitude as what is reported in the literature, they are still quite low. Many

reports have focused on the optimization of canthaxanthin production yields using *D. maris*, where Goswami *et al.* [23], conducted a comprehensive study on this topic, achieving extremely high yields of 16,509 µg/g (122 mg/L). As was done in this project, Goswami *et al.* used a growth medium with a pH value of 5.5, albeit a liquid medium in their case, and they used methanol as the extraction solvent. Their growth media was composed of glucose, NaCl, bacteriological peptone and yeast extract. Furthermore, they argued that incubation at 25 °C, while being shaken at 120 RPM in an Erlenmeyer flask for five days, exposed to light, with a 2 % inoculum are the optimal conditions for both growth and canthaxanthin production by the *D. maris*. The growth medium used in this project is highly similar to the one used by Goswami *et al.* in the sense that the primary carbon source is glucose, which, according to Khodaiyan *et al.* [36], is the most effective carbon source for the production of canthaxanthin by *Dietzia* species. In addition, The growth medium used in this project contains both yeast extract and peptone, which are reported to be the optimal nitrogen sources for canthaxanthin production *Dietzia* species, followed by casein [24]. For the pH 7.3 agar plates used in this project, casein and peptone were the primary nitrogen sources, while it was casein, peptone and yeast extract in the pH 5.5 plates. The main difference between the study by Goswami and the present project, besides a one day longer incubation period, is the fact, that they used liquid media while agar plates were used in this project for the production of the carotenoid. Thus, the agar plates should perhaps be used more as a pre-culture, which also serves as an inducer for the carotenoid production, after which the biomass is to be transferred into a liquid medium, increasing the biomass significantly over time. Lastly, Goswami *et al.* did not attempt to optimize the extraction process.

Another study by Khodaiyan *et al.* [36], found that a pH of 7 and a temperature of 31 °C was optimal conditions for the production of canthaxanthin by *Dietzia natronolimnaea* HS-1. In addition, Khodaiyan *et al.* found that when they switched from a Erlenmeyer flask system to a batch fermenter system, they could extract yields of 699 µg/g (4.28 mg/L) of canthaxanthin.

### 3.3 Bioproduction of Astaxanthin by *R. opacus*

In order to determine the conversion of canthaxanthin by *R. opacus* DSM 43250, into astaxanthin, the phenol-induced *R. opacus* cells were fed the water-extracted liposome samples. The water-extracted samples were utilized due to their solubility into the culture and their high concentration of canthaxanthin. In addition, it was interesting to observe whether the *R. opacus* cells were able to utilize the canthaxanthin when encapsulated in liposomes. The transformation was monitored at 0 and 24 hours of incubation. See Figure 3.43 for the extracted ion chromatograms of the reference cultures incubated with no canthaxanthin for 0 and 24 hours.

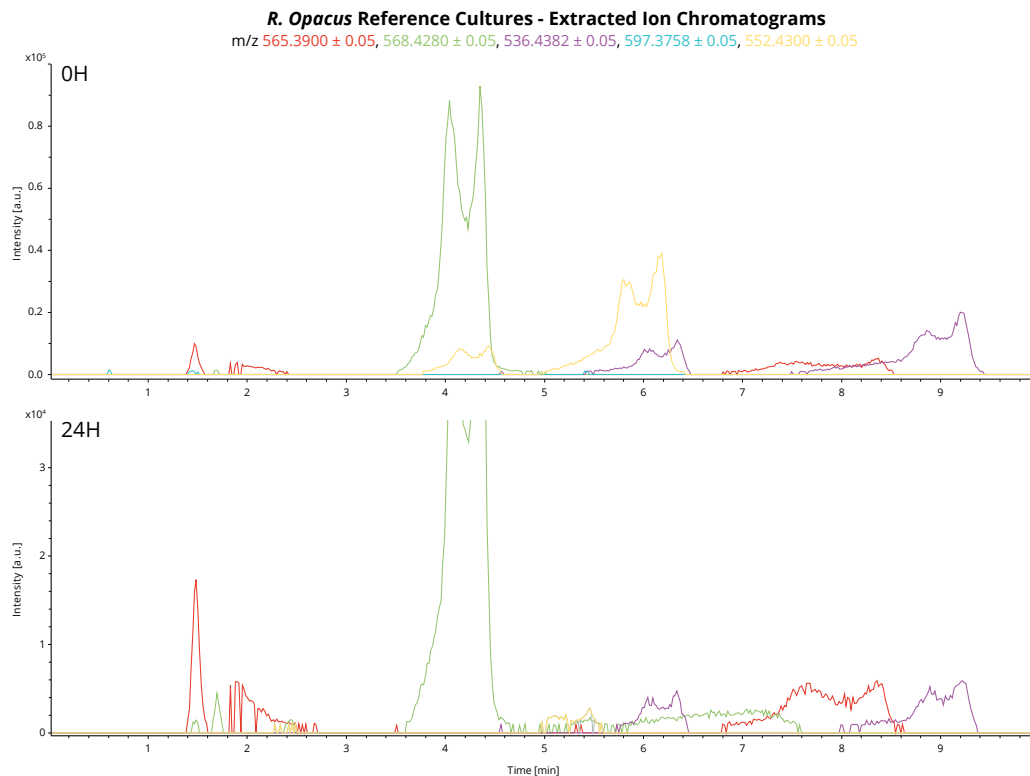


**Figure 3.43:** HPLC/ESI-MS extracted ion chromatograms of the *R. opacus* reference cultures after 0 and 24 hours of incubation, at positive ionization. The mass chromatogram is measured with an isocratic mobile phase of 99 % acetonitrile on the C18 HPLC column, dissolved in chloroform. In addition, a 10 minute pre-run with pure acetonitrile, followed by a running time of 10 minutes, was utilized with a 15  $\mu$ L injection volume. Canthaxanthin at m/z 565.3900  $\pm$  0.05 ( $[M + H]^+$ ), zeaxanthin/lutein at m/z 568.4280  $\pm$  0.05,  $\beta$ -carotene at m/z 536.4382  $\pm$  0.05 ( $[M]^+$ ), astaxanthin at m/z 597.3758  $\pm$  0.05 ( $[M + H]^+$ ), and  $\beta$ -cryptoxanthin at m/z 552.4300  $\pm$  0.05 ( $[M + H]^+$ ) have been extracted from the full chromatogram. *R. opacus* appears to produce relatively high concentrations of both zeaxanthin/lutein and  $\beta$ -cryptoxanthin under normal growth conditions.

In Figure 3.43, it can be seen that *R. opacus* DSM 43250 synthesises a range of carotenoids during incubation, including zeaxanthin/lutein at m/z 568.4280  $\pm$  0.05 and  $\beta$ -cryptoxanthin at m/z 552.4300  $\pm$  0.05. This conforms with the fact that the genus of *Rhodococcus* is known to produce a wide range of carotenoids naturally [31, 32, 90]. Furthermore, it can be seen from the extracted ion chromatograms that the intensity of the carotenoids mass peaks decreases with increasing incubation time. This might be explained by the lack of available carbon sources during incubation, as the cells were incubated in mineral medium without the water-extracted liposomes containing canthaxanthin, or any other carbon sources. It has been proposed that the synthesis of carotenoids is highly dependent on a sufficient carbon content of the growth medium [10]. Therefore, one could argue that the carotenoids

### 3.3. Bioproduction of Astaxanthin by *R. opacus*

found in the reference culture extracted after 0 hours of incubation is a result of the normal growth of the bacterium in the main GS culture, and when the cells are subsequently grown in the mineral medium for 24 hours, the intracellular carbon content was utilized for energy production and survival rather than the synthesis of secondary metabolites like carotenoids. In addition, the intracellular carotenoids might have served as an available carbon source during the starvation, explaining the decrease in concentration over time [91]. Furthermore, canthaxanthin appears to be present in the reference cultures, even though they were incubated without canthaxanthin. But canthaxanthin is not present at the expected retention time, and it can therefore be argued that what is observed in Figure 3.43, is another compound or fragment with difficulties separating from the C18 HPLC column (like  $\beta$ -carotene), and therefore not canthaxanthin.

Canthaxanthin is, however, present in the cultures which were incubated with the water-extracted liposomes as the sole carbon source. See Figure 3.44 for the extracted ion chromatograms of one of the cultures incubated for 0 and 24 hours, each containing  $26.465 \pm 0.15 \mu\text{g}$  canthaxanthin encapsulated in *D. maris* liposomes.

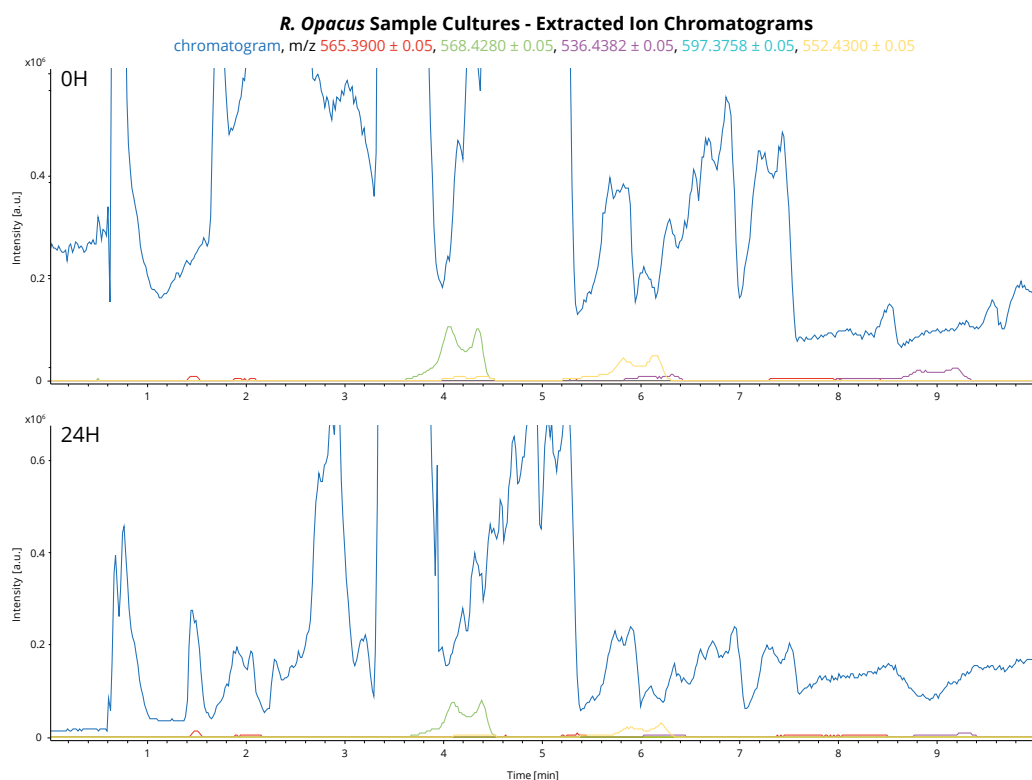


**Figure 3.44:** HPLC/ESI-MS full mass chromatogram and extracted ion chromatograms of one of the *R. opacus* cultures after 0 and 24 hours of incubation containing canthaxanthin, at positive ionization. The mass chromatogram is measured with an isocratic mobile phase of 99 % acetonitrile on the C18 HPLC column, dissolved in chloroform. In addition, a 10 minute pre-run with pure acetonitrile, followed by a running time of 10 minutes, was utilized with a 15  $\mu\text{L}$  injection volume. Canthaxanthin at  $m/z 565.3900 \pm 0.05$  ( $[\text{M} + \text{H}]^+$ ), zeaxanthin/lutein at  $m/z 568.4280 \pm 0.05$ ,  $\beta$ -carotene at  $m/z 536.4382 \pm 0.05$  ( $[\text{M}]^+$ ), astaxanthin at  $m/z 597.3758 \pm 0.05$  ( $[\text{M} + \text{H}]^+$ ), and  $\beta$ -cryptoxanthin at  $m/z 552.4300 \pm 0.05$  ( $[\text{M} + \text{H}]^+$ ) have been extracted from the full chromatogram (dark blue).

From Figure 3.44, it is visible that *R. opacus* DSM 43250 synthesises a range of carotenoids during incubation, and that their concentration appear to decrease with increasing incubation times. Contrary to the reference cultures however, canthaxanthin is observed at the expected retention time, but at very low concentrations, where no astaxanthin was observed in any of the cultures. From the extracted ion chromatograms of the *R. opacus* cultures, it appears that the concentration of canthaxanthin

present in the samples increases with increasing incubation time. The integrals of the extracted ion chromatograms of canthaxanthin were compared to the canthaxanthin MS standard curve, and averaged for the triplicates. See Figure 3.45 for the extracted mass in relation to the added canthaxanthin.

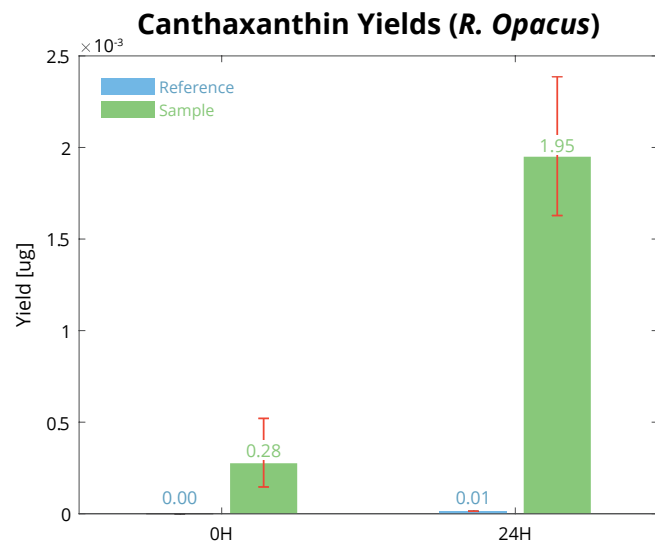


**Figure 3.45:** Bar plot showing the average canthaxanthin yields for both the reference and sample cultures of *R. opacus*, incubated for 0 and 24 hours, and extracted with chloroform. It is evident that the yield increases with the incubation time, while the reference yield is effectively non-existent.

From Figure 3.45 it is visible that only small concentrations of canthaxanthin was present in the *R. opacus* extracts. The water-soluble liposomes were suspended into the *R. opacus* broths, colouring the cultures red, for at least 24 hours of incubation. The broths were then discarded and the remaining *R. opacus* cells were extracted with chloroform. This means that the canthaxanthin present in the *R. opacus* extracts might be a result of either absorption of the compound from the liposomes, or the adsorption of the liposomes onto the envelope of the *R. opacus* cells. This effect was more pronounced over time, as the *R. opacus* extracts after 24 hours of incubation contained 1.65 % of the added canthaxanthin, compared to the 0.03 % after 0 hour of incubation. Even though no astaxanthin was produced by the *R. opacus* DSM 43250 cells, this absorption or adsorption of canthaxanthin might be the first step to such a production. In order to elucidate how well the actual transformation of canthaxanthin is carried out by *R. opacus*, experiments with higher concentrations (ideally 1 mM) of pure canthaxanthin must be carried out. However, as mentioned before, due to the poor quality of the canthaxanthin received in the early stages of the experiment period, these experiments were not accomplished in this project. In addition, in order to verify the absorption of significant concentrations of canthaxanthin over time by *R. opacus*, much higher concentrations of the liposomes are required along with longer incubation times.

The *R. opacus* cells have been proven to be able to degrade a wide range of hydrophobic compounds, including phospholipids. Thus, it is a distinct possibility, that the bacterial cells will degrade the liposomes of the water-extracted sample over time, after which the canthaxanthin molecules become available for metabolism, which would lead to insignificant concentrations of the compound being extracted after a certain amount of incubation time. This could potentially explain the low extraction yields after 24 hours of incubation. However, this process would likely lead to an initial large increase in the canthaxanthin concentration inside the cells, due to the liposomes being degraded relatively fast,

as they are the most available carbon source. An additional extraction on the sample sometime between 0 and 24 hours would be required in order to verify a decrease in canthaxanthin over time. On the other hand, if an absorption or adsorption of the liposomes were occurring, leading to an incorporation of the carotenoid into the bacterial cells, the concentration of the extracted canthaxanthin would likely continue to increase during longer incubation times. Both theories demand additional extractions of the intracellular carotenoid content for verification.

#### 3.3.1 Thin-Layer Chromatography

Since it was impossible to observe any canthaxanthin in the NMR spectra done on the vesicle samples at the current concentrations, a TLC was prepared in the hope of drawing out canthaxanthin from the liposomes, and compare them with both the canthaxanthin found in the *R. opacus* extracts, and to known standards of the compound. In addition, if it was possible to separate the canthaxanthin from the vesicles, it might be possible to utilize TLC as a purification method in the reach of higher concentrations of natural canthaxanthin. See Figure 3.46 for the thin-layer chromatograph of one of the water-extracted liposome samples, some of the *R. opacus* extracts, and analytical standards of canthaxanthin, astaxanthin, and  $\beta$ -carotene.

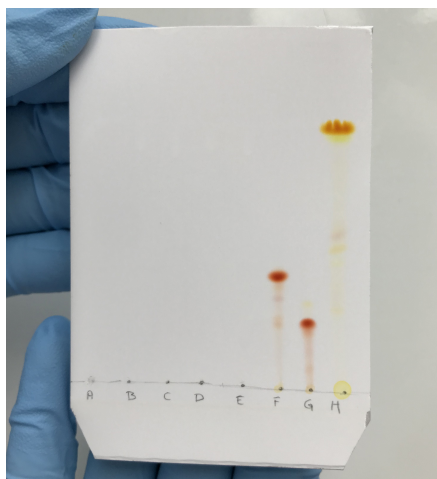


**Figure 3.46:** Visualization of the thin-layer chromatograph of the following extracts; water-extracted liposomes (A), *R. opacus* extract 0H reference (B), *R. opacus* extract 0H (C), *R. opacus* extract 24H reference (D), *R. opacus* extract 24H (E), analytical canthaxanthin (F), analytical astaxanthin (G), and analytical  $\beta$ -carotene (H), in visible light. The chromatograph was developed with a petroleum ether:acetone (75:25) mobile phase. Only the analytical standards are visible in visible light, and they are well separated.

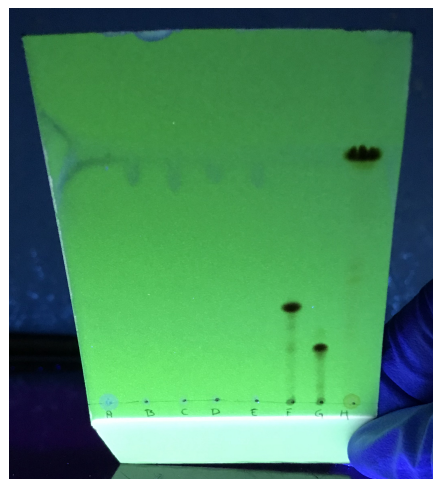


**Figure 3.47:** Visualization of the thin-layer chromatograph of the following extracts; water-extracted liposomes (A), *R. opacus* extract 0H reference (B), *R. opacus* extract 0H (C), *R. opacus* extract 24H reference (D), *R. opacus* extract 24H (E), analytical canthaxanthin (F), analytical astaxanthin (G), and analytical  $\beta$ -carotene (H), in UV light. The chromatograph was developed with a petroleum ether:acetone (75:25) mobile phase. Only the analytical standards are visible in UV light, and they are well separated.

From Figures 3.46 and 3.47 it became evident that the mobile phase utilized for the development of the thin-layer chromatograph was able to separate canthaxanthin, astaxanthin and  $\beta$ -carotene.  $\beta$ -carotene however, followed the solvent front. In both UV and visible light, no carotenoids were visible in any of the *R. opacus* extracts or in the water-extracted liposome sample, even though the presence of canthaxanthin was verified in both the 24H *R. opacus* extract and inside the liposomes. It is however, possible that the concentrations of canthaxanthin in the *R. opacus* and water-extracts were too low for visible detection during the TLC measurement. Furthermore, it was discovered earlier that

the vesicles containing canthaxanthin were not destroyed during extraction with chloroform, due to their high degree of stability, and it is therefore plausible that the organic mobile phase consisting mainly of petroleum ether is not able to separate canthaxanthin from the vesicles either. Thus the vesicles have probably not been developed using this mobile phase.

During this project, a bioproduction of canthaxanthin by *D. maris* was achieved, and the carotenoid was extracted in such a manner, that it could be either absorbed or adsorbed by the *R. opacus* cells. However, the incorporation of canthaxanthin by the *R. opacus* was not pronounced, and no transformation of the compound into astaxanthin was observed. Thus, the concept of the two-organism batch reactor system for bioproduction of astaxanthin still needs considerable development before it can be realised.

---

## 4. Conclusion

---

The goal of this project was initially to develop a two-organism batch reaction system for the bioproduction of astaxanthin, using *D. maris* for the production of canthaxanthin which would be used as precursor in the biosynthesis of astaxanthin by *R. opacus*. However, due to problems with acquiring sufficient amounts of canthaxanthin, the focus shifted towards the optimization of the production and extraction of the compound by *D. maris* DSM 43672, which then could be fed to *R. opacus* DSM 43250 for the synthesis of astaxanthin.

Firstly, in order to quantitate any production of both canthaxanthin and astaxanthin, MS standard curves were prepared. In addition, comprehensive NMR and MS measurements were conducted in order quickly and securely verify any presence of the desired carotenoids in complex biological samples.

Secondly, the optimum light conditions for carotenoid production were determined for *D. maris*. As expected, due to the anti-oxidant nature of the carotenoids, the production of canthaxanthin by *D. maris* was 118.4 % higher during incubation in full light, compared to incubation in complete darkness. Therefore, agar plates were prepared with high surface areas, and incubated in full light, in order to maximize the light and oxygen exposure to each cell. Two types of agar plates were utilized in the production of canthaxanthin, TS agar plates at pH 7.3 and TS agar plates at pH 5.5 containing yeast extract. In addition, a total of both four and eight days of incubation was utilized. As the most effective extraction solvent, chloroform was utilized to extract carotenoids from the *D. maris* cells with low levels of contaminations from cell debris. The extracted canthaxanthin was quantitated using the corresponding MS standard curve, resulting in yields between 100.09 and 121.52 µg per g bacterial cells. The canthaxanthin yield nearly doubled as the biomass proportionally increased. The highest canthaxanthin yield was obtained after a total of eight days of growth, using the pH 7.3 plates where the complete biomass was transferred onto new agar plates at pH 5.5 after four days of growth.

As an eco-friendly non-toxic alternative to chloroform extraction, edible sunflower oil was utilized for the extraction of carotenoids from *D. maris* cells. This proved unsuccessful however, but in the process, it was discovered that after sonication of the bacterial cells, the canthaxanthin seemed to readily dissolve into the aqueous phase instead of the oil. This was unexpected due to the highly hydrophobic nature of the compound. During two sets of quadruplicates, this phenomenon was verified to be reproducible. NTA was used to verify that the bacterial membrane formed vesicles during the sonication of the bacterium, ultimately encapsulating the carotenoids and making them water-soluble. The mean diameter of the vesicles were 255.79 nm, conforming with the hypothesis that larger bilayer vesicles, like liposomes, were formed from the membrane constituents. Lastly, the canthaxanthin extraction yield when using water as the extraction solvent, was between 128.04 and 153.72 µg per g bacterial cells. The highest canthaxanthin yield was again obtained from the pH 5.5 agar plates. The extraction yield from the water-extraction experiments were approximately 25 % higher, than the chloroform-extracted samples. The water-extracted samples were, however, highly contaminated with cell debris, primarily in the vesicle form, and efforts should therefore be made to separate the canthaxanthin from the vesicles before the compound can be utilized in human products. In the end, the water-extracted samples were fed to phenol-induced *R. opacus* cells. No production of astaxanthin was observed, but the bacterium appears to produce significant amounts of carotenoids itself, and to absorb or adsorb the vesicles containing canthaxanthin over time.



---

# Bibliography

---

- [1] G. Singh. *Chemistry of Terpenoids and Carotenoids*. Discovery Publishing House, 3 edition, 2007.
- [2] B. Hammond. Carotenoids. *Adv. Nutr.*, 4(12):474–476, 2013.
- [3] P. Vachali, P. Bhosale, and P. S. Bernstein. Microbial Carotenoids. In *Microb. Carotenoids From Fungi Methods Protoc. - Methods Mol. Biol.*, volume 898, pages 41–59. 2012.
- [4] H. J. Nelis and A. P. De Leenheer. Microbial sources of carotenoid pigments used in foods and feeds. *J. Appl. Bacteriol.*, 70(3):181–191, 1991.
- [5] A. Vershinin. Biological functions of carotenoids - diversity and evolution. *BioFactors*, 10(2-3):99–104, 1999.
- [6] Q. Ashton Acton, editor. *Carotenoids: Advances in Research and Application*. ScholarlyEditions TM, 2013.
- [7] C. K. Venil, Z. A. Zakaria, and W. A. Ahmad. Bacterial pigments and their applications. *Process Biochem.*, 48(7):1065–1079, 2013.
- [8] D. B. Rodriguez-Amaya. Natural food pigments and colorants. *Curr. Opin. Food Sci.*, 7:20–26, 2016.
- [9] P. Kaiser, P. Surmann, G. Vallentin, and H. Fuhrmann. A small-scale method for quantitation of carotenoids in bacteria and yeasts. *J. Microbiol. Methods*, 70(1):142–149, 2007.
- [10] G. K. Chandi and B. S. Gill. Production and characterization of microbial carotenoids as an alternative to synthetic colors: A review. *Int. J. Food Prop.*, 14(3):503–513, 2011.
- [11] J. C. De Carvalho, L. Cardoso, A. L. Woiciechowski, and L. Vandenberghe. Microbial Pigments. In *Exploit. Agro-Industrial Wastes to Prod. Low-Cost Microb. Surfactants*, pages 73–97. 2014.
- [12] M. Ravaghi, S. H. Razavi, S. M. Mousavi, C. Sinico, and A. M. Fadda. Stabilization of natural canthaxanthin produced by *Dietzia natronolimnaea* HS-1 by encapsulation in niosomes. *LWT - Food Sci. Technol.*, 73:498–504, 2016.
- [13] A. M. Goula, M. Ververi, A. Adamopoulou, and K. Kaderides. Green ultrasound-assisted extraction of carotenoids from pomegranate wastes using vegetable oils. *Ultrason. Sonochem.*, 34:821–830, 2017.
- [14] P. S. Nigam and J. S. Luke. Food additives: Production of microbial pigments and their antioxidant properties. *Curr. Opin. Food Sci.*, 7:93–100, 2016.
- [15] L. Dufossé. Microbial Production of Food Grade Pigments. *Food Technol. Biotechnol.*, 44(3):313–321, 2006.
- [16] R. L. Ausich. Commercial opportunities for carotenoid production by biotechnology. *Pure Appl. Chem.*, 69(10):2169–2174, 1997.

- [17] R. T.M. Baker. Canthaxanthin in aquafeed applications: Is there any risk? *Trends Food Sci. Technol.*, 12(7):240–243, 2001.
- [18] M. Lu, Y. Zhang, C. Zhao, P. Zhou, and L. Yu. Analysis and identification of astaxanthin and its carotenoid precursors from *Xanthophyllomyces dendrorhous* by high-performance liquid chromatography. *Zeitschrift fur Naturforsch. - Sect. C J. Biosci.*, 65 C(7-8):489–494, 2010.
- [19] H. J. Nelis and A. P. De Leenheer. Reinvestigation of *Brevibacterium* sp. Strain KY-4313 as a Source of Canthaxanthin. *Appl. Environ. Microbiol.*, 55(10):2505–2510, 1989.
- [20] K. Malik, J. Tokkas, and S. Goyal. Microbial Pigments: A review. *Int. J. Microb. Resour. Technol. Accept.*, 41(4):361–365, 2012.
- [21] B. H. Lee. *Fundamentals of Food Biotechnology*. John Wiley & Sons Ltd, 2014.
- [22] D. Asker and Y. Ohta. Production of canthaxanthin by *Haloferax alexandrinus* under non-aseptic conditions and a simple, rapid method for its extraction. *Appl. Microbiol. Biotechnol.*, 58(6):743–750, 2002.
- [23] G. Goswami, S. Chakraborty, S. Chaudhuri, and D. Dutta. Optimization of process parameters by response surface methodology and kinetic modeling for batch production of canthaxanthin by *Dietzia maris* NIT-D (accession number: HM151403). *Bioprocess Biosyst. Eng.*, 35(8):1375–1388, 2012.
- [24] S. M. T. Gharibzahedi, S. H. Razavi, and M. Mousavi. Potential applications and emerging trends of species of the genus *Dietzia*: A review. *Ann. Microbiol.*, 64(2):421–429, 2014.
- [25] S. M. T. Gharibzahedi, S. H. Razavi, and S. M. Mousavi. Characterization of bacteria of the genus *Dietzia*: An updated review. *Ann. Microbiol.*, 64(1):1–11, 2014.
- [26] S. M. T. Gharibzahedi, S. H. Razavi, and M. Mousavi. Kinetic analysis and mathematical modeling of cell growth and canthaxanthin biosynthesis by *Dietzia natronolimnaea* HS-1 on waste molasses hydrolysate. *RSC Adv.*, 3(45):23495, 2013.
- [27] E. Ryckebosch, K. Muylaert, M. Eeckhout, T. Ruysen, and I. Foubert. Influence of drying and storage on lipid and carotenoid stability of the Microalga *Phaeodactylum tricornutum*. *J. Agric. Food Chem.*, 59(20):11063–11069, 2011.
- [28] I. E. Apanasenko, O.Yu. Selyutina, N. E. Polyakov, L. P. Suntsova, E. S. Meteleva, A. V. Dushkin, P. Vachali, and P. S. Bernstein. Solubilization and Stabilization of Macular Carotenoids by Water Soluble Oligosaccharides and Polysaccharides Irina. *Arch Biochem Biophys.*, 572:58–65, 2015.
- [29] S. Rath, Z. Olempska-Beer, and P. Kuznesof. Lycopene extract from tomato is a lycopene-rich extract prepared from the ripe fruits of tomato (CTA). *Fao*, (9):1–9, 2007.
- [30] E. Yara-Varón, Y. Li, M. Balcells, R. Canela-Garayoa, A. S. Fabiano-Tixier, and F. Chemat. Vegetable oils as alternative solvents for green oleo-extraction, purification and formulation of food and natural products. *Molecules*, 22(9), 2017.
- [31] Michael Goodfellow, editor. *The Actinobacteria, Part A and B*, volume Five. Springer, second edition, 2011.

- [32] S. Ichiyama, K. Shimokata, and M. Tsukamura. Carotenoid Pigments of Genus *Rhodococcus*. *Microbiol. Immunol.*, 33(6):503–508, 1989.
- [33] A. Søbbye, M. L. K. Lund, and A. Kolding. Biodegradation of 4-Fluorophenol by *Rhodococcus opacus*. 2017.
- [34] A. Søbbye, M. L. K. Lund, and A. Kolding. Biodegradation of Nitrile Compounds by *Rhodococcus opacus*. 2017.
- [35] H. M. Alvarez, editor. *Biology of Rhodococcus*, volume 16. Springer, 2010.
- [36] F. Khodaiyan, S. H. Razavi, Z. Emam-Djomeh, S. M. A. Mousavi, and M. A. Hejazi. Effect of culture conditions on canthaxanthin production by *Dietzia natronolimnaea* HS-1. *J. Microbiol. Biotechnol.*, 17(2):195–201, 2007.
- [37] H. J. Gross. *Mass spectrometry*. Springer, 3rd edition, 2017.
- [38] P. L. Urban. Quantitative mass spectrometry: an overview. *Philos. Trans. A. Math. Phys. Eng. Sci.*, 374(2079):20150382, 2016.
- [39] A LaFountain, S. Kaligotla, S. Cawley, K. Riedl, S. J. Schwartz, H. A. Frank, and R. Prum. Novel methoxy-carotenoids from the burgundy colored plumage of the Pompadour Cotinga *Xipholena punicea*. *Arch. Biochem. Biophys.*, 504(1):142–153, 2010.
- [40] G. Goswami, S. Chaudhuri, and D. Dutta. Effect of pH and inoculum percentage on canthaxanthin production by *Dietzia maris*. In A. Mendez-Vilas, editor, *Microorg. Ind. Environ. From Sci. Ind. Res. to Consum. Prod.*, pages 318–322. Lisbon, 2010.
- [41] E. Lesellier, A. Tchaplá, C. Marty, and A. Lebert. Analysis of carotenoids by high-performance liquid chromatography and supercritical fluid chromatography. *J. Chromatogr. A*, 633(1-2):9–23, 1993.
- [42] T. Glaser, A. Lienau, D. Zeeb, M. Krucker, M. Dachtler, and K. Albert. Qualitative and quantitative determination of carotenoid stereoisomers in a variety of spinach samples by use of MSPD before HPLC-UV, HPLC-APCI-MS, and HPLC-NMR on-line coupling. *Chromatographia*, 57(SUPPL.):19–25, 2003.
- [43] A. Tchaplá, S. Heron, E. Lesellier, and H. Colin. General view of molecular interaction mechanisms in reversed-phase liquid chromatography. *J. Chromatogr. A*, 656:81–112, 1993.
- [44] S. M. Rivera and R. Canela-Garayoa. Analytical tools for the analysis of carotenoids in diverse materials. *J. Chromatogr. A*, 1224:1–10, 2012.
- [45] S. Taylor Mayne and R. S. Parker. Cis-Canthaxanthin and other Carotenoid-Like Compounds in Canthaxanthin Preparations. *J. Agric. Food Chem.*, 36(3):478–482, 1988.
- [46] G. L. Glish and R. W. Vachet. *The basics of mass spectrometry in the twenty-first century*, 2003.
- [47] David R. Lide, editor. *CRC Handbook of Chemistry and Physics, 94th Edition, 2013-2014*. CRC Press, volume 53 edition, 2013.
- [48] G. P. Moss. Carbon-13 NMR spectra of carotenoids. *Pure Appl. Chem*, 47(2-3):97–102, 1976.

- [49] NMR Sample Preparation, 2009.
- [50] A. Yokoyama, H. Izumida, and W. Miki. Production of astaxanthin and 4-ketozeaxanthin by the marine bacterium, *agrobacterium aurantiacum*. *Biosci. Biotechnol. Biochem.*, 58(10):1842–1844, 1994.
- [51] W. Sun, H. Lin, Y. Zhai, L. Cao, K. Leng, and L. Xing. Separation, Purification, and Identification of (3S,3S)- trans -Astaxanthin from *Haematococcus pluvialis*. *Sep. Sci. Technol.*, 50(9):1377–1383, 2015.
- [52] R. J. Bushway and A. M. Wilson. Determination of  $\alpha$ - and  $\beta$ -Carotene in Fruit and Vegetables by High Performance Liquid Chromatography. *Can. Inst. Food Sci. Technol. J.*, 15(3):165–169, 1982.
- [53] D. Benhaim and E. Grushka. Characterization of Ascentis RP-Amide column: Lipophilicity measurement and linear solvation energy relationships. *J. Chromatogr. A*, 1217(1):65–74, 2010.
- [54] A. Marin and C. Barbas. Systematic comparison of different functionality columns for a classical pharmaceutical problem. *J. Pharm. Biomed. Anal.*, 40(2):262–270, 2006.
- [55] R. J. Bushway. Separation of carotenoids in fruits and vegetables by high performance liquid chromatography. *J. Liq. Chromatogr.*, 8(8):1527–1547, 1985.
- [56] R. J. Seviour and R. C. Codner. Effect of Light on Carotenoid and Riboflavin Production by the Fungus *Cephalosporium diospyri*. *J. Gen. Microbiol.*, 77(May):403–415, 1973.
- [57] L. C. Sander, K. E. Sharpless, N. E. Craft, and S. A. Wise. Development of Engineered Stationary Phases for the Separation of Carotenoid Isomers. *Anal. Chem.*, 66(10):1667–1674, 1994.
- [58] I. Hvidsten, S. A. Mjøs, G. Bødtker, and T. Barth. Data on pigments and long-chain fatty compounds identified in *Dietzia* sp. A14101 grown on simple and complex hydrocarbons. *Data Br.*, 4:622–629, 2015.
- [59] S. Joseph and P. Thankam. Process for the Production of Zeaxanthin, 2005.
- [60] R. Mitra, A. K. Samanta, S. Chaudhuri, and D. Dutta. Effect of Selected Physico-Chemical Factors on Bacterial B-Cryptoxanthin Degradation: Stability and Kinetic Study. *Food Proces Eng.*, 40(2), 2016.
- [61] A Wo, K. F. Van, and A. L. Carolas. Patentes Production of high- purity carotenoids by fermenting selected bacterial strains. pages 1–14, 2015.
- [62] L. I. Ardis. *Testosterone Research Trends*. Nova Publishers, 2007.
- [63] F. Mijangos, F. Varona, and N. Villota. Changes in Solution Color During Phenol Oxidation by Fenton Reagent. 40(17):5538–5543, 2017.
- [64] T. de Miguel, C. Sieiro, T. G Villa, and M. Poza. Isolation and taxonomic study of a new canthaxanthin-containing bacterium, *Gordonia jacobaea* MV-1 sp. nov. *Int. Microbiol.*, 3:107–111, 2000.
- [65] H. F. Haas and L. D. Bushneli. The Production of Carotenoid Pigments from Mineral Oil by Bacteria. *J. Bacteriol.*, 48(2):219–31, 1944.

- [66] Y. Li, A. S. Fabiano-Tixier, V. Tomao, G. Cravotto, and F. Chemat. Green ultrasound-assisted extraction of carotenoids based on the bio-refinery concept using sunflower oil as an alternative solvent. *Ultrason. Sonochem.*, 20(1):12–18, 2013.
- [67] C. Qian, E. A. Decker, H. Xiao, and D. J. McClements. Inhibition of  $\beta$ -carotene degradation in oil-in-water nanoemulsions: Influence of oil-soluble and water-soluble antioxidants. *Food Chem.*, 135(3):1036–1043, 2012.
- [68] R. S. Pohndorf, T. R. S. Cadaval, and L. A. A. Pinto. Kinetics and thermodynamics adsorption of carotenoids and chlorophylls in rice bran oil bleaching. *J. Food Eng.*, 185:9–16, 2016.
- [69] H. Arvayo-Enríquez, I. Mondaca-Fernández, P. Gortárez-Moroyoqui, J. López-Cervantes, and R. Rodríguez-Ramírez. Carotenoids extraction and quantification: a review. *Anal. Methods*, 5(12):2916, 2013.
- [70] N. M. Sachindra and N. S. Mahendrakar. Process optimization for extraction of carotenoids from shrimp waste with vegetable oils. *Bioresour. Technol.*, 96(10):1195–1200, 2005.
- [71] N. Gera and S. Doores. Kinetics and Mechanism of Bacterial Inactivation by Ultrasound Waves and Sonoprotective Effect of Milk Components. *J. Food Sci.*, 76(2), 2011.
- [72] E. Joyce, A. Al-Hashimi, and T. J. Mason. Assessing the effect of different ultrasonic frequencies on bacterial viability using flow cytometry. *J. Appl. Microbiol.*, 110(4):862–870, 2011.
- [73] S. Gao, G. Lewis, and Y. Hemar. Handbook of Ultrasonics and Sonochemistry. pages 1–27, 2017.
- [74] S. Batzri and E. D. Korn. Single bilayer liposomes prepared without sonication. *BBA - Biomembr.*, 298(4):1015–1019, 1973.
- [75] V. Filipe, A. Hawe, and W. Jiskoot. Critical evaluation of nanoparticle tracking analysis (NTA) by NanoSight for the measurement of nanoparticles and protein aggregates. *Pharm. Res.*, 27(5):796–810, 2010.
- [76] B. J. Frisken. Revisiting the method of cumulants for the analysis of dynamic light-scattering data. *Appl. Opt.*, 40(24):4087, 2001.
- [77] I. Tatischeff, E. Larquet, J. M. Falcon-Perez, P. Y. Turpin, and S. G. Kruglik. Fast characterisation of cell-derived extracellular vesicles by nanoparticles tracking analysis, cryo-electron microscopy, and Raman tweezers microspectroscopy. *J. Extracell. Vesicles*, 1(1), 2012.
- [78] E. Van Der Pol, A. G. Hoekstra, A. Sturk, C. Otto, T. G. Van Leeuwen, and R. Nieuwland. Optical and non-optical methods for detection and characterization of microparticles and exosomes. *J. Thromb. Haemost.*, 8(12):2596–2607, 2010.
- [79] T. Lundqvist and S. Bredenberg. Pharmaceutical Development. In Raymond Hill, editor, *Drug Discov. Dev.*, chapter 16, pages 227–238. Churcill Livingstone, 2nd edition, 2013.
- [80] J. H. Crowe, S. B. Leslie, and L. M Crowe. Is vitrification Sufficient to Preserve Liposomes during Freeze-Drying. *Cryobiology*, 31:355–366, 1994.
- [81] J. Santhanalakshmi and S. I. Maya. Solvent effects on reverse micellisation of Tween 80 and Span 80 in pure and mixed organic solvents. *Proc. Indian Acad. Sci. (Chemical Sci.)*, 109(1):27–38, 1997.

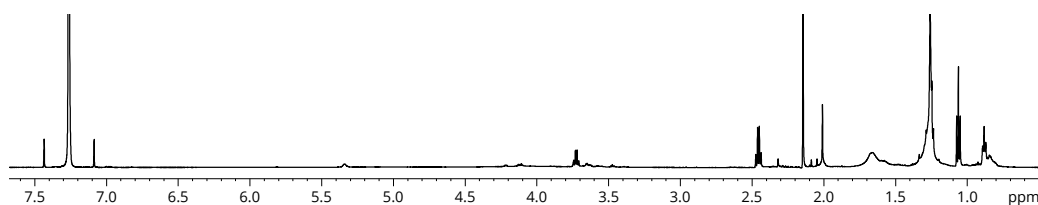
- 
- [82] I. Furo. NMR spectroscopy of micelles and related systems. *J. Mol. Liq.*, 117(1-3):117–137, 2005.
- [83] O. Cruciani, L. Mannina, A. P. Sobolev, C. Cametti, and A. Segre. An improved NMR study of liposomes using 1-palmitoyl-2-oleoyl-sn-glycero-3-phosphatidylcholine as model. *Molecules*, 11(5):334–344, 2006.
- [84] D. D. Lasic. Magnetic Resonance Methods in The Studies of Liposomes Liposomes NMR and EPR of Lipo- somes. *Bull. Magn. Reson.*, 13(1):3–13, 1991.
- [85] S. Spisák, N. Solymosi, P. Ittész, A. Bodor, D. Kondor, G. Vattay, B. K. Barták, F. Sipos, O. Galamb, Zsolt Tulassay, Zoltán Szállási, Simon Rasmussen, Thomas Sicheritz-Ponten, Søren Brunak, Béla Molnár, and István Csabai. Complete Genes May Pass from Food to Human Blood. *PLoS One*, 8(7):1–11, 2013.
- [86] H. I. Elsner and E. B. Lindblad. Ultrasonic Degradation of DNA. *DNA*, 8(10):697–701, 1989.
- [87] J. Sambrook and D. W. Russel. Fragmentation of DNA by Sonication. *Cold Spring Harbor Protoc.*, 2006.
- [88] S. H. Razavi, F. Blanchard, and I. Marc. UV-HPLC / APCI-MS method for separation and identification of the carotenoids produced by *Sporobolomyces ruberrimus* H110. *Iran. J. Chem. Chem. Eng.*, 25(2):1–10, 2006.
- [89] A. Sujak, W. Okulski, and W. I. Gruszecki. Organization of xanthophyll pigments lutein and zeaxanthin in lipid membraned formed with dipalmitoylphosphadylcholine. *Biochim. Biophys. Acta*, 1509:255–263, 2000.
- [90] A. Thanapimmetha, T. Suwaleerat, M. Saisriyoot, Y. Chisti, and P. Srinophakun. Production of carotenoids and lipids by *Rhodococcus opacus* PD630 in batch and fed-batch culture. *Bioprocess Biosyst. Eng.*, 40(1):133–143, 2017.
- [91] K. Rabaey and W. Verstraete. Microbial fuel cells: Novel biotechnology for energy generation. *Trends Biotechnol.*, 23(6):291–298, 2005.

---

# A. *D. maris* and *R. ruber* NMR Measurements

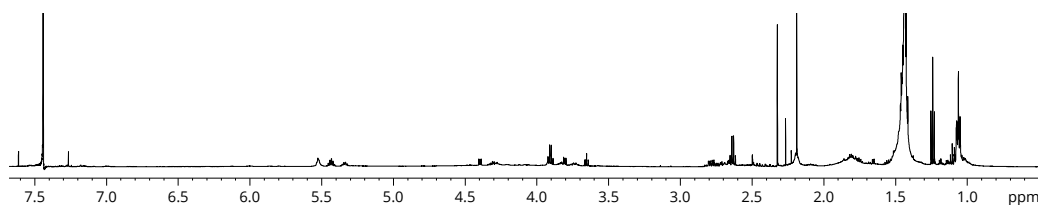
---

***D. maris* Dark Sample -  $^1\text{H}$  NMR Spectrum**



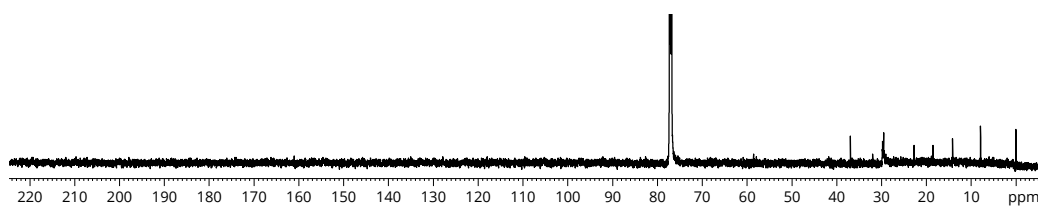
**Figure A.1:** PULCON  $^1\text{H}$  NMR spectrum of the *D. maris* sample shielded from light, diluted into deuterium-locked chloroform. No shifts related to either canthaxanthin, or any other carotenoid can be seen.

***D. maris* Light Sample -  $^1\text{H}$  NMR Spectrum**

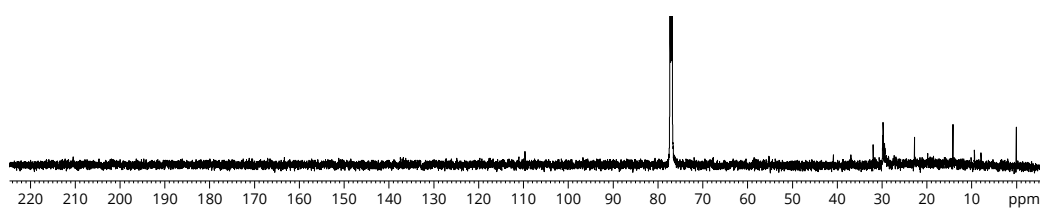


**Figure A.2:** PULCON  $^1\text{H}$  NMR spectrum of the *D. maris* sample exposed to light, diluted into deuterium-locked chloroform. No shifts related to either canthaxanthin, or any other carotenoid can be seen.

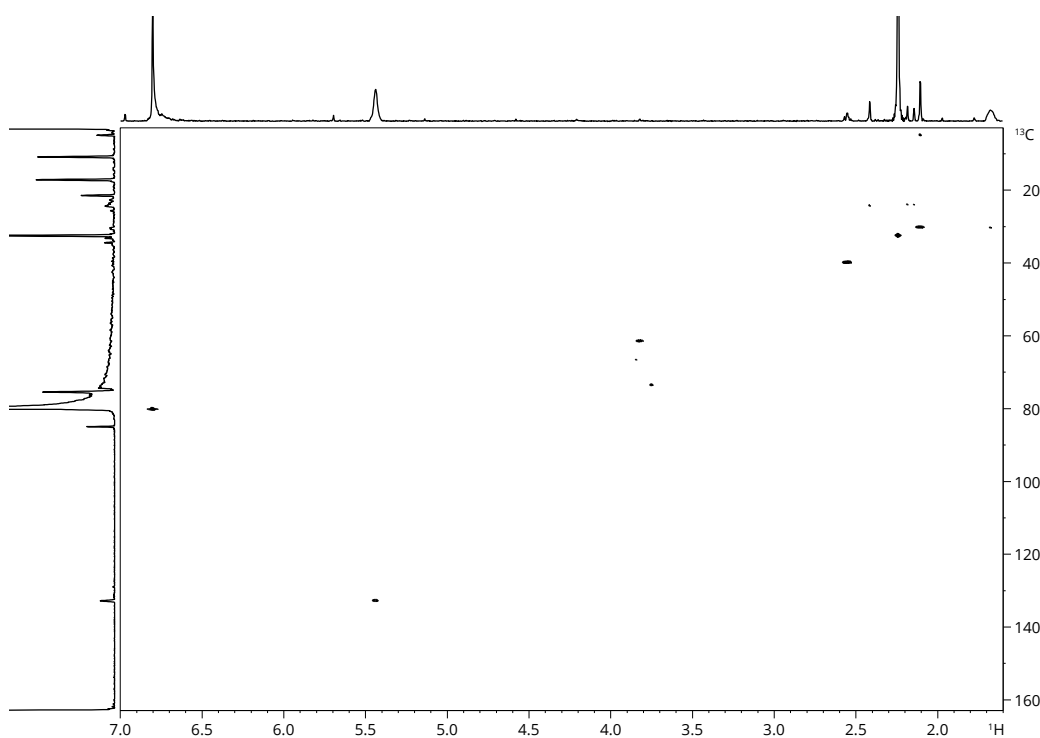
***D. maris* Dark Sample -  $^{13}\text{C}$  NMR Spectrum**



**Figure A.3:**  $^{13}\text{C}$  NMR spectrum of the *D. maris* sample shielded from light, diluted into deuterium-locked chloroform. No shifts related to either canthaxanthin, or any other carotenoid can be seen.

***D. maris* Light Sample -  $^{13}\text{C}$  Spectrum**

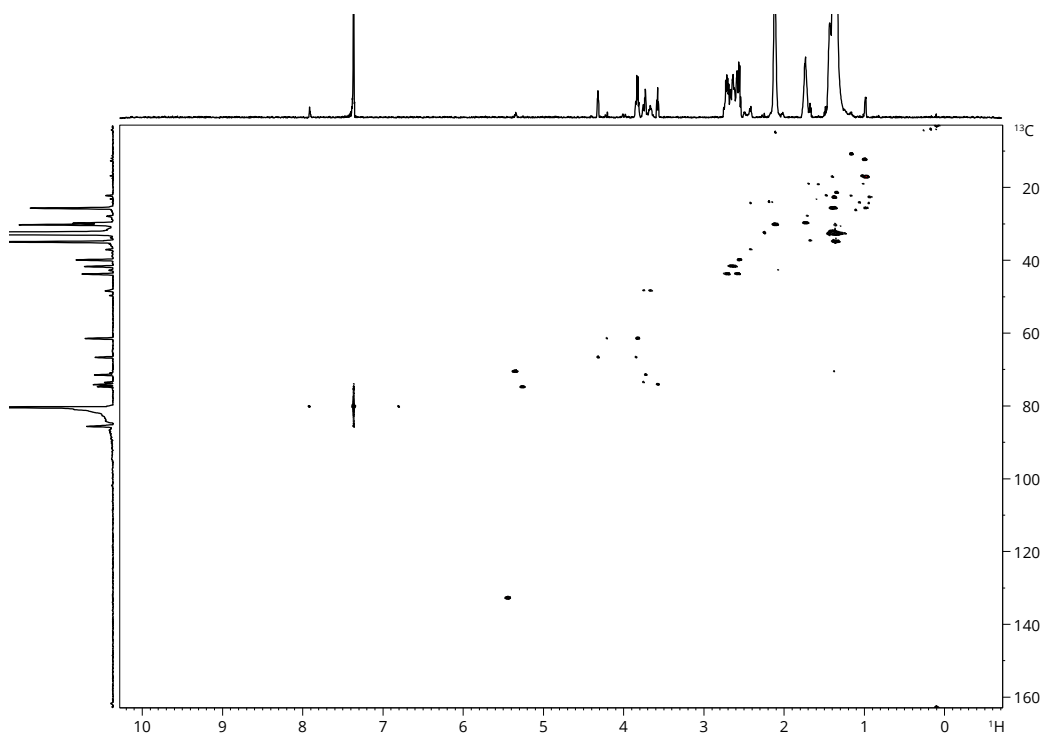
**Figure A.4:**  $^{13}\text{C}$  NMR spectrum of the *D. maris* sample exposed to light, diluted into deuterium-locked chloroform. No shifts related to either canthaxanthin, or any other carotenoid can be seen.

***D. maris* Dark Sample - HSQC Spectrum**

**Figure A.5:**  $^1\text{H}$  coupled  $^{13}\text{C}$  HSQC 2D NMR spectrum of the *D. maris* sample shielded from light during incubation, diluted into deuterium-locked chloroform. No couplings related to either canthaxanthin, or any other carotenoid can be seen.

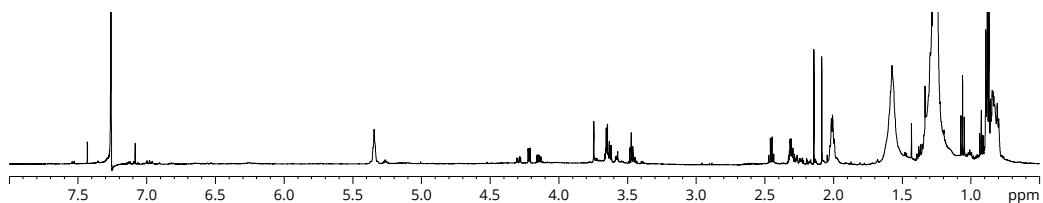
---

### *D. maris* Light Sample - HSQC Spectrum



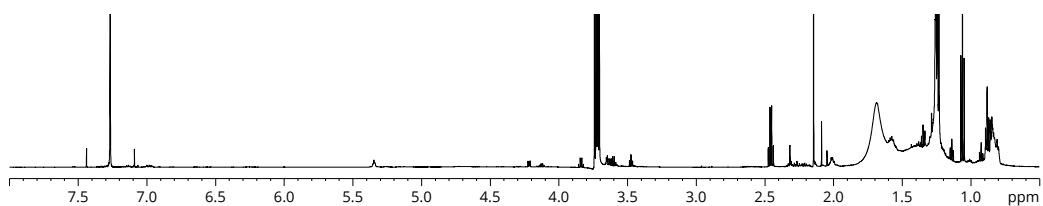
**Figure A.6:**  $^1\text{H}$  coupled  $^{13}\text{C}$  HSQC 2D NMR spectrum of the *D. maris* sample exposed to light during incubation, diluted into deuterium-locked chloroform. No couplings related to either canthaxanthin, or any other carotenoid can be seen.

### *R. ruber* Dark Sample - $^1\text{H}$ NMR Spectrum

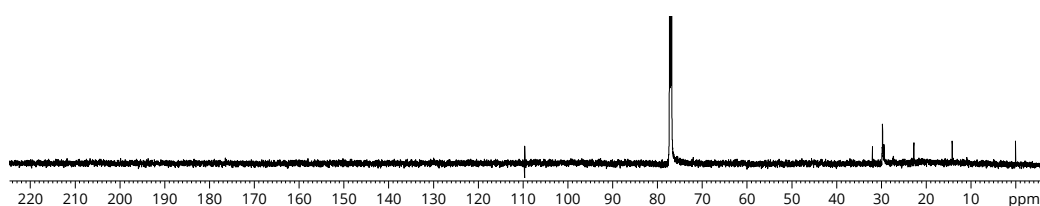


**Figure A.7:** PULCON  $^1\text{H}$  NMR spectrum of the *R. ruber* sample shielded from light, diluted into deuterium-locked chloroform. No shifts related to either  $\beta$ -carotene, or any other carotenoid can be seen.

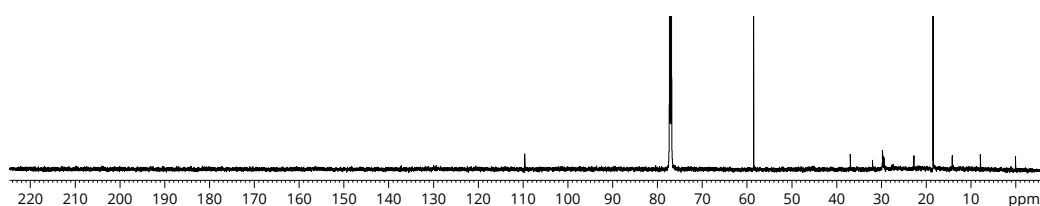
### *R. ruber* Light Sample - $^1\text{H}$ NMR Spectrum



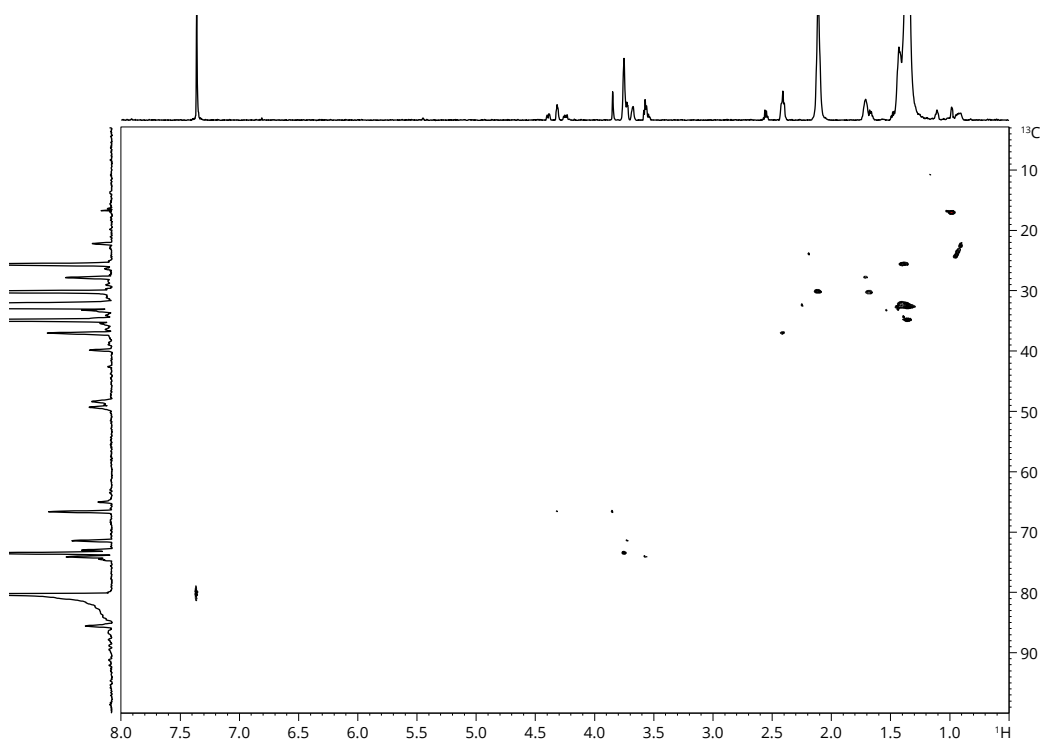
**Figure A.8:** PULCON  $^1\text{H}$  NMR spectrum of the *R. ruber* sample exposed to light, diluted into deuterium-locked chloroform. No shifts related to either  $\beta$ -carotene, or any other carotenoid can be seen.

***R. ruber* Dark Sample -  $^{13}\text{C}$  NMR Spectrum**

**Figure A.9:**  $^{13}\text{C}$  NMR spectrum of the *R. ruber* sample shielded from light, diluted into deuterium-locked chloroform. No shifts related to either  $\beta$ -carotene, or any other carotenoid can be seen.

***R. ruber* Light Sample -  $^{13}\text{C}$  NMR Spectrum**

**Figure A.10:**  $^{13}\text{C}$  NMR spectrum of the *R. ruber* sample exposed to light, diluted into deuterium-locked chloroform. No shifts related to either  $\beta$ -carotene, or any other carotenoid can be seen.

***R. ruber* Dark Sample - HSQC Spectrum**

**Figure A.11:**  $^1\text{H}$  coupled  $^{13}\text{C}$  HSQC 2D NMR spectrum of the *R. ruber* sample shielded from light, diluted into deuterium-locked chloroform. No couplings related to either  $\beta$ -carotene, or any other carotenoid can be seen.

***R. ruber* Light Sample - HSQC Spectrum**

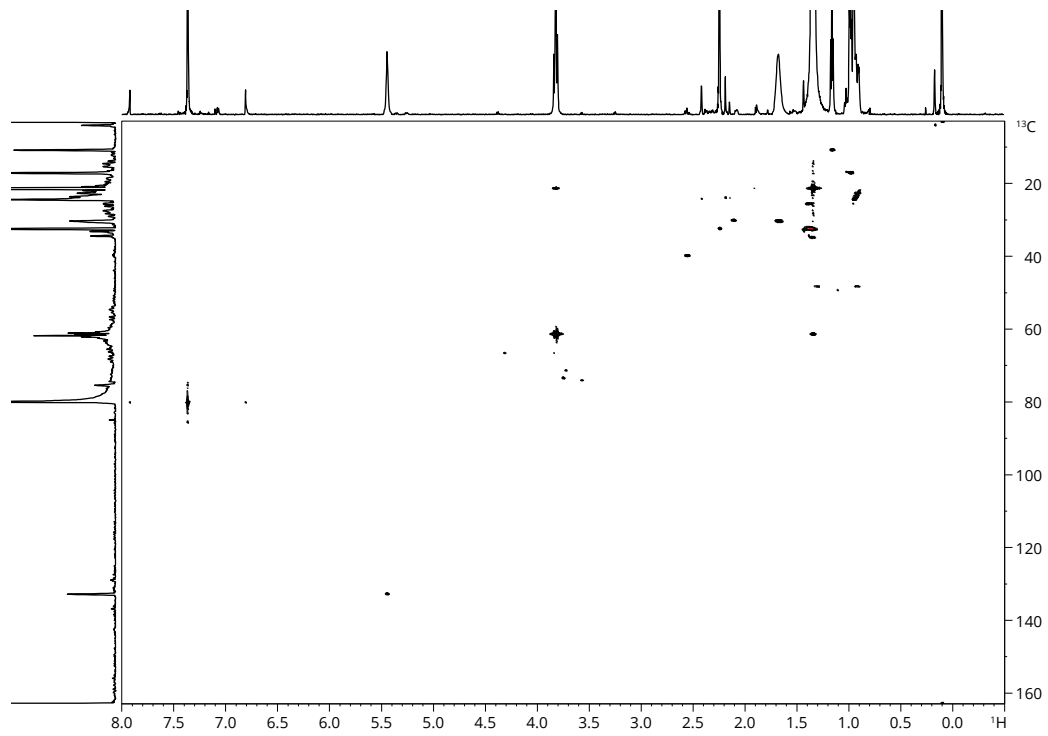


**Figure A.12:**  $^1\text{H}$  coupled  $^{13}\text{C}$  HSQC 2D NMR spectrum of the *R. ruber* sample exposed to light, diluted into deuterium-locked chloroform. No couplings related to either  $\beta$ -carotene, or any other carotenoid can be seen.



## B. Mass Chromatograms of Extracted Agar Plates

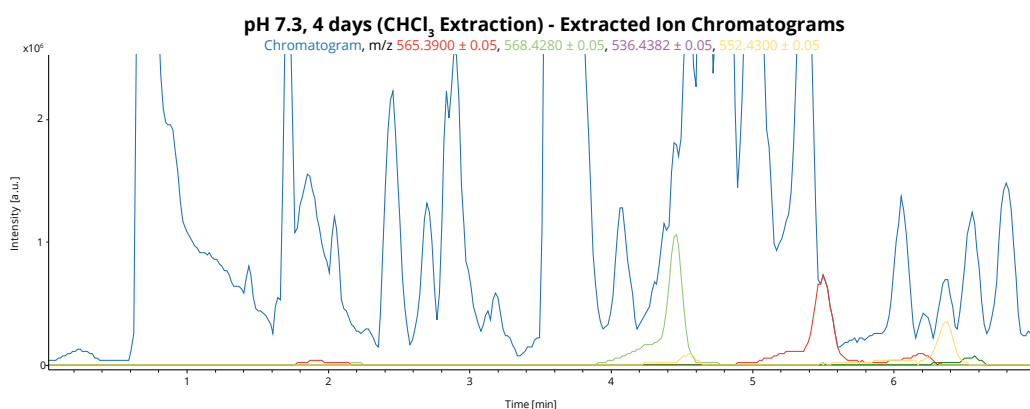


**Figure B.1:** HPLC/ESI-MS full mass chromatogram and extracted ion chromatograms the *D. maris* agar plate B which had been incubated at pH 7.3 for 4 days, at positive ionization. The mass chromatogram is measured in chloroform with an isocratic mobile phase of 99 % acetonitrile on the C18 HPLC column. In addition, a 10 minute pre-run with pure acetonitrile, followed by a running time of 10 minutes, was utilized with a 5  $\mu$ L injection volume. Canthaxanthin at  $m/z$  565.3900  $\pm$  0.05 ( $[M+H]^+$ ), zeaxanthin/lutein at  $m/z$  568.4280  $\pm$  0.05 ( $[M]^+$ ),  $\beta$ -carotene/lycopene at  $m/z$  536.4382  $\pm$  0.05 ( $[M]^+$ ), and  $\beta$ -cryptoxanthin at  $m/z$  552.4331  $\pm$  0.05 ( $[M]^+$ ) have been extracted from the full chromatogram (dark blue).

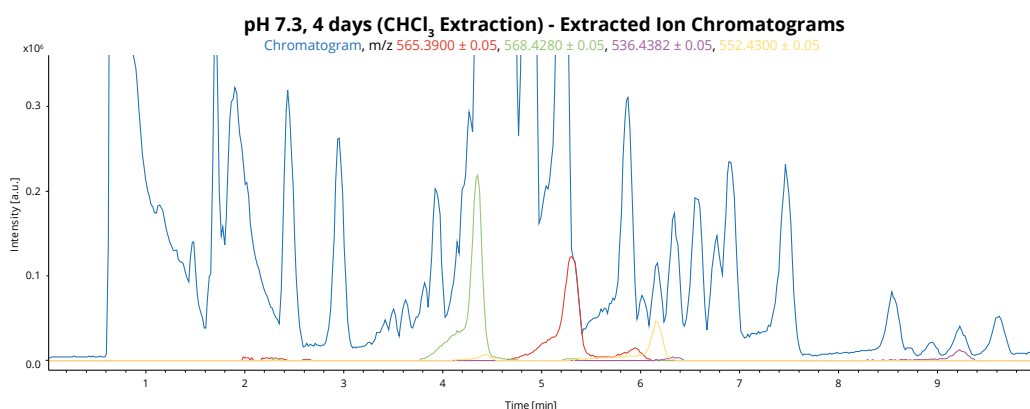


**Figure B.2:** HPLC/ESI-MS full mass chromatogram and extracted ion chromatograms the *D. maris* agar plate C which had been incubated at pH 7.3 for 4 days, at positive ionization. The mass chromatogram is measured in chloroform with an isocratic mobile phase of 99 % acetonitrile on the C18 HPLC column. In addition, a 10 minute pre-run with pure acetonitrile, followed by a running time of 10 minutes, was utilized with a 5  $\mu$ L injection volume. Canthaxanthin at  $m/z$  565.3900  $\pm$  0.05 ( $[M+H]^+$ ), zeaxanthin/lutein at  $m/z$  568.4280  $\pm$  0.05 ( $[M]^+$ ),  $\beta$ -carotene/lycopene at  $m/z$  536.4382  $\pm$  0.05 ( $[M]^+$ ), and  $\beta$ -cryptoxanthin at  $m/z$  552.4331  $\pm$  0.05 ( $[M]^+$ ) have been extracted from the full chromatogram (dark blue).

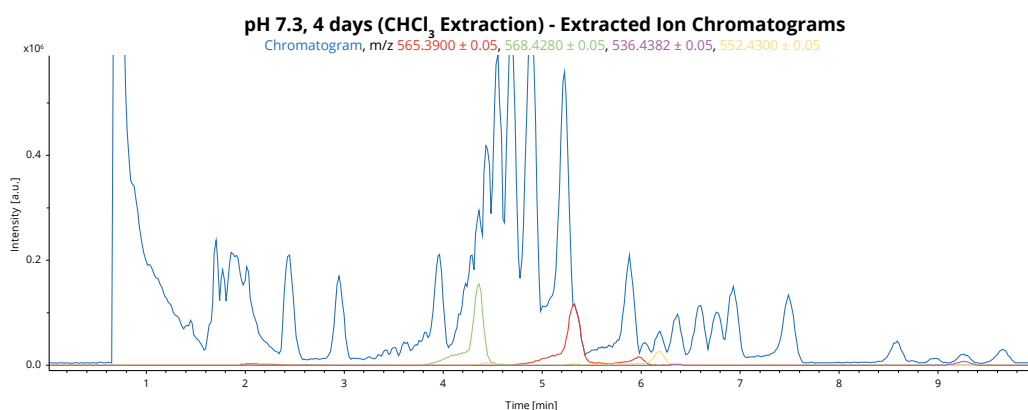


**Figure B.3:** HPLC/ESI-MS full mass chromatogram and extracted ion chromatograms the *D. maris* agar plate D which had been incubated at pH 7.3 for 4 days, at positive ionization. The mass chromatogram is measured in chloroform with an isocratic mobile phase of 99 % acetonitrile on the C18 HPLC column. In addition, a 10 minute pre-run with pure acetonitrile, followed by a running time of 10 minutes, was utilized with a 5  $\mu$ L injection volume. Canthaxanthin at  $m/z$  565.3900  $\pm$  0.05 ( $[M+H]^+$ ), zeaxanthin/lutein at  $m/z$  568.4280  $\pm$  0.05 ( $[M]^+$ ),  $\beta$ -carotene/lycopene at  $m/z$  536.4382  $\pm$  0.05 ( $[M]^+$ ), and  $\beta$ -cryptoxanthin at  $m/z$  552.4331  $\pm$  0.05 ( $[M]^+$ ) have been extracted from the full chromatogram (dark blue).

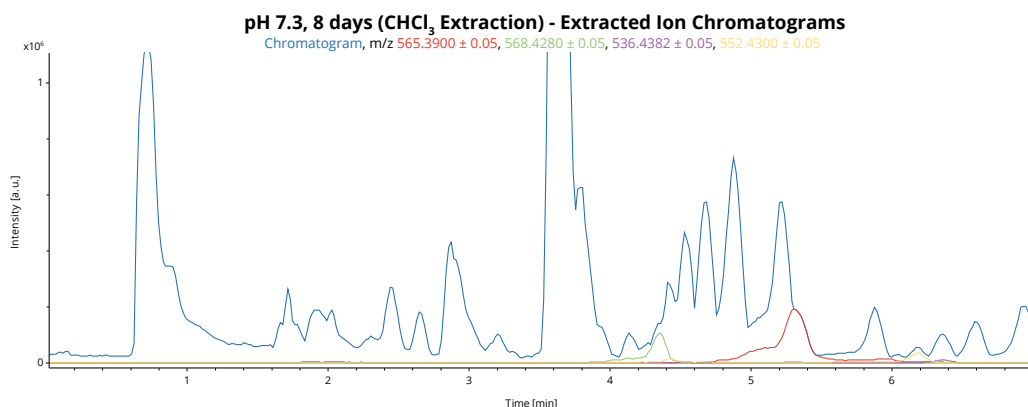


**Figure B.4:** HPLC/ESI-MS full mass chromatogram and extracted ion chromatograms of the *D. maris* agar plate B which had been incubated at pH 7.3 for 8 days, at positive ionization. The mass chromatogram is measured in chloroform with an isocratic mobile phase of 99 % acetonitrile on the C18 HPLC column. In addition, a 10 minute pre-run with pure acetonitrile, followed by a running time of 10 minutes, was utilized with a 5  $\mu$ L injection volume. Canthaxanthin at  $m/z$  565.3900  $\pm$  0.05 ( $[M+H]^+$ ), zeaxanthin/lutein at  $m/z$  568.4280  $\pm$  0.05 ( $[M]^+$ ),  $\beta$ -carotene/lycopene at  $m/z$  536.4382  $\pm$  0.05 ( $[M]^+$ ), and  $\beta$ -cryptoxanthin at  $m/z$  552.4300  $\pm$  0.05 ( $[M]^+$ ) have been extracted from the full chromatogram (dark blue).

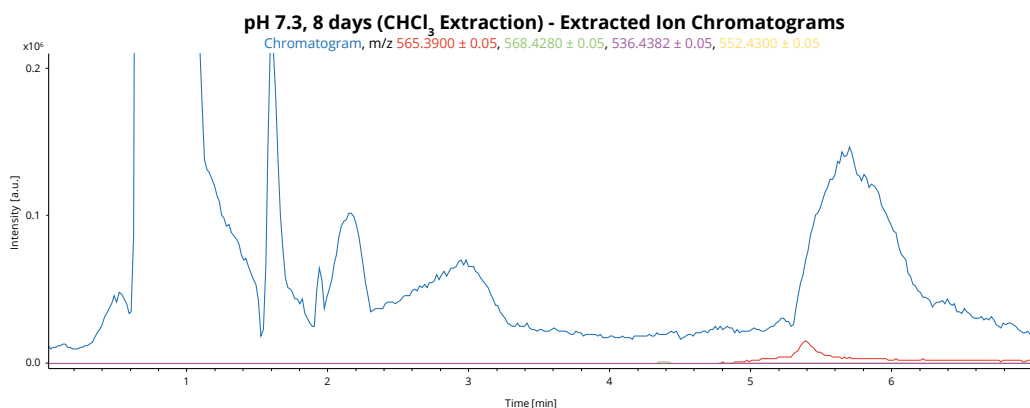


**Figure B.5:** HPLC/ESI-MS full mass chromatogram and extracted ion chromatograms of the *D. maris* agar plate C which had been incubated at pH 7.3 for 8 days, at positive ionization. The mass chromatogram is measured in chloroform with an isocratic mobile phase of 99 % acetonitrile on the C18 HPLC column. In addition, a 10 minute pre-run with pure acetonitrile, followed by a running time of 10 minutes, was utilized with a 5  $\mu$ L injection volume. Canthaxanthin at  $m/z$   $565.3900 \pm 0.05$  ( $[M+H]^+$ ), zeaxanthin/lutein at  $m/z$   $568.4280 \pm 0.05$  ( $[M]^+$ ),  $\beta$ -carotene/lycopene at  $m/z$   $536.4382 \pm 0.05$  ( $[M]^+$ ), and  $\beta$ -cryptoxanthin at  $m/z$   $552.4300 \pm 0.05$  ( $[M]^+$ ) have been extracted from the full chromatogram (dark blue).

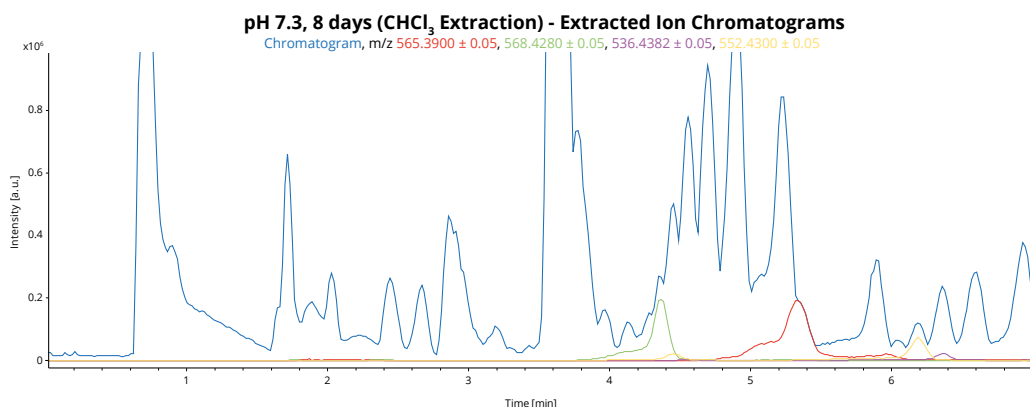


**Figure B.6:** HPLC/ESI-MS full mass chromatogram and extracted ion chromatograms of the *D. maris* agar plate D which had been incubated at pH 7.3 for 8 days, at positive ionization. The mass chromatogram is measured in chloroform with an isocratic mobile phase of 99 % acetonitrile on the C18 HPLC column. In addition, a 10 minute pre-run with pure acetonitrile, followed by a running time of 10 minutes, was utilized with a 5  $\mu$ L injection volume. Canthaxanthin at  $m/z$   $565.3900 \pm 0.05$  ( $[M+H]^+$ ), zeaxanthin/lutein at  $m/z$   $568.4280 \pm 0.05$  ( $[M]^+$ ),  $\beta$ -carotene/lycopene at  $m/z$   $536.4382 \pm 0.05$  ( $[M]^+$ ), and  $\beta$ -cryptoxanthin at  $m/z$   $552.4300 \pm 0.05$  ( $[M]^+$ ) have been extracted from the full chromatogram (dark blue).

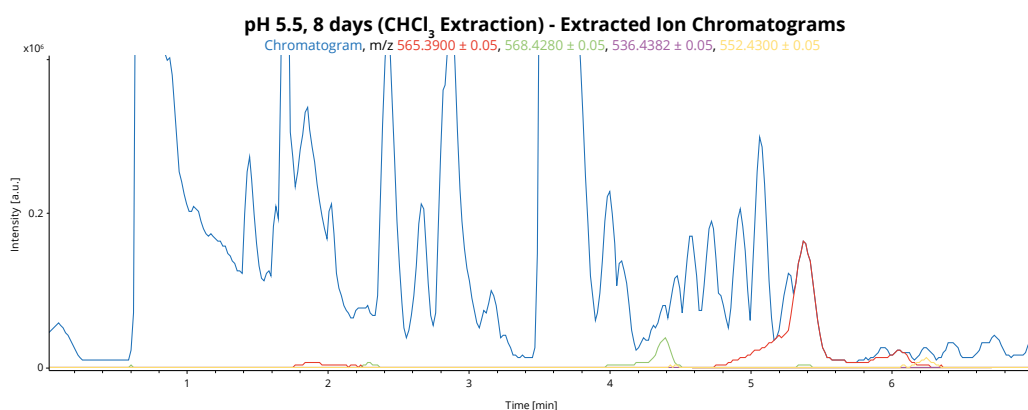


**Figure B.7:** HPLC/ESI-MS full mass chromatogram and extracted ion chromatograms of the *D. maris* agar plate B which had been incubated at pH 5.5 for 8 days, at positive ionization. The mass chromatogram is measured in chloroform with an isocratic mobile phase of 99 % acetonitrile on the C18 HPLC column. In addition, a 10 minute pre-run with pure acetonitrile, followed by a running time of 10 minutes, was utilized with a 5  $\mu$ L injection volume. Canthaxanthin at  $m/z$  565.3900  $\pm$  0.05 ( $[M+H]^+$ ), zeaxanthin/lutein at  $m/z$  568.4280  $\pm$  0.05 ( $[M]^+$ ),  $\beta$ -carotene/lycopene at  $m/z$  536.4382  $\pm$  0.05 ( $[M]^+$ ), and  $\beta$ -cryptoxanthin at  $m/z$  552.4300  $\pm$  0.05 ( $[M]^+$ ) have been extracted from the full chromatogram (dark blue).

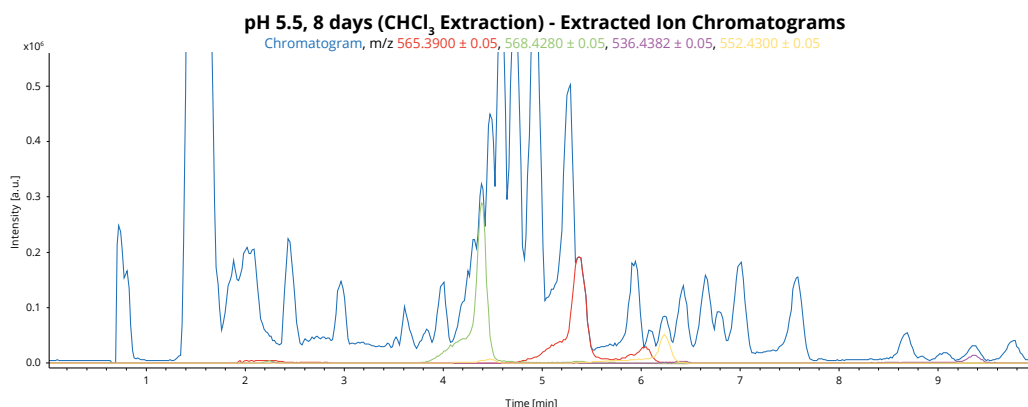


**Figure B.8:** HPLC/ESI-MS full mass chromatogram and extracted ion chromatograms of the *D. maris* agar plate C which had been incubated at pH 5.5 for 8 days, at positive ionization. The mass chromatogram is measured in chloroform with an isocratic mobile phase of 99 % acetonitrile on the C18 HPLC column. In addition, a 10 minute pre-run with pure acetonitrile, followed by a running time of 10 minutes, was utilized with a 5  $\mu$ L injection volume. Canthaxanthin at  $m/z$  565.3900  $\pm$  0.05 ( $[M+H]^+$ ), zeaxanthin/lutein at  $m/z$  568.4280  $\pm$  0.05 ( $[M]^+$ ),  $\beta$ -carotene/lycopene at  $m/z$  536.4382  $\pm$  0.05 ( $[M]^+$ ), and  $\beta$ -cryptoxanthin at  $m/z$  552.4300  $\pm$  0.05 ( $[M]^+$ ) have been extracted from the full chromatogram (dark blue).

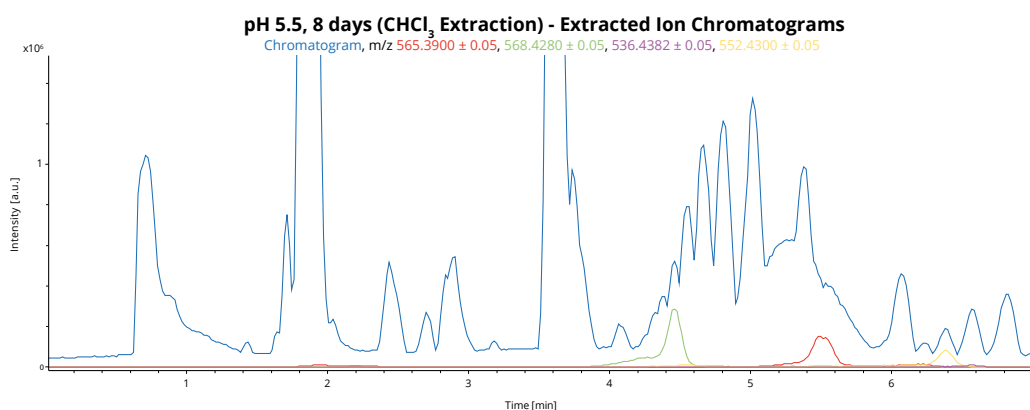


**Figure B.9:** HPLC/ESI-MS full mass chromatogram and extracted ion chromatograms of the *D. maris* agar plate D which had been incubated at pH 5.5 for 8 days, at positive ionization. The mass chromatogram is measured in chloroform with an isocratic mobile phase of 99 % acetonitrile on the C18 HPLC column. In addition, a 10 minute pre-run with pure acetonitrile, followed by a running time of 10 minutes, was utilized with a 5  $\mu$ L injection volume. Canthaxanthin at m/z 565.3900  $\pm$  0.05 ( $[M + H]^+$ ), zeaxanthin/lutein at m/z 568.4280  $\pm$  0.05 ( $[M]^+$ ),  $\beta$ -carotene/lycopene at m/z 536.4382  $\pm$  0.05 ( $[M]^+$ ), and  $\beta$ -cryptoxanthin at m/z 552.4300  $\pm$  0.05 ( $[M]^+$ ) have been extracted from the full chromatogram (dark blue).

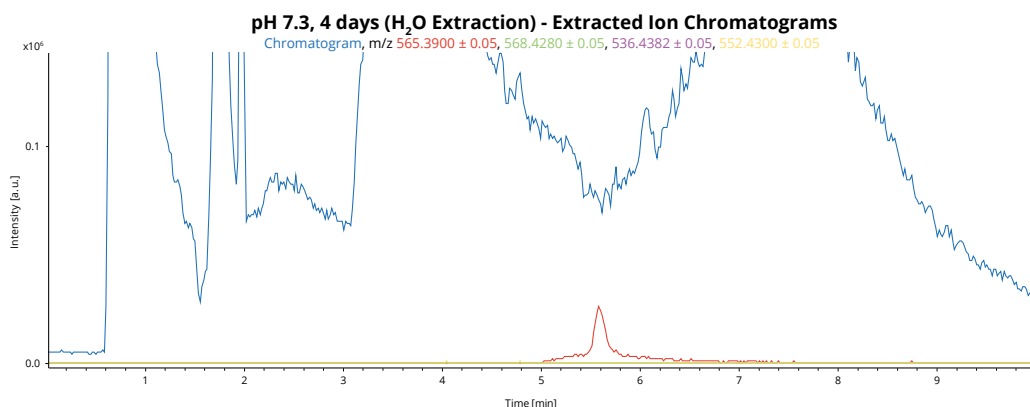


**Figure B.10:** HPLC/ESI-MS full mass chromatogram and extracted ion chromatograms of the water-extracted sample A which had been incubated for 4 days at pH 7.3, at positive ionization. The mass chromatogram is measured in methanol (1:1) with an isocratic mobile phase of 99 % acetonitrile on the C18 HPLC column. In addition, a 10 minute pre-run with pure acetonitrile, followed by a running time of 10 minutes, was utilized with a 5  $\mu$ L injection volume. Canthaxanthin at m/z 565.3900  $\pm$  0.05 ( $[M + H]^+$ ), zeaxanthin/lutein at m/z 568.4280  $\pm$  0.05,  $\beta$ -carotene/lycopene at m/z 536.4382  $\pm$  0.05 ( $[M]^+$ ), and  $\beta$ -cryptoxanthin at m/z 552.4300  $\pm$  0.05 ( $[M + H]^+$ ) have been extracted from the full chromatogram (dark blue).

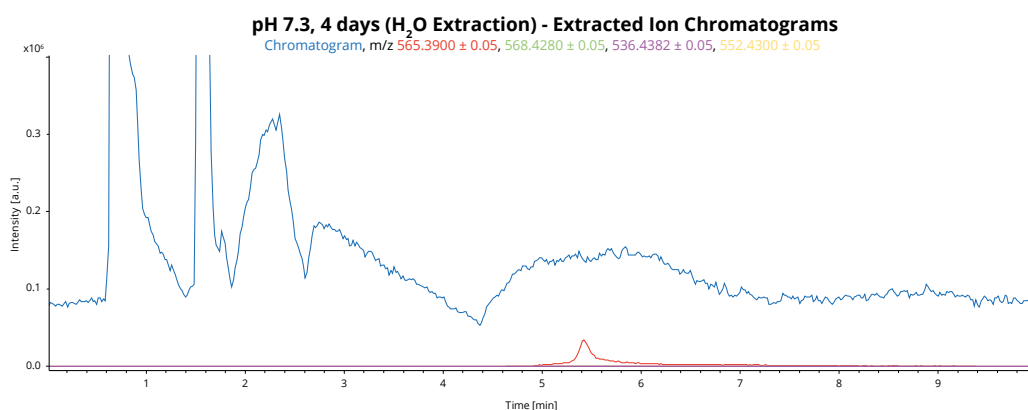


**Figure B.11:** HPLC/ESI-MS full mass chromatogram and extracted ion chromatograms of the water-extracted sample B which had been incubated for 4 days at pH 7.3, at positive ionization. The mass chromatogram is measured in methanol (1:1) with an isocratic mobile phase of 99 % acetonitrile on the C18 HPLC column. In addition, a 10 minute pre-run with pure acetonitrile, followed by a running time of 10 minutes, was utilized with a 5  $\mu$ L injection volume. Canthaxanthin at m/z 565.3900  $\pm$  0.05 ( $[M+H]^+$ ), zeaxanthin/lutein at m/z 568.4280  $\pm$  0.05,  $\beta$ -carotene/lycopene at m/z 536.4382  $\pm$  0.05 ( $[M]^+$ ), and  $\beta$ -cryptoxanthin at m/z 552.4300  $\pm$  0.05 ( $[M+H]^+$ ) have been extracted from the full chromatogram (dark blue).

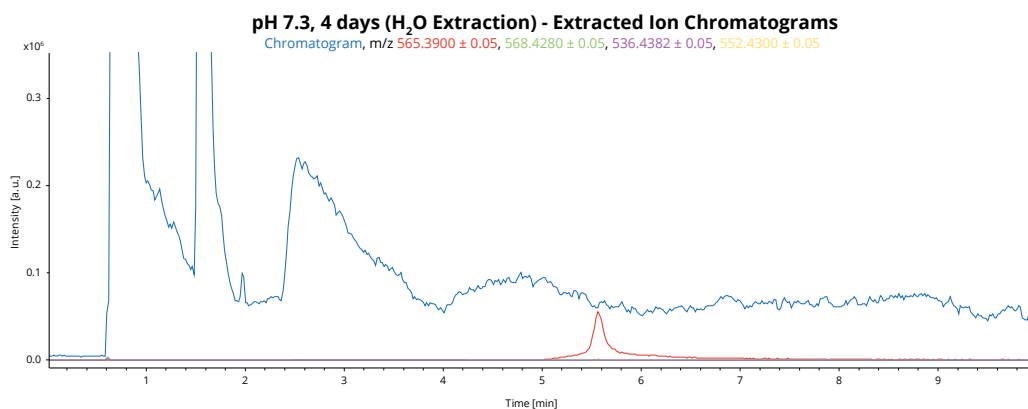


**Figure B.12:** HPLC/ESI-MS full mass chromatogram and extracted ion chromatograms of the water-extracted sample C which had been incubated for 4 days at pH 7.3, at positive ionization. The mass chromatogram is measured in methanol (1:1) with an isocratic mobile phase of 99 % acetonitrile on the C18 HPLC column. In addition, a 10 minute pre-run with pure acetonitrile, followed by a running time of 10 minutes, was utilized with a 5  $\mu$ L injection volume. Canthaxanthin at m/z 565.3900  $\pm$  0.05 ( $[M+H]^+$ ), zeaxanthin/lutein at m/z 568.4280  $\pm$  0.05,  $\beta$ -carotene/lycopene at m/z 536.4382  $\pm$  0.05 ( $[M]^+$ ), and  $\beta$ -cryptoxanthin at m/z 552.4300  $\pm$  0.05 ( $[M+H]^+$ ) have been extracted from the full chromatogram (dark blue).

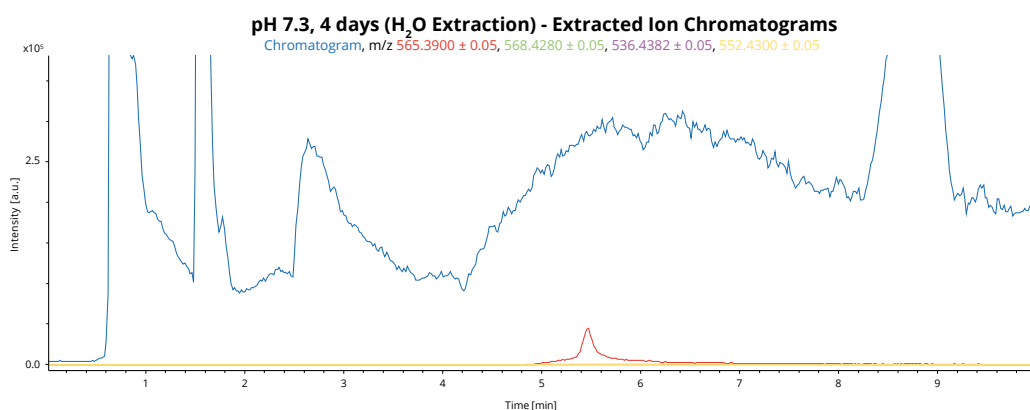


**Figure B.13:** HPLC/ESI-MS full mass chromatogram and extracted ion chromatograms of the water-extracted sample D which had been incubated for 4 days at pH 7.3, at positive ionization. The mass chromatogram is measured in methanol (1:1) with an isocratic mobile phase of 99 % acetonitrile on the C18 HPLC column. In addition, a 10 minute pre-run with pure acetonitrile, followed by a running time of 10 minutes, was utilized with a 5  $\mu$ L injection volume. Canthaxanthin at m/z 565.3900  $\pm$  0.05 ( $[M + H]^+$ ), zeaxanthin/lutein at m/z 568.4280  $\pm$  0.05,  $\beta$ -carotene/lycopene at m/z 536.4382  $\pm$  0.05 ( $[M]^+$ ), and  $\beta$ -cryptoxanthin at m/z 552.4300  $\pm$  0.05 ( $[M + H]^+$ ) have been extracted from the full chromatogram (dark blue).

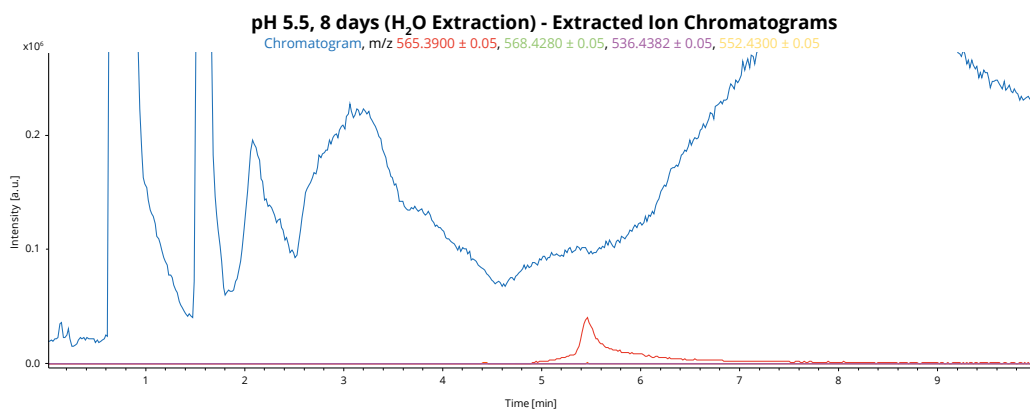


**Figure B.14:** HPLC/ESI-MS full mass chromatogram and extracted ion chromatograms of the water-extracted sample B which had been incubated for 8 days at pH 5.5, at positive ionization. The mass chromatogram is measured in methanol (1:1) with an isocratic mobile phase of 99 % acetonitrile on the C18 HPLC column. In addition, a 10 minute pre-run with pure acetonitrile, followed by a running time of 10 minutes, was utilized with a 5  $\mu$ L injection volume. Canthaxanthin at m/z 565.3900  $\pm$  0.05 ( $[M + H]^+$ ), zeaxanthin/lutein at m/z 568.4280  $\pm$  0.05,  $\beta$ -carotene/lycopene at m/z 536.4382  $\pm$  0.05 ( $[M]^+$ ), and  $\beta$ -cryptoxanthin at m/z 552.4300  $\pm$  0.05 ( $[M + H]^+$ ) have been extracted from the full chromatogram (dark blue).

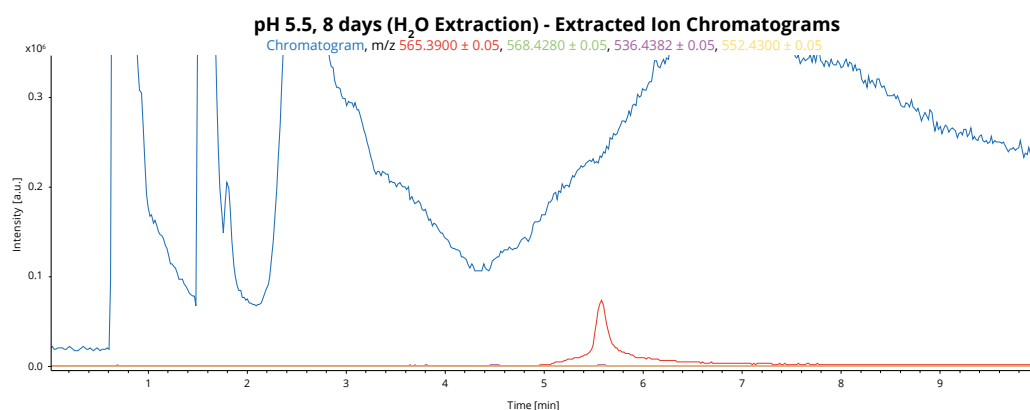


**Figure B.15:** HPLC/ESI-MS full mass chromatogram and extracted ion chromatograms of the water-extracted sample C which had been incubated for 8 days at pH 5.5, at positive ionization. The mass chromatogram is measured in methanol (1:1) with an isocratic mobile phase of 99 % acetonitrile on the C18 HPLC column. In addition, a 10 minute pre-run with pure acetonitrile, followed by a running time of 10 minutes, was utilized with a 5  $\mu$ L injection volume. Canthaxanthin at  $m/z$  565.3900  $\pm$  0.05 ( $[M+H]^+$ ), zeaxanthin/lutein at  $m/z$  568.4280  $\pm$  0.05,  $\beta$ -carotene/lycopene at  $m/z$  536.4382  $\pm$  0.05 ( $[M]^+$ ), and  $\beta$ -cryptoxanthin at  $m/z$  552.4300  $\pm$  0.05 ( $[M+H]^+$ ) have been extracted from the full chromatogram (dark blue).

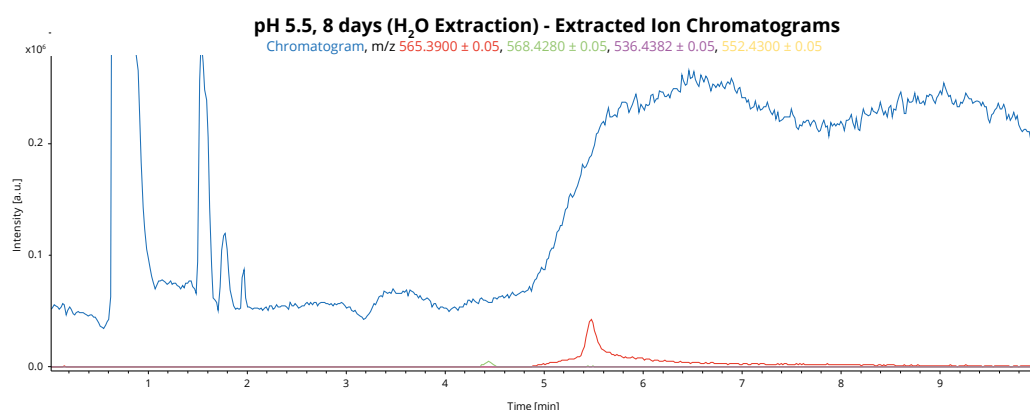


**Figure B.16:** HPLC/ESI-MS full mass chromatogram and extracted ion chromatograms of the water-extracted sample D which had been incubated for 8 days at pH 5.5, at positive ionization. The mass chromatogram is measured in methanol (1:1) with an isocratic mobile phase of 99 % acetonitrile on the C18 HPLC column. In addition, a 10 minute pre-run with pure acetonitrile, followed by a running time of 10 minutes, was utilized with a 5  $\mu$ L injection volume. Canthaxanthin at  $m/z$  565.3900  $\pm$  0.05 ( $[M+H]^+$ ), zeaxanthin/lutein at  $m/z$  568.4280  $\pm$  0.05,  $\beta$ -carotene/lycopene at  $m/z$  536.4382  $\pm$  0.05 ( $[M]^+$ ), and  $\beta$ -cryptoxanthin at  $m/z$  552.4300  $\pm$  0.05 ( $[M+H]^+$ ) have been extracted from the full chromatogram (dark blue).

---

# C. Nanoparticle Tracking Analysis Measurements

---

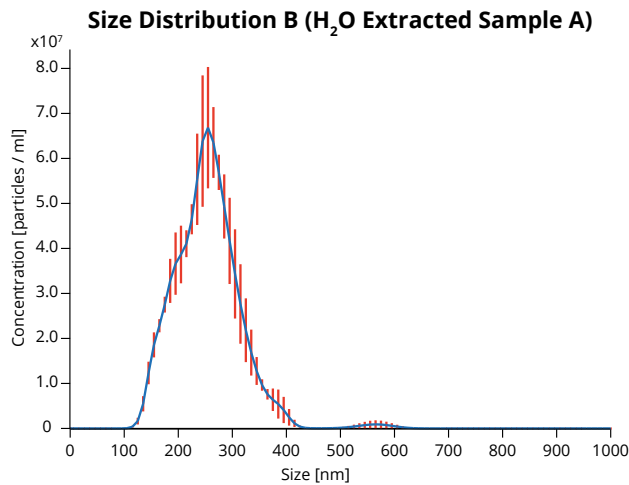


**Figure C.1:** A plot showing the average size distribution of the vesicles in one spot of one water-extracted sample, formed during ultra-sonication of the *D. maris* cells from the membrane constituents, encapsulating the bacterial canthaxanthin.

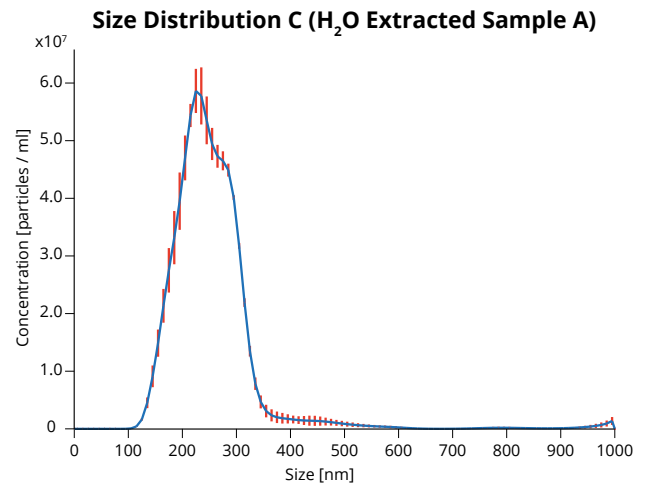


**Figure C.2:** A plot showing the average size distribution of the vesicles in one spot of one water-extracted sample, formed during ultra-sonication of the *D. maris* cells from the membrane constituents, encapsulating the bacterial canthaxanthin.

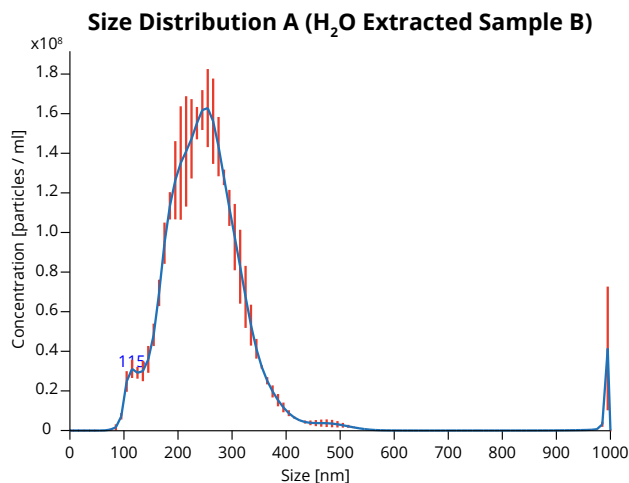


**Figure C.3:** A plot showing the average size distribution of the vesicles in one spot of one water-extracted sample, formed during ultra-sonication of the *D. maris* cells from the membrane constituents, encapsulating the bacterial canthaxanthin.

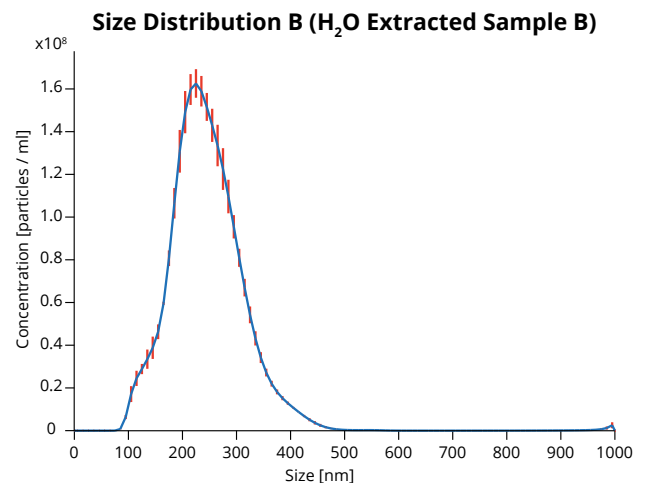


**Figure C.4:** A plot showing the average size distribution of the vesicles in one spot of one water-extracted sample, formed during ultra-sonication of the *D. maris* cells from the membrane constituents, encapsulating the bacterial canthaxanthin.

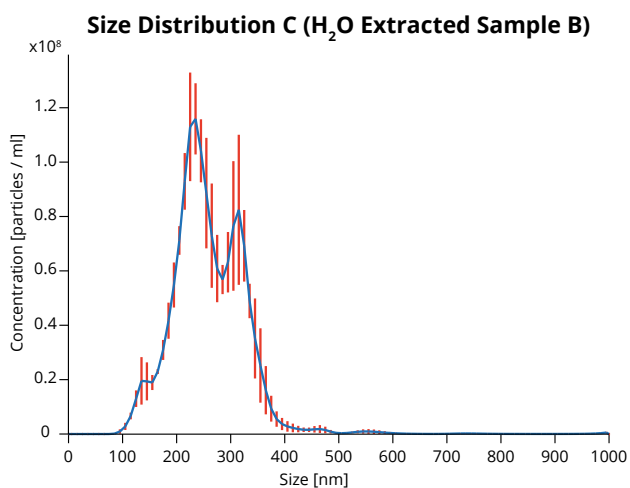


**Figure C.5:** A plot showing the average size distribution of the vesicles in one spot of one water-extracted sample, formed during ultra-sonication of the *D. maris* cells from the membrane constituents, encapsulating the bacterial canthaxanthin.

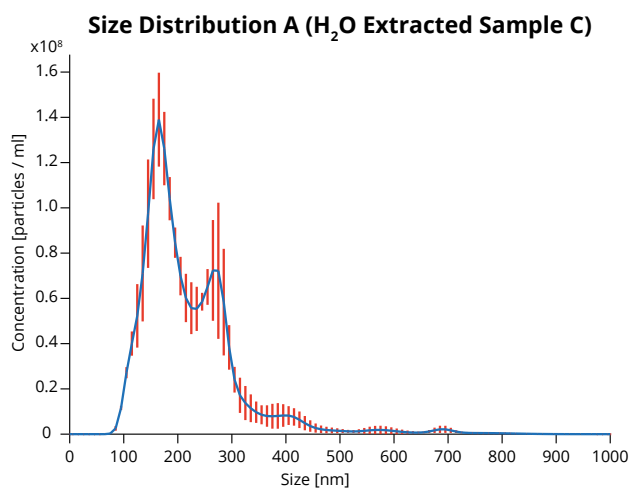


**Figure C.6:** A plot showing the average size distribution of the vesicles in one spot of one water-extracted sample, formed during ultra-sonication of the *D. maris* cells from the membrane constituents, encapsulating the bacterial canthaxanthin.

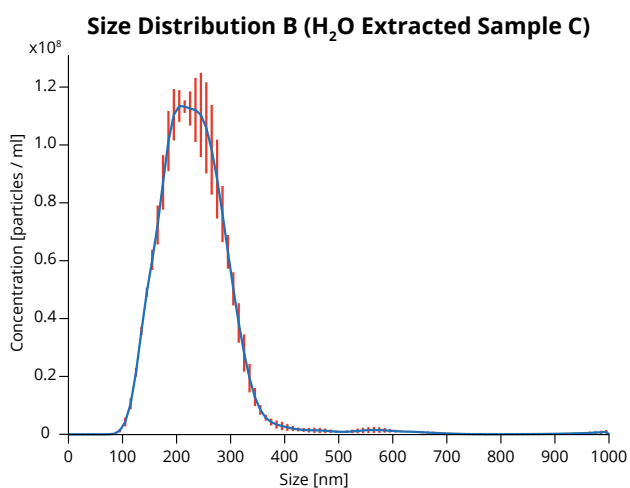


**Figure C.7:** A plot showing the average size distribution of the vesicles in one spot of one water-extracted sample, formed during ultra-sonication of the *D. maris* cells from the membrane constituents, encapsulating the bacterial canthaxanthin.

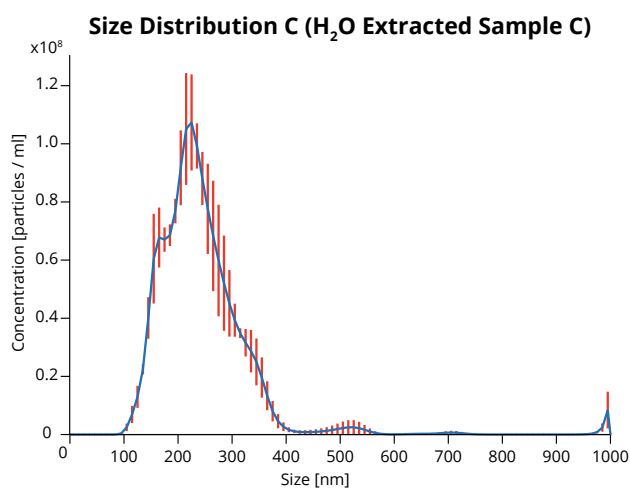


**Figure C.8:** A plot showing the average size distribution of the vesicles in one spot of one water-extracted sample, formed during ultra-sonication of the *D. maris* cells from the membrane constituents, encapsulating the bacterial canthaxanthin.

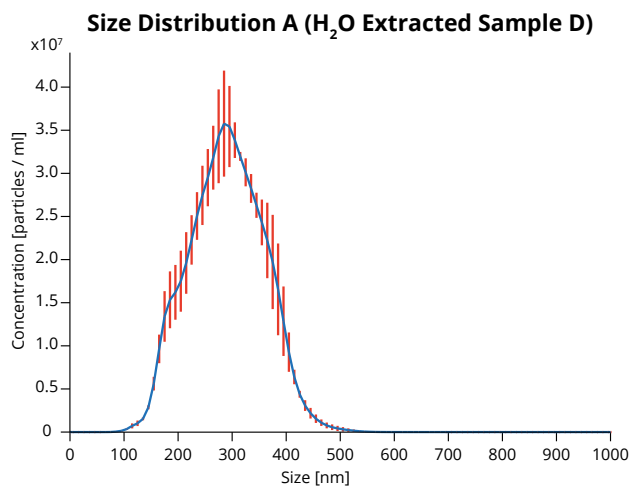


**Figure C.9:** A plot showing the average size distribution of the vesicles in one spot of one water-extracted sample, formed during ultra-sonication of the *D. maris* cells from the membrane constituents, encapsulating the bacterial canthaxanthin.

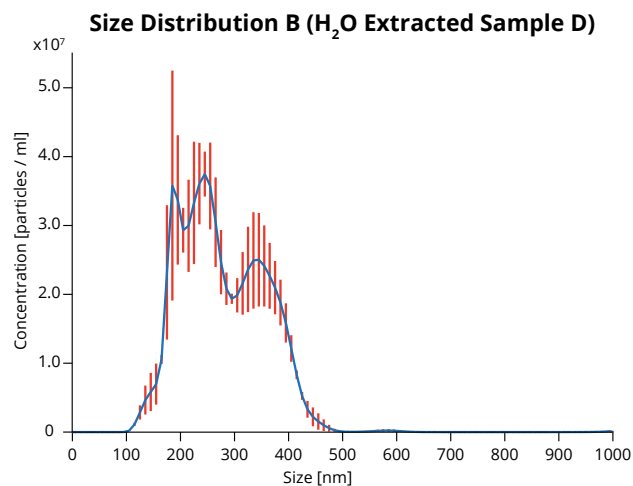


**Figure C.10:** A plot showing the average size distribution of the vesicles in one spot of one water-extracted sample, formed during ultra-sonication of the *D. maris* cells from the membrane constituents, encapsulating the bacterial canthaxanthin.

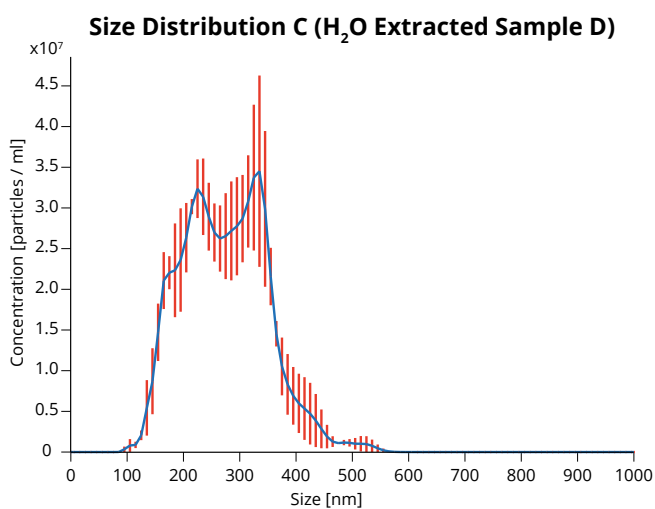


**Figure C.11:** A plot showing the average size distribution of the vesicles in one spot of one water-extracted sample, formed during ultra-sonication of the *D. maris* cells from the membrane constituents, encapsulating the bacterial canthaxanthin.